NTNU
Norwegian University of
Science and Technology

Hywind Powering Utsira

A reliability study of offshore wind connected
to multiple oil and gas platforms

Idun Vetvik

Master of Energy and Environmental Engineering
Submission date: June 2017
Supervisor: Kjetil Uhlen, IEL

Norwegian University of Science and Technology
Department of Electric Power Engineering

Problem Description

The aim of this thesis is to evaluate the reliability of the generation system and the composite generation and transmission system when wind power is added to the system or the grid topology is changed. For this thesis, the Utsira High area, consisting of four oil and gas platforms, is used as a basis for the analysis.

To evaluate the reliability of the system, different ways to incorporate and model wind power in reliability evaluations will be investigated and compared. In addition to the impact of including the technical availability of wind turbine generators, the availability of the wind power due to wind speed will be studied in this thesis. How the wind turbine availability will affect the overall reliability of the system will be explored in the reliability assessment.

The study consists of a generation adequacy analysis and a composite generation and transmission reliability analysis. The reliability of the composite generation and transmission system will be evaluated to quantify the possible benefits from changing the grid topology from a radial grid to a ring grid, the benefits from the additional wind power, and to study the impact on the reliability from including the transmission system. The generation adequacy analysis will evaluate possible benefits from additional wind power, as well as studying the impact on reliability from different reliability parameters and wind model methodologies.

The layouts that are to be studied in the composite reliability analysis are the Base Case, in which each the platforms are connected in a radial network, Case 1, in which the platforms are connected in a radial network and a wind farm is connected to platform 1, Case 2, in which the platforms are connected in a ring network, and Case 3, in which the platforms are connected in a ring network and a wind farm is connected to platform 1. The layouts that are to be studied in the generation adequacy analysis are the existing generation system at Utsira High, with and without additional wind power.

Acknowledgements

First, I would like to thank my supervisor Kjetil Uhlen for help and guidance throughout the project and support in shaping the problem description. The work has been rewarding and educational.

I would also like to thank Vijay Venu Vadlamudi. His expertise and contribution in the field of reliability analysis have been very helpful. He helped a great deal with the understanding and implementation of different wind power modelling methodologies for adequacy assessments of composite wind-integrated systems.

Idun Deildokk Vetvik
(I.D.V)

Abstract

Today four oil and gas platforms are being commissioned at the Utsira High area on the Norwegian Continental Shelf. One of the platforms is already powered from shore by a 120MW/+-80 kV high voltage direct current (HVDC) cable. The other platforms are equipped with gas turbines in order to generate their required electric power before a second HVDC-cable rated at 200 MW is connected. Following this, all the platforms will be powered from shore and linked together in a radial grid [1]. The gas turbines will work as backup generators. Connecting floating wind turbines to the platforms could be a way of decreasing emissions from the gas turbines, and/or decreasing the power imported from shore, while at the same time improve the reliability of the system.

The aim of this master thesis is to investigate the possible benefits of including an additional connection between the platforms at the Utsira Hight area and connecting a floating wind farm. Wind speed fluctuations and unpredictable power production may affect the reliability and operation of power systems. The impact of integrating offshore wind to the power system at Utsira High needs to be carefully investigated. Different ways of incorporating wind power in reliability evaluations will be investigated and compared. The study consists of a generation adequacy analysis and a composite generation and transmission reliability analysis.

In this thesis, two different connecting schemes and two different generation options have been studied, creating four different cases for the composite generation and transmission reliability study.

Base Case: Radial grid, no connected wind power
Case 1: Radial grid, 60 MW connected wind power
Case 2: Ring grid, no connected wind power
Case 3: Ring grid, 60 MW connected wind power

All the different cases are assumed to have both HVDC connections to shore connected and to have the gas turbines installed. In addition, several analyses have been made on variations of these cases. Among these variations were varying reliability parameters and different load values.

For the generation adequacy analysis, only the generation system is studied, and the transmission system is neglected. The simplified system models in the generation system adequacy consist of the installed generating units (three gas turbine generators and two HVDC-connections to shore) and the total system load. Hence the different composite cases, the Base Case, Case 1, 2, and 3 are not studied in the generation adequacy analysis. In this thesis, the generation system adequacy is studied with and without 60 MW wind power, with different system load values, different reliability parameters for the wind turbines, and different methodologies to model the wind farm.

For the generation reliability analysis, a tool was developed in MatLab to analytically calculate the reliability indices for different input. Wind was modelled using different methodologies, incorporating technical unavailability (forced outage rate) of each wind turbine as well as unavailability due to the wind speed. Varying reliability parameters were used and compared to see the impact of the technical availability of wind turbines. For the composite generation and transmission system reliability analysis, Matlab and Microsoft Excel was used to build a mathematical model of the system and calculate the reliability indices using an analytical method.

By performing several reliability analyses and considering the actual production from the generating units and the different power demands, the amount of energy that is not served has been calculated for the different cases and for the generation systems.

Based on the analyses performed on the different cases in the composite analysis, it is fair to conclude that adding wind power has a larger impact on the reliability compared to the impact from creating a ring grid. The results yielded by the analyses show that Case 3 is the best option among the four when focusing on improved reliability. The improvement from adding both wind power and the extra cable proved to be less than the combined improvement of adding the cable and the wind farm individually, and was almost equal to the improvement from wind alone, hence Case 1 would be a preferable solution. From the generation system analysis, it is clear that the choice of wind model methodology has a larger impact on the reliability compared to the forced outage rate of the wind turbines.

Sammendrag

I dag bygges det fire olje- og gassplattformer på Utsirahøyden. En av plattformene forsynes med strøm fra land via en 120MW/+-80 kV HVDC-kabel. De tre andre plattformene skal forsynes av gassturbiner som er plassert på plattformene før en annen HVDC-kabel på 200 MW blir tilkoblet. Etter tilkoblingen, blir plattformene koblet sammen med AC-kabler i et radialt nettverk, og alle plattformene vil få kraft fra land. Når området er fullt elektrifisert fra land, vil gassturbinene fungere som reservekraft i tider da kraft fra land er utilgjengelig. Tilkobling av flytende vindturbiner kan være en måte å redusere utslippene fra gassturbinene, redusere kraftimporten fra land, og samtidig forbedre systemets pålitelighet.

Målet i denne masteroppgaven er å undersøke de mulige fordelene med å inkludere en ekstra forbindelse mellom plattformene på Utsirahøyden for å danne et ringnett og å koble til en flytende vindmøllepark. Vindhastighetsfluktuasjoner og uforutsigbar kraftproduksjon kan påvirke påliteligheten og driften av et kraftsystem, og effekten av tilkoblingen av vindkraft i dette systemet må undersøkes nøye. Ulike metoder å integrere vindkraft i pålitelighetsevalueringer vil bli undersøkt og sammenlignet. Masteroppgaven består av en pålitelighetsanalyse av produksjonssystemet og av det kombinerte produksjons- og overføringssystemet.

I denne oppgaven er det to ulike nett-topologier og to ulike kraftproduksjonssystemer som undersøkes, dette fører til fire ulike alternativer for den kombinerte analysen.

Base Case: radielt nett, ingen vindkraft tilkoblet systemet
Case 1: radielt nett, 60 MW vindkraft tilkoblet systemet
Case 2: ringnett, ingen vindkraft tilkoblet
Case 3: ringnett, 60 MW vindkraft tilkoblet systemet

I alle de ulike casene er det antatt at begge HVDC-tilkoblingene til land er tilkoblet og alle gassturbinene er installert. I tillegg er det utført flere analyser med varierende parametere for de samme casene. Blant disse variasjonene er det undersøkt ulike pålitelighetsparametere og ulike lastverdier. I pålitelighetsanalysene av produksjonssystemet, er det kun systemet bestå-

ende av genererende enheter og last som er analysert, og selve overføringsnettet med kabler mellom plattformene er neglisjert. Den forenklede systemmodellen i produksjonsanalysen består av de installerte genererende enhetene (tre gassturbiner og to HVDC-tilkoblinger til land) og den totale lasten. Derfor er ikke de ulike casene, Base Case, Case 1, 2, og 3, studert i denne analysen. I denne masteroppgaven er produksjonssystemet studert med og uten 60 MW vindkraft, med ulike lastverder, ulike pålitelighetsparametere, og med ulike metoder å modellere vindkraft i pålitelighetsanalyser på.

For pålitelighetsanalysene for produksjonssystemet ble det utviklet et verktøy i MatLab som analytisk regner ut pålitelighetsindekser for ulik systeminformasjon. Vindkraft er modellert ved bruk av ulike metoder der både teknisk utilgjengelighet og utilgjengelighet av vindkraft grunnet vindhastighet er inkludert. Varierende tekniske pålitelighetsparametere på alle individuelle vindmøller ble brukt for å evaluere påvirkningen av mekaniske feil på påliteligheten til hele systemet. For de kombinerte pålitelighetsanalysene for produksjons- og overføringssystemet ble Matlab og Microsoft Excel brukt til å bygge en matematisk modell av systemet og beregne pålitelighetsindeksene ved hjelp av en analytisk metode.

Ved å utføre pålitelighetsanalyser, ta i betraktning den faktiske produksjonen fra alle de genererende enhetene, og de ulike kraftbehovene ved plattformene, beregnes mengden ikke levert energi for alle de fire casene og for de to ulike produksjonssystemene.

Ved sammenligning av de ulike casene in den kombinerte analysen, kommer det klart frem at å koble til vindkraft til systemet hadde større påvirkning på påliteligheten enn å endre nettet fra et radialnett til et ringnett. Resultatene fra den kombinerte analysen viser at Case 3 er det beste alternativet når man fokuserer på forbedret pålitelighet. Forbedringen fra å koble til både vindkraft og en ekstra kabel (Case 3) viste seg å være mindre enn summen av forbedringen fra å koble til vindkraft og koble til en ekstra kabel individuelt, og er nesten lik forbedringen fra kun vindkraft alene. Dermed kan Case 1 være en gunstig løsning. Fra produksjonssystemanalysen kom det klart frem at valg av vindkraftmodell hadde større påvirkning på pålitelighetsresultatene enn utilgjengeligheten til de individuelle vindturbinene.

Preface

This thesis is the final report of a five-year master degree in electrical power engineering at the Norwegian University of Science and Technology, NTNU. The problem to be studied concerns the electrification project of the Utsira High area.

Studying the potential benefits of connecting wind power to the Utsira High platforms and interconnecting different grid layouts has been both interesting and challenging. The master thesis follows a pre-master thesis project, a specialisation project, in which the generation system adequacy of Utsira High was studied, with and without wind power.

One of the main obstacles that has been encountered is the choice of methodology and simulation software for the analysis. As work was started on the thesis, a lot of effort was put into the understanding of the fundamentals of composite reliability. One of the other main obstacles was the modelling of the wind power. For this thesis, including the technical unavailability of the wind farm was an essential part of the analyses. To do this, methodologies that allow all the wind turbines to be modelled as one generating unit, including both the unavailability due to wind deficiency and technical unavailability of all the wind turbines was utilized. The choice of different modelling methodologies was done based on advice and help from Vijay Vadlamudi.

For the generation system adequacy analyses, both Matlab and PowerFactory can be used. Using Matlab and an analytical methodology to obtain the reliability indices was suitable for the generation adequacy analysis. In addition, the choice of Matlab as the preferred platform was made due to familiarity. Power Factory uses Monte Carlo simulations, making it possible to compare the results from analytical methodologies using contingency enumerations in Matlab and Monte Carlo Simulations. Due to an uncertainty of the methodology in PowerFactory for the composite simulation and the obtained results, this will not be described or used in this thesis. Microsoft Excel was used to process the contingency lists created in Matlab and perform a contingency analysis for the composite cases.

Contents

List of Abbreviations

LOLP	Loss of Load Probability
LOLE	Loss of Load Expectation
FOR	Forced Outage Rate
COPT	Capacity Outage Probability Table
ELCC	Effective Load Carrying Capability
EENS	Expected Energy Not Served
HVDC	High Voltage Direct Current
HVAC	High Voltage Alternating Current
O&G	Oil and Gas
ILCC	Ideal Load Carrying Capability
LOEE	Loss of Energy Expectation
LOEP	Loss of Energy Probability
ENS	Energy Not Served
IC	Installed Capacity
MTTR	Mean Time To Repair
MTTF	Mean Time To Failure
BES	Bulk Electric System
WECS	Wind Energy Conversion System
WTG	Wind Turbine Generator
DAFOR	Derated Adjusted Forced Outage Rate
EFOR	Equivalent Forced Outage Rate
LC	Load Curtailment
NA	Not Applicable
U	Unavailability
A	Availability
MCS	Monte Carlo Simulation
HL-I	Hiarchial Level One (generation)
HL-II	Hiarchial Level Two (generation and transmission)

List of Figures

List of Tables

1 Introduction

1.1 Background and Objective

Today four oil and gas platforms are being commissioned at the Utsira High area on the Norwegian Continental Shelf. One of the platforms is already powered from shore by a 120MW/+-80 kV HVDC cable. The other platforms are equipped with gas turbines in order to generate their required electric power before a second HVDC-cable rated at 200 MW is connected. Following this, all the platforms will be powered from shore and linked together in a radial grid [1]. The gas turbines already placed on the platforms have high emissions and low efficiency compared to onshore power plants and will work as backup generators.

In this thesis, the option of connecting offshore floating wind turbines to the platforms is investigated. There is no current experience with offshore wind connected to oil and gas platforms, but there are plenty of possible benefits as well as challenges and risks. Offshore wind turbines can either be fixed to the ocean floor or have a floating construction. There is more experience with fixed constructions, but due to high water depth at Utsira High, floating constructions should be considered. In Norway, Statoil has a concept for floating offshore wind turbines called Hywind. The demonstration unit was first tested in 2009 with a generator rating of 2.3 MW. This was the first and only operating Norwegian floating wind turbine [2]. A floating wind park, called Hywind Scotland Pilot Park, is planned outside Scotland with generator units rated at 6 MW and a total capacity of 30 MW. The park is planned to be operating within 2017 and this will be the world's first floating wind farm [3].This wind turbines utilized in Hywind Scotland Pilot Park will be used as a basis for wind power calculations at Utsira High.

The objective of this master thesis is to investigate the possible benefits from connecting an offshore wind farm and including an additional connection between the platforms at the Utsira High area. The study consists of a generation adequacy analysis and a composite generation and transmission reliability analysis. The benefits will be measured in increased reliability of the system. In the composite generation and transmission reliability analysis four different cases are studied. In the generation adequacy analysis, the

system is evaluated both with and without the connected wind farm. Different ways of incorporating wind power in the reliability evaluations will be investigated and compared.

1.2 Motivation

Today there is no experience with connecting offshore wind as power supply to offshore oil and gas platforms. A motivation for a reliability study on offshore wind as power supply for oil and gas platforms is to gain understanding of how potential solutions can improve the reliability of the system, and decrease the CO_2-emissions from the backup power supply. By investigating both the generation and the composite system, the impact of different potential solutions can be compared on a wider basis. The impact on the reliability of the system from either improving the grid and/or adding wind power generation can be compared.

Today there is no consensus on how to treat wind power in a composite adequacy evaluation. Wind power cannot be treated the same way as conventional generation in these methods due to its intermittent nature. Considerable work has been done on developing methods for generating capacity adequacy evaluations and reliability assessment of conventional generating systems incorporating wind power. However, these studies focus on generation system reliability, the ability to supply the total system load, not composite system reliability [4]. Relatively little work has been done on the integration of wind power in composite generation and transmission system reliability analysis [4]. A motivation for this thesis is to gain an understanding of how to integrate wind power in a composite generation and transmission system reliability analysis, and how different wind modelling methodologies will affect the results. Finding a methodology to include technical unavailability of wind turbines and the unavailability of the wind resources in order to model the wind farm in both the generating system and the composite system is also a part of the motivation for this thesis.

1.3 Scope of Work

In this thesis, the reliability of the generation system and the composite generation and transmission system of four oil and gas platforms at the Utsira High area are studied. In addition, possible benefits of connecting offshore wind to the system and creating a ring grid are investigated. The study consists of a generation adequacy analysis and a composite generation and transmission reliability analysis. Even though power system reliability is a multifaceted problem, this report focuses on power system adequacy.

For the generation adequacy analysis, the system is studied with and without 60 MW wind power. In the composite analysis, two different connecting schemes and two different generation options have been studied, creating four different cases in the composite reliability analysis.

Base Case: Radial grid, no connected wind power
Case 1: Radial grid, 60 MW connected wind power
Case 2: Ring grid, no connected wind power
Case 3: Ring grid, 60 MW connected wind power

In both the generation and the composite system, the analyses are performed using varying reliability parameters and load levels. In this thesis, the wind is modelled using different methodologies, including technical unavailability of the wind turbine generators (WTG) in order to obtain a more accurate representation of the total unavailability of the wind farm. The different methodologies, multi-state unit models, derated adjusted forced outage rate (DAFOR), and negative load, and the impact from technical failure of WTG are compared and evaluated.

Using PowerFactory the power flow in Case 2 and 3 was simulated, while Matlab and Microsoft Excel was used to build a mathematical model of the system and to calculate the reliability indices using an analytical method. For the conventional generation, the focus is on a two-state model. For the reliability adequacy analysis, analytical methodologies are used to obtain the reliability indices for the composite systems. For the generation adequacy analysis, both analytical methods and Monte Carlo simulations (MCS) are used. In this thesis, Hywind as well as wind data from the Utsira High area is used as a base for the calculation of wind power.

1.4 Relation with the Specialisation Project

This master thesis is a continuation of a specialisation project titled "Reliability study on offshore wind connected to multiple oil and gas platforms" written for NTNU autumn 2016. Some parts of the specialisation project report are reused in this thesis. Data, theory, and background information that are essential for the thesis and are unchanged are reused. This applies to the reliability analysis theory about the generation system adequacy, "Wind Power and Offshore Wind", and parts of the background information, including the sections "The Utsira High Area", "Load Demand", and "Wind Data" under "Background Information and Data".

2 Background Information and Data

2.1 The Utsira High Area

As a basis for the analysis and calculations in this project, the Utsira High area is used. The area consists of four oil and gas deposits, out of which platform 1 is the largest, consisting of multiple platforms linked together as one. This platform is the one closest to the shore and will be supplied directly from land. The other fields vary in size and distance to shore. The approximately distances between the platforms are given in Table 1, found by a map in the status report of the area from 2012 [5]. The planned power solution will be used as a Base Case for the composite generation and transmission reliability study. This is solution is illustrated in Figure 1 and Figure 22, showing the connections between the platforms and the power supply.

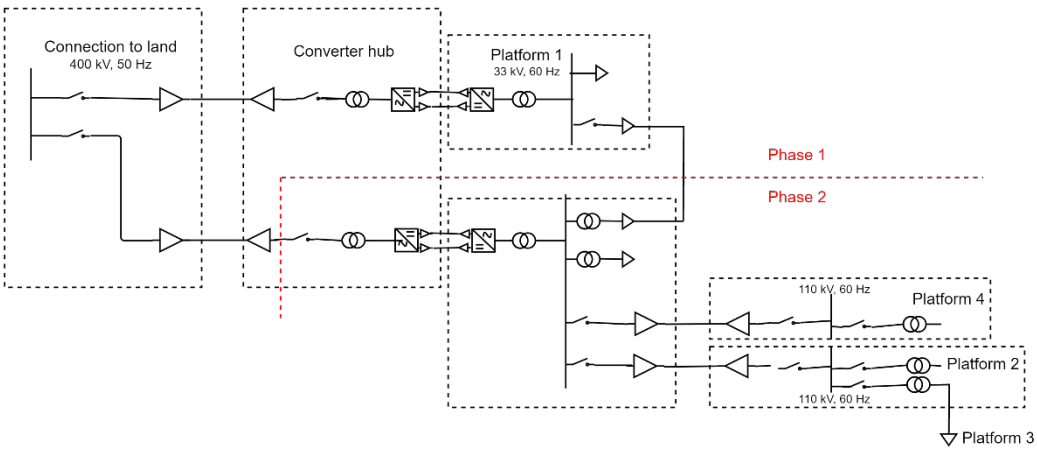

Figure 1: Base Case power solution

Table 1: Distances between platforms given in km

Platforms/Platforms	1	2	3
1	0	13.5	19.8
2	13.5	0	8.1
3	19.8	8.1	0
4	51.3	42.3	47.7

Figure 1 is based on a figure from the report on power solutions for Utsira High [1].Platform 1 will first be powered from a 120MW/+-80 kV HVDC cable from shore, which is expected to be in operation from 2018. The other platforms will be powered by gas turbines before an additional 200 MW

HVDC cable is connected to platform 1. After this installation, all platforms will be fully electrified from shore and inter-connected in a radial grid as illustrated in Figure 1 [1]. The gas generators will only serve as backup generation.

2.2 Different Power Solutions and Layouts

In this thesis, two different connecting schemes and two different generation options have been studied, creating four different cases in the composite analysis.

Base Case: Radial grid, no connected wind power
Case 1: Radial grid, 60 MW connected wind power
Case 2: Ring grid, no connected wind power
Case 3: Ring grid, 60 MW connected wind power

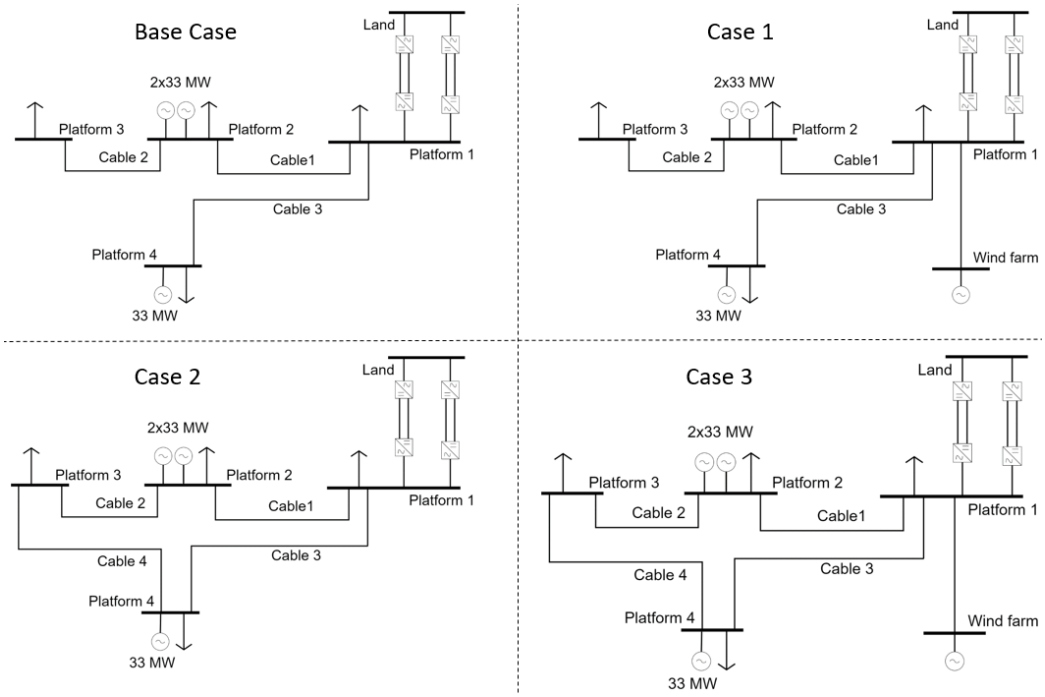

Figure 2: Different Cases for Utsira High area

The Base Case is the planned power solution and configuration of Utsira High, depicted in Figure 22. It consists of two HVDC connections to shore that combined can draw 300 MW and gas turbines on platform 2 and 3 that can serve as backup generation. In Case 1, 60 MW of wind power is added to the Base Case and connected to platform 1 as a power supply for the

whole area. In Case 2, a cable between platform 3 and 4 is connected to the Base Case, creating a ring grid topology. In Case 3, both wind power and the cable is added to the Base Case configuration. For all four cases, both connections from shore to platforms 1 are installed, platform 2 has two gas generators installed and platform 4 has one gas generator installed. The four cases were chosen to be studied to investigate the impact of adding wind power, the impact of strengthening the grid by creating a ring topology, and the impact of both additions to the planned power solution. All four cases are more thoroughly explained and illustrated in section 7.2 Composite Adequacy Test Systems. For the generation adequacy analysis, there are two systems being evaluated, the generation system as planned, with three gas generators and two HVDC-connections to shore, and one system where 60 MW of wind power is added to the planned system. These two generation systems are illustrated and explained in section 7.1 Generation Adequacy Test Systems.

2.3 Load Demand

The total power demand of the whole area was estimated to be approximately 200-250 MW [1]. In later estimates, the peak load of the area is assumed to reach approximately 281 MW in the year 2028 [1, 6-8]. The different platforms have a peak power demand and production at different years. Combined, platform 3 and 4, have an estimated peak demand of 43.6 MW in 2019, and platform 4 is estimated to reach peak power demand in 2023 with 25 MW. Due to the high power demand at platform 1, peaking at 237 MW in 2028, the peak demand for the whole area is at during the peak time of platform 1 [1, 6-8]. Throughout the operational lifetime of the platforms the load demand will increase and decrease. However, the system needs to be rated for the maximum values. Maximum load values also give a worst-case scenario for the reliability analysis, i.e. more pessimistic results and a higher security margin.

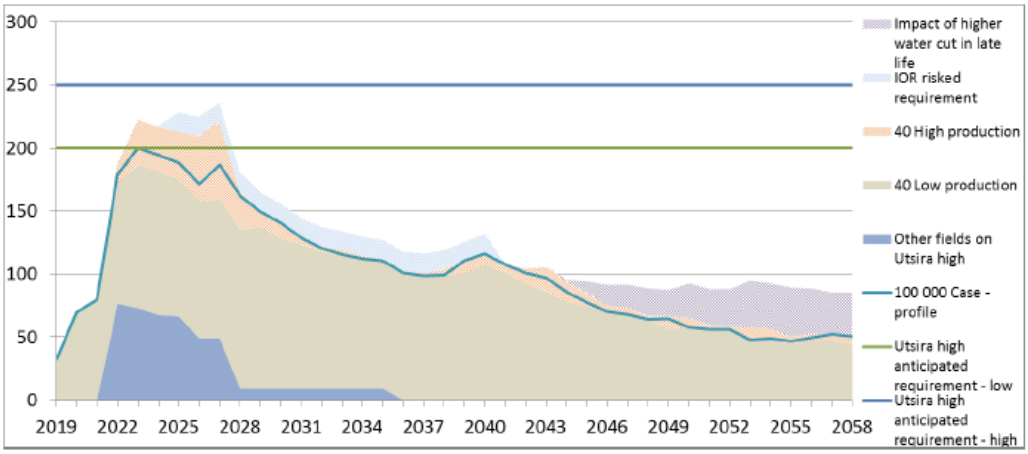

Figure 3: Load profiles [1]

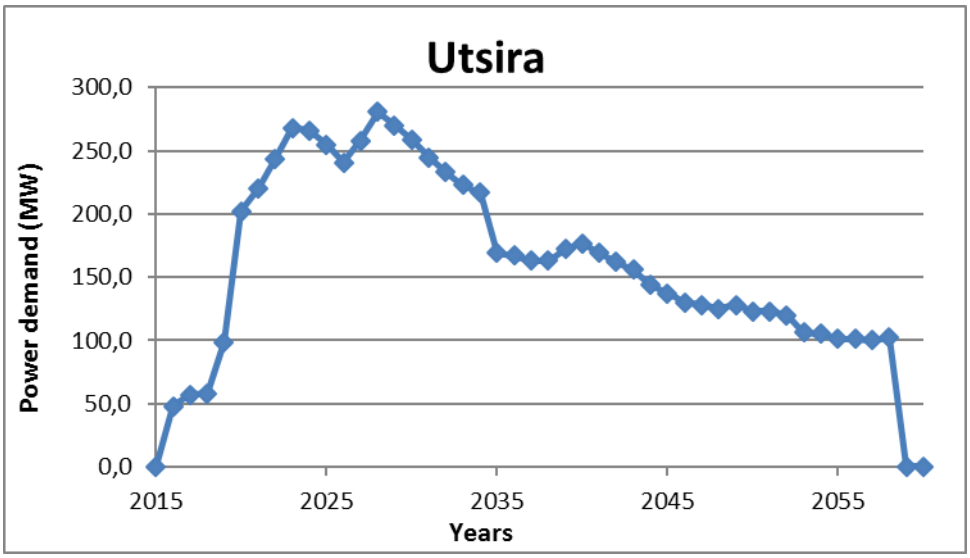

Figure 4: Power demand [1, 6-8]

For more accurate results, an hourly load demand profile is used. For this, a reference platform is used as a base and scaled to fit the load demand for the whole area. These load curves and the hourly load data is the load demand at a reference platform provided by Statoil. As observed from Figure 6, the load is not constant even though the curve is relatively flat at around 70% to 80% of the annual peak. The annual peak value for the reference platform is assumed to be equal to 100%, the load curve can be scaled according to different peak loads. In this thesis, the estimated load values for the platforms and the whole system is assumed to be the annual peak values. The load data from Figure 5 indicates that the platform had five short operation stops, planned or unplanned, over one year.

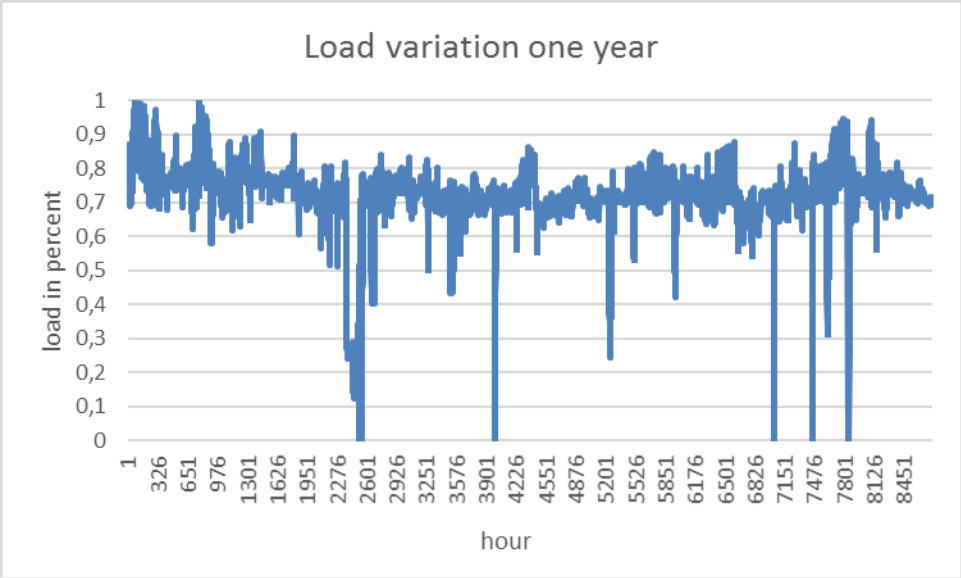

Figure 5: Load variation one year from a reference platform in per unit

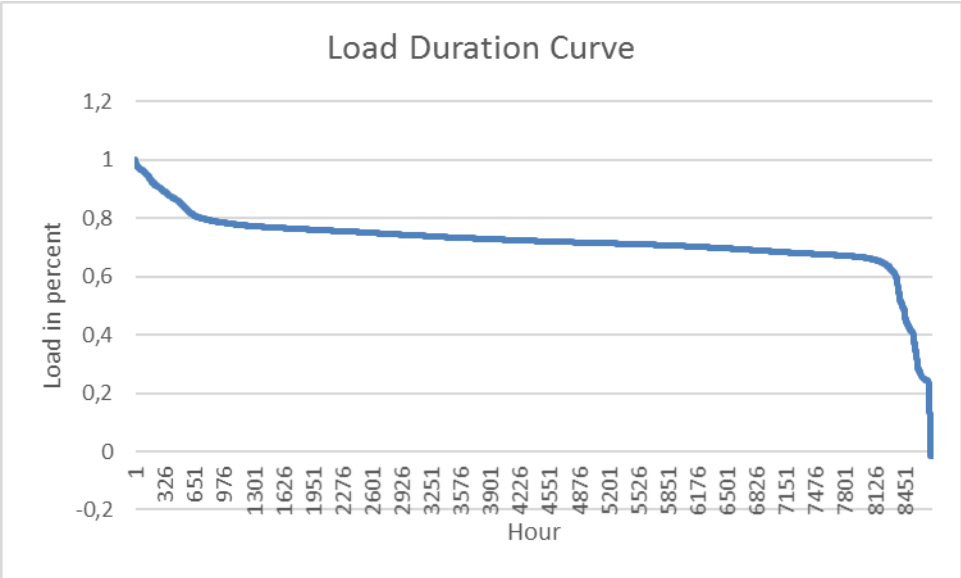

Figure 6: Load duration curve from a reference platform in per unit

2.4 Wind Data

The wind data used in this thesis is from https://www.renewables.ninja/. The website creates output, consisting of wind power, time, and wind speed, based on the type of generator, placement, installed capacity, hub height and time period. The different generators affect the output due to different power curves. Renewables.ninja is used in different scientific papers as a source of wind and solar data. The methodology of the wind speed measurement and output power calculation is thoroughly explained in "Using bias-corrected reanalysis to simulate current and future wind power output" by Staffell and Pfenninger [9]. The program in Renewables.ninja provides hourly data outputs with wind speed, and power output for the specific conditions. There are 8760 data points for one year, correlating with the load data from the reference platform provided by Statoil.

To get a realistic data for the actual energy output, the location chosen for wind measurements and data is the Utsira High area. The generator used to calculate the output power based on the wind measurements is a Siemens SWT 3.6 107. This generator is the closest alternative to the Hywind generator used at the offshore wind farm project Hywind Scotland Pilot Park, a Siemens SWT 6.0 154 [3]. The wind speed is measured approximately at the hub height of the Siemens SWT 6.0 154. The cut-in, nominal and cut-out wind speeds of the two wind turbines are almost the same. The only difference is that for the 6.0 MW turbine nominal power can be produced at 12 m/s as compared to 13 m/s for the 3.6 MW turbine [10, 11]. The power curve of the 6.0 MW turbine, is not available, hence the power curve of the 3.6 MW turbine is used as a basis for the power output calculations. The installed capacity is set to one turbine, and the data series is changed to be in per unit. The per unit can either be per unit of rated power, or per unit of maximum power output. Using per unit based on maximum output, and then scaling it up to the wanted installed capacity removes the losses that are initially in the data. Using per unit of rated power, the losses in the wind turbine generator are included. In this thesis, the losses are included in the wind data to give a more realistic data set. The per unit data is scaled up to the installed capacity of 60 MW (10x6 MW wind turbine generators).

However, one weakness in this data is that the sample is for one year only, treating the output wind power as fixed values and effectively assuming that every year is identical. Using multiple historical data could give a better estimation [12]. Because the program calculates the power output based on the power characteristics of a chosen turbine and measured wind speed, the effect of wind turbine placement and wind wake from other turbines are not considered [12]. Hence, the wind data should be used with reservations regarding the accuracy. In this thesis, the assessments of different methodologies and the benefits from connecting wind power are the main focus areas, and for this purpose, the accuracy of the hourly wind data is less important and thus is neglected.

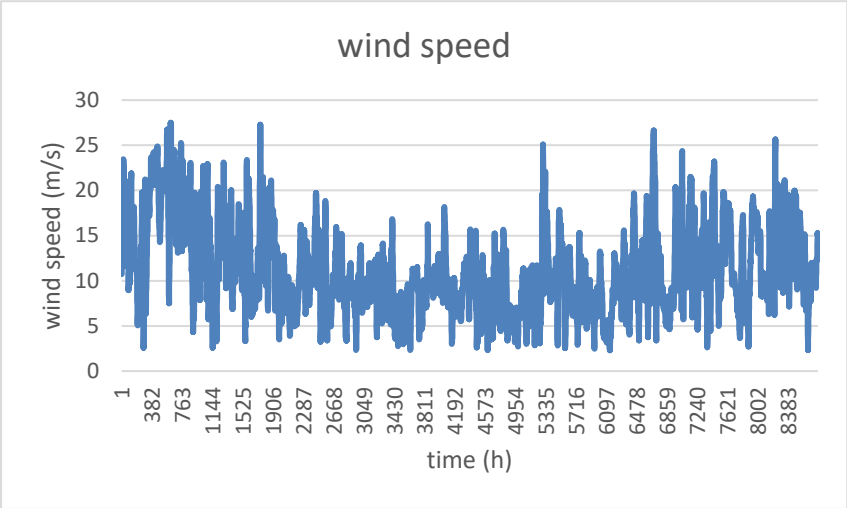

Figure 7: Hourly wind data Utsira High

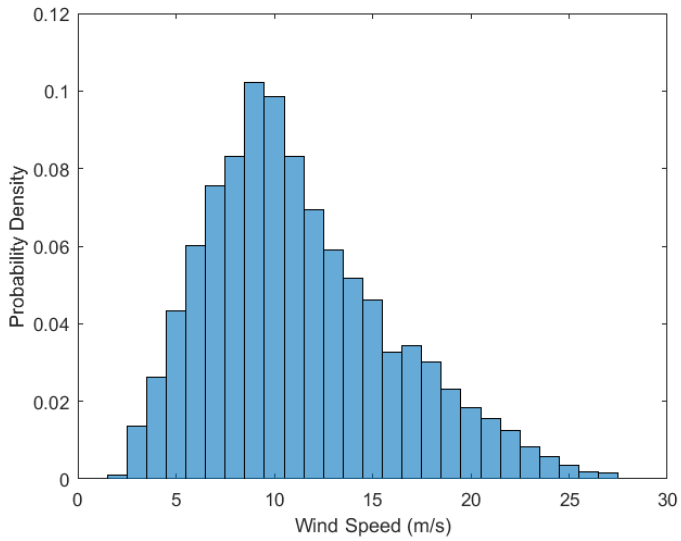

Figure 8: Wind speed probability density Utsira High

3 Wind Power and Offshore Wind

Offshore wind turbines can either be fixed to the ocean floor or have a floating construction. There is more experience with fixed constructions, but due to high water depth at some locations, floating constructions are needed. In Norway, Statoil has a concept for floating offshore wind turbines called Hywind. The demonstration unit was first tested in 2009 with a generator rating of 2.3 MW. This was the first and only operating Norwegian floating wind turbine[2]. A floating wind park, called Hywind Scotland Pilot Park, is planned outside Scotland with generator units rated at 6 MW and a total capacity of 30 MW. The park is planned to be operating within 2017 and this will be the world's first floating wind park [3]. Other floating wind turbine concepts from other companies and countries are Foundation, Windfloat, Hexagon Energy Design and HiPRwind [13].

3.1 Available Wind Power

The power in the wind that hits the wind turbine is given by Equation 3.1 [14]:

$$P = \frac{1}{2}\rho A v^3 \tag{3.1}$$

- ρ is the density of air, that for standard conditions are given as 1.225 kg/m^3
- A is sweeping area of the turbine, given in m^2
- v is the wind velocity given in m/s
- P is the power given in watts

There is a limit of how much power a wind turbine can extract from the wind. The amount of power extracted is determined from by power coefficient, C_p, and the actual power from a turbine is given by Equation 3.2.

$$P = \frac{1}{2}\rho A v^3 C_p(\lambda) \tag{3.2}$$

$$\lambda = \frac{tip\ speed\ of\ the\ blade}{wind\ speed} = \frac{\omega R}{U} \tag{3.3}$$

- R is the radius of the sweeping area or the length of the blade
- ω is the rotational speed in radians/second
- C_p is the power coefficient determined by the tip speed ratio λ
- P is the produced power from the wind turbine, given in watts

The power coefficient can be found using C_p-λ curves, these curves are given from the manufacturer or by turbine testing and modelling [14].

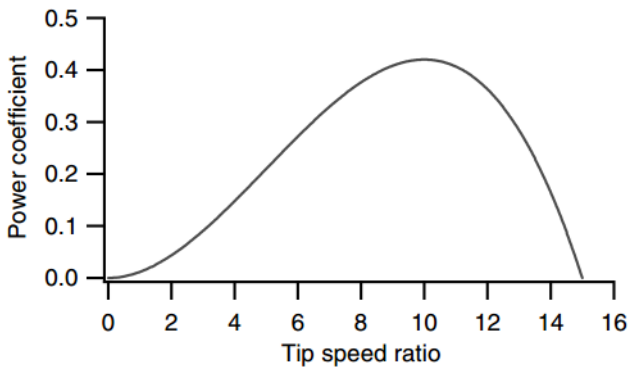

Figure 9: Example Cp-lambda curve [14]

From Betz' law, it is given that the maximum value of the power coefficient is 16/24 = 0.5926 [14]. Hence there is no wind turbine with a higher performance than the Betz' limit. Commercial wind turbines today have a maximum power coefficient between 0.45 and 0.5 [13].

To illustrate how much power a turbine can generate, a power curve is used. This can be seen in Figure 10 and is based on the maximum output of a turbine, and the blades are pitched or controlled in other ways to keep the same maximum power output at wind speeds higher than the rated speed. Turbines usually have a cut-in wind speed at around 3-5 m/s and a cut-out wind speed at around 20-25 m/s, but these values vary and the manufacturers of the turbines provide power curves and specifications. Too high wind speed can cause damage to the turbine. It is protected from high speeds by forcing the blades to stall, causing the wind turbine to stop rotating, decreasing the power output to zero. The rated power of a turbine is the maximum power output under perfect wind conditions and is the flat top part of the power curve seen in Figure 10.

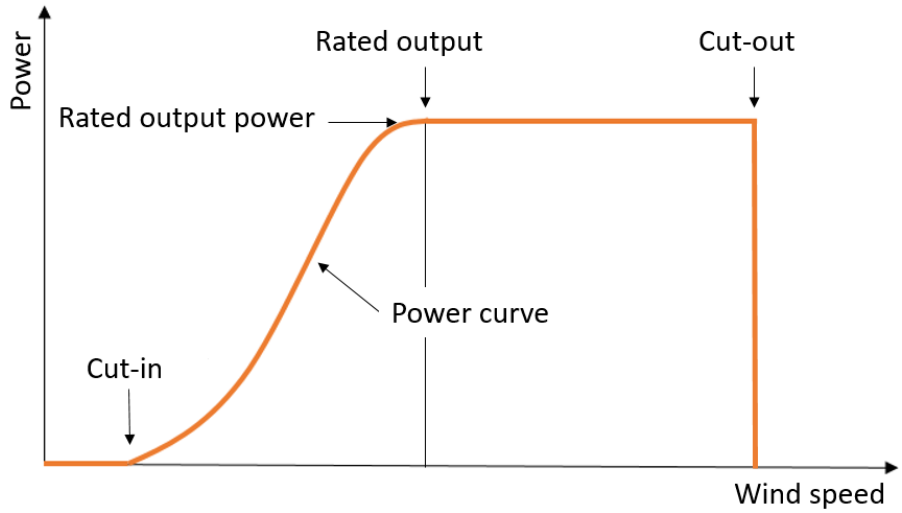

Figure 10: Example power curve

Mathematically the operation of the wind turbine can be explained as follows [15],

$$P = \begin{cases} 0 & v < v_{cut-in} \\ \frac{1}{2}\rho A v^3 C_p(\lambda) & v_{cut-in} \leq v < v_r \\ P_r & v_r \leq v < v_{cut-out} \\ 0 & v \geq v_{cut-out} \end{cases} \tag{3.4}$$

where P_r is the rated output power, v_{cut-in} is the designed cut-in wind speed, $v_{cut-out}$ is the designed cut-out wind speed, and v_r is the rated wind speed [15].

3.2 Statistical Analysis of Wind Data

There are two commonly used probability distributions, the Rayleigh and the Weibull. The Rayleigh distribution only uses the mean wind speed as a parameter, while the Weibull distribution uses two different parameters, and can therefor better represent a wider range of wind regimes. The Weibull probability density function and the cumulative distribution function are as given as [14],

$$p(v) = \left(\frac{k}{c}\right)\left(\frac{v}{c}\right)^{k-1} \exp\left[-\left(\frac{v}{c}\right)^k\right] \tag{3.5}$$

$$F(v) = 1 - \exp\left[-\left(\frac{v}{c}\right)^k\right] \tag{3.6}$$

Where k and c respectively are called the shape factor and the scale factor. Both parameters are based on the mean wind speed, $\bar{v}$, and the standard wind speed deviation, σ_v[14].

$$k = \left(\frac{\sigma_v}{\bar{v}}\right)^{-1.086} \tag{3.7}$$

$$c = \frac{\bar{v}}{\Gamma(1+\frac{1}{k})} \tag{3.8}$$

Equation 3.7 and 3.8 are analytical approximations for the parameters k and c [14].

4 Power System Reliability

4.1 Introduction

To evaluate the possible benefit of connecting a wind farm and interconnecting platform 3 and 4, reliability analyses are performed for the different layout cases. Reliability evaluations of a system are important for the comparison of the probability of load curtailment and investment cost [16]. This part of the thesis is dedicated to discussing reliability evaluation of the whole system and present the chosen methodology.

Power system reliability can be split into two parts, power system adequacy and power system security. In this context, security is the system's ability to respond to both transient and dynamic contingencies or other disturbances, relating to the robustness of the system. Power system adequacy will be the focus area is this thesis. It covers the planned and unplanned outages of the system components, while still able to supply the load demand at all times. Adequacy studies do not include transient or dynamic disturbances [17, 18]. Adequacy can be split into three different hierarchical levels, HL-I: Generation, HL-II: Generation and transmission, and HL-III: Generation, transmission, and distribution. In this thesis, HL-I and HL-II are studied.

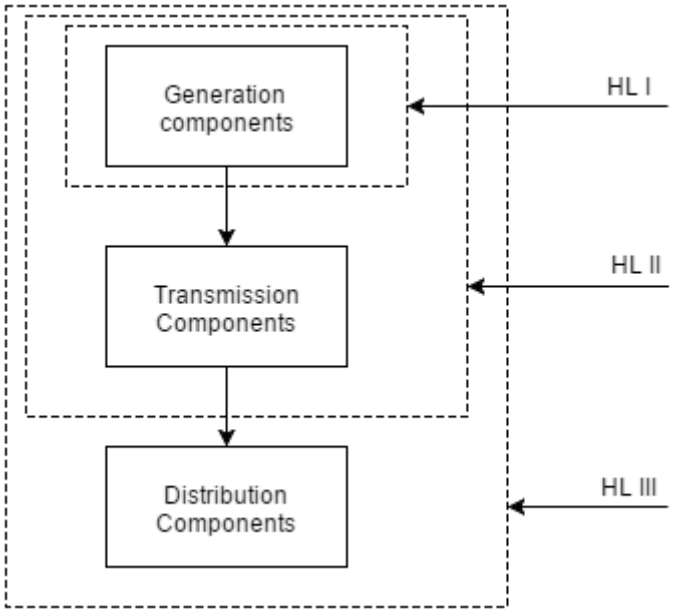

Figure 11: Hierchial levels in adequacy analysis [12]

4.2 Adequacy Assessment of Generation Systems

4.2.1 Theory

In this section, the focus is on the HL-I: Generation. To evaluate the adequacy of a system, a generation capacity model and a load model must be constructed before convolving the two models into a risk model [12, 17].

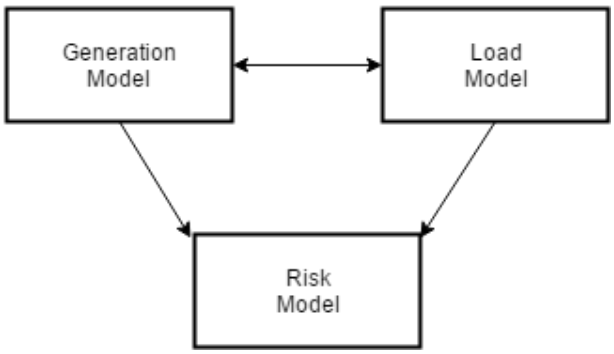

Figure 12: Conceptual tasks in HL-I evaluation [12]

The load model for the generation adequacy evaluation is based on estimated values of the total power demand of all four platforms. Both high and low estimates with constant and varying loads are used. In a HL-I analysis, the transmission system is neglected and the system can be simplified into the model depicted in Figure 13. The load model consists of hourly peak values for a full year in per unit and is scaled to the yearly peak load. This model is used for the HL-I analysis. The same load model is used for HL-II adequacy evaluations, but here the load is considered to be constant throughout the year.

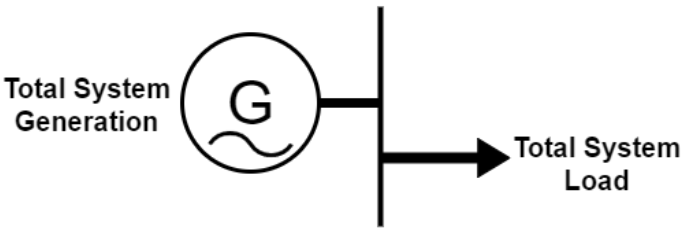

Figure 13: Generation load model [12]

In this thesis, only the two-state generation model is used for the conventional generation. Each generating unit is assumed to be either fully available (Up) or out of service (Down). No derated state, i.e.where a generating

unit work at 50% capacity or another capacity between 0% and 100%, is considered for the conventional generators. The two-state model is illustrated in Figure 14 where λ is the expected failure rate and μ is the expected repair rate [19].

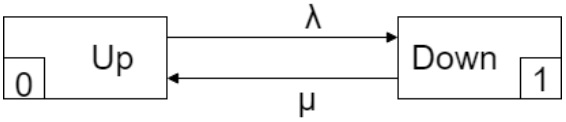

Figure 14: Two-state model

Availability of a component is the probability that the component is in the up-state, and unavailability is the probability that the component is in the down-state. If the forced outage rate (FOR) or the unavailability (U) of a component is not given, it can be computed using the expected failure rate and expected repair rate [16]. The availability (A) of a component is equals 1-U.

$$U = FOR = \frac{\lambda}{\mu + \lambda} = \frac{r}{m + r} \tag{4.1}$$

$$A = \frac{\mu}{\mu + \lambda} = \frac{m}{m + r} \tag{4.2}$$

- λ is the expected failure rate or number of failure per year (1/yr)
- μ is the expected repair rate
- m is the MTTR (mean time to repair) = 1/ λ
- r is the MTTF (mean time to failure) = 1/ μ

These indices can be used for generation units, but also for other components like circuit breakers, subsea cables, and other components in the system. These indices are also used for the composite generation and transmission analysis (HL-II) [16].

The capacity outage probability table (COPT) is a table containing the different outage states of the system, with the individual and cumulative

probability of each state. The COPT is used as a generator model in adequacy analyses. Each state equals the amount of available and unavailable generation capacity in the system. The cumulative probability is the probability that the capacity outage is larger than the outage of the state in question, and is described mathematically in Equation 4.4. The COPT for a simple system is presented in Table 2. The system consists of three generators with a rating of 1 MW, 2 MW, and 5 MW, and with the same unavailability, U, and thus the same availability, A. This system is not directly related to this thesis, but used as an example of how the COPT is constructed.

Table 2: Example COPT

Capacity outage State	Available Capacity	Capacity Outage, C_k	State Probability, $f_y(y)$	Cumulative Probability. $F_Y(y)$
1	8	0	AAA	UAA+AUA+UUA+AAU+UAU+AUU+UUU
2	7	1	UAA	AUA+UUA+AAU+UAU+AUU+UUU
3	6	2	AUA	UUA+AAU+UAU+AUU+UUU
4	5	3	UUA	AAU+UAU+AUU+UUU
5	3	5	AAU	UAU+AUU+UUU
6	2	6	UAU	AUU+UUU
7	1	7	AUU	UUU
8	0	8	UUU	0

The COPT include the capacity that is available in the system, the capacity outage, the individual probability for each state and the cumulative probability. The different states are all the possible operating states, different combinations of generating units that are either functioning or not functioning [17]. In the COPT, the contingencies and whether generation units are in the up- or down-state, are considered as independent events. A fault in one generator is considered as an independent event, and will not cause faults or increase the probability of a fault in another generator due to for example overloading. The state probability is the probability of the combination of operating states. For example, in capacity outage state 1 in Table 2, all three generators are in up-state, such that the state probability equals the up-state probability (the availability) for each generator multiplied by

each other. The capacity outage state probability is given by statistic mathematical formula for independent events, where the capacity outage state 1 probability can be mathematically explained as:

$$\begin{aligned} P(Gen1\ up\ \cap Gen2\ up\ \cap Gen3\ up) \\ &= P(Gen1\ up) * P(Gen2\ up) * P(Gen3\ up) \\ &= AAA \end{aligned} \tag{4.3}$$

The cumulative probability is the probability that the capacity outage (C_k) is larger than the specific outage capacity for that state. This can be calculated as the sum of all the other probabilities for states with a larger capacity outage, as mathematically described in Equation 4.4 [20].

$$F_Y(y) = P(Y > y) = \sum_{y_j > y} f_y(y_j) \tag{4.4}$$

- $F_Y(y)$ is the cumulative probability for a specific outage state, y
- $f_y(y)$ is the probability for a specific outage state, y
- P is probability
- y is the state outage
- Y is the capacity outage

There are different adequacy indices used in reliability analyses. The loss of load probability (LOLP) is a basic risk index, reflecting the probability of losing load at a given time interval, but not the amount of load that is lost. It is the probability that the available generation at a specific time is less than the load demand at the same time. The loss of load expectation (LOLE), is given in days per year or hours per year, i.e. the amount of expected time where the generation is not sufficient to supply the demand [17, 21]. LOLE gives the same reliability information about a system as LOLP, but is the sum of LOLP over the time interval and thus returns time units. The basic risk model includes both the LOLP and LOLE [12, 17].

The loss of load probability (LOLP) is given as the probability that the capacity outage (C_k) is larger than the reserve capacity. The reserve capacity

is the installed capacity (IC) minus the load demand (d). Hence the loss of generation is larger than the reserve generation, causing a loss of load [20]. This can be described as:

$$LOLP(d) = P(C_k > (IC - d)) \tag{4.5}$$

- d is the load demand
- IC is the installed capacity
- P is the probability
- LOLP(d) is the loss of load probability at load demand d
- C_k is the capacity outage

Using the simple system from above and a load demand of 2 MW, the maximum allowable outage would be 6 MW. Outages larger than 6 MW will cause a loss of load. Hence, in order to find the loss of load probability, the COPT is used as a look-up table to find the probability for outages larger than 6 MW. In the simple system above, the probability for outages larger than 6 MW is the cumulative probability equal to AUU+UUU. Further, the loss of load expectation (LOLE) can be computed. This is usually given in days/year or hours/year. Using a load model with hourly peak load is used, the LOLE can be expressed as[20]:

$$LOLE = \sum_{t=1}^{8760} LOLP(d(t)) \tag{4.6}$$

- d(t) is the load demand at time t
- LOLP(d) is the loss of load probability at load demand d
- t is the time in hours, out of 8760 hours in one year

For a constant peak load curve, the system will fail to meet its peak demand if the capacity outage is greater than the reserve capacity. The reserve capacity is the difference between the installed capacity and the load demand[22]. A normal LOLE criterion for a power system is 0.1 days in one

year. This is equals 2.4 hours/year or 1 day in 10 years, and usually corresponds by having 15% of reserve installed capacity [17]. This criterion, called the target or goal LOLE, is the specified risk value of the system [23].

There are also other reliability indices that not only reflects the probability or frequency of losing the load, but also the severity of the incident. Loss of energy expectation and loss of energy probability (LOEE/LOEP), and expected energy not served (EENS) are such indices. The latter reflects the amount of load lost and the duration. For reliability analyses, both basic risk indices such as LOLE/LOLP, and severity based indices such as EENS should be included to give a detailed description on the reliability of the system [17].

Table 3: Overview of adequacy indices

Index type	Symbol	Explanation
Risk indices	LOLE	Loss of Load Expectation (hours/year)
	LOLP	Loss of Load Probability (%)
	U	Unavailability (%)
	A	Availability (%)
Severity indices		
	LOEE	Loss of Energy Expectation (kWh)
	LOEP	Loss of Energy Probability (%)
	EENS	Expected Energy Not Served (kWh)

The EENS is found by using different capacity outage states in the capacity outage probability table (COPT), checking the difference between supply and demand for each hour. If the available generating capacity is insufficient to supply the load demand, the load difference in that hour is added to the ENS, energy not served, for that state. After going through all hours in one year, comparing the load and available generation for one state, the total ENS for that state is multiplied by the individual state probability found in the COPT. This is then repeated for all remaining capacity outage states. After this is done for all states, the ENS values are added together, resulting in the EENS. This is described mathematically in Equation 4.7 [17].

$$\begin{aligned} EENS = \sum & (Probability\ of\ capacity\ outage\ state) \\ & \times (ENS\ due\ to\ capacity\ outage\ state) \end{aligned} \tag{4.7}$$

4.2.2 Adequacy Assessment of Generation Systems Containing Wind Capacity

In the specialisation project, only the generation system was considered. Here the method of choice was finding the effective load carrying capability (ELCC) of the wind farm connected to the system. The ELCC is a measure of the capacity value of renewable power generation. It is used as the standard measure in evaluating the contribution of the intermittent generation, providing the additional load to the system while keeping the same loss of load expectation (LOLE) level of the system [12, 21]. The ELCC of the wind power generation is computed by using the capacity outage probability table (COPT) of the power system together with an hourly load duration curve and time series of wind power output.

In the calculation of ELCC, the wind power is treated as negative load, assuming that the wind turbine generators (WTG) there is no mechanical failure or downtime. Using this method, the technical availability of the individual WTG is not considered, and the resulting reliability indices are therefore more optimistic. For this reason, different ways of model wind in power system reliability assessments are studied. The wind power can be modelled as a two-state generating unit with an equivalent forced outage rate based on both wind speed and technical unavailability (DAFOR), and as a multi-state model with several derated states based on the capacity probabilities of the output power of the wind farm. The two-state and multi-state generating unit model of the wind farm can be incorporated in the COPT with the conventional two-state generators, and the adequacy indices can be calculated using the same methodologies. Calculating the EENS and LOLE as systems without wind power explained mathematically in Equation 4.6 and 4.7. The wind model methodologies used in the generation adequacy assessment and in the composite generation and transmission adequacy assessment are explained in the theory section 4.4 Modelling of Wind Power in Adequacy Assessments and in the methodology section 5.1 Wind Power Modelling.

4.3 Adequacy Assessment of Composite Generation and Transmission Systems

4.3.1 Concept of Bulk Electric System Reliability Analysis

In this section, the focus is on the HL-II analysis. HL-II adequacy evaluation is often termed as composite generation and transmission adequacy evaluation or bulk power system reliability evaluation [24]. In power system planning, the determination of the amount of generation capacity necessary to satisfy the system load demand at all times is one of the most basic and important elements. The planning and development of the network to deliver the power generated are equally important. Composite power system reliability analysis provides an assessment of the ability of the generation and transmission system to satisfy the load and energy demands of the overall system and for the major load points. The evaluation of the reliability of composite generation and transmission systems or bulk electric systems (BES) is complex [4].

As of today, there is no general consensus within the electric power industry on how to perform an adequacy analysis on a composite system. Different adequacy indices and method can be implemented, but the most important indices relate to load curtailment [16]. In order to evaluate the ability to meet the load and energy requirements at the major load points and the overall system, both analytical methods or Monte Carlo simulations (MCS) can be used. Analytical methods represent the system by mathematical models and usually involve some form of contingency enumeration. This method frequently requires assumptions to simplify the overall problem and direct numerical analysis is used to derive the reliability indices[4].

One of the common indices in composite systems adequacy analysis is the expected energy not served (EENS). The EENS combines the frequency and magnitude of outages into one single index. To get an evaluation of the adequacy of a BES, both load point indices and system indices are needed. The load point indices provide information for each major load point in the system, while indices provide information on the overall system performance. The different load point indices are dependent on the priority and the load curtailment system due to different load bus priorities in the actual system[4].

4.3.2 Theory

The generation system model used in the composite generation and transmission analysis is the same COPT as used in the generation system reliability analysis. The transmission system model can be created using the same algorithm as for the generation system model. To calculate the LOLP, and other reliability indices, it is critical to know which cable is out. Some outages cause isolation of platforms and may lead load curtailment. One example is platform 3. If cable 2 (C2) is out in the Base Case or Case 1, platform 3 is isolated with no available generation and there will be a load curtailment. Therefore, load point failure needs to be considered, creating a more complex model.

Reliability indices used for composite systems [16]:

$$F_k = \sum F(B_j)(P_{gj} + P_{1j} - P_{gj}P_{1j}) \tag{4.8}$$

$$Q_k = \sum P(B_j)(P_{gj} + P_{1j} - P_{gj}P_{1j}) \tag{4.9}$$

- B_j is an outage state in the transmission network, including the state with zero outages
- P_{gj} is the probability of the generating capacity outage exceeding the reserve capacity
- P_{1j} is the probability of the load at bus K to exceed the maximum load that can be supplied to that bus without failure

For states where the load point has sufficient transmission capacity, P_{gj} is the loss of load probability (LOLP), calculated in the same way as in HL-I. The reserve capacity is the difference between the available generation and the load demand and is the same definition used for LOLP. For a constant load demand, P_{1j} is either 1 or 0. P_{1j} at bus two is the probability of the load at platform 2 exceeding the maximum power that can be supplied to the platform without failure during outage state j. Equations 4.8 and 4.9 consider the generating facility as a single entity and is applicable to radial configurations such as Base Case and Case 1. A more general set of equations applicable to both radial and ring/meshed grid are Equation 4.10 and 4.11.[16]

$$Probability\ of\ failure\ Q_k = \sum P_j P_{Kj} \tag{4.10}$$

$$Frequency\ of\ failure\ F_k = \sum F_j P_{Kj} \tag{4.11}$$

- j is an outage state in the network
- P_j is the probability of existence of outage j
- F_j is the frequency of occurrence of outage j
- P_{Kj} is the probability of the load at bus K exceeding the maximum load that can be supplied to that bus during the outage j

In ring/meshed networks, overloading of cables needs to be considered. This causes P_{Kj} to be equal to one at times where the connection to the load point is overloaded.

$$Expected\ number\ of\ load\ curtailments = \sum_{j \in x,y} F_j \tag{4.12}$$

- $j \in x$ includes all contingencies which result in cable overloads which are alleviated by load curtailment at bus K
- $j \in y$ includes all contingencies which result in an isolation of bus K.

$$Expected\ load\ curtailed = \sum_{j \in x,y} L_{Kj} F_j \tag{4.13}$$

- L_{Kj} is the load not supplied at an isolated bus K due to the contingency j.

The expected loss curtailed is a different way of calculating the loss of load expectation (LOLE) using the frequency of events and amount of load not served instead off the loss of load probability (LOLP).

$$EENS = \sum_{j \in x,y} L_{Kj} P_j \times 8760 \ MWh \tag{4.14}$$

The expected energy not served is the total energy not served at an isolated bus K due to contingency j. Equation 4.14 is applicable to systems with a constant load demand.

$$\begin{aligned} &Expected\ duration\ of\ load\ curtailmant \\ &= \sum_{j \in x,y} P_j \times 8760\ hours \end{aligned} \tag{4.15}$$

Table 4: Overview of reliability indices [25]

Index type	Symbol	Explanation
Primary indices	λ	Number of failures per year (1/yr)
	μ	Number of repairs per year (1/yr)
	MTTR	Mean Time To Repair (h)
	MTTF	Mean Time To Failure (h)
	U	Unavailability (h/yr or %)
Load/Energy-oriented indices		
	EENS	Expected Energy Not Served (kWh/year)
	ELC	Expected Load Curtailment (MW)
	AENS	Average Energy Not Served (kWh)

The calculation methods used for evaluation of the composite generation and transmission systems are taken from Chapter 6 "Composite generation and transmission systems" from "Reliability Evaluation of Power System" by Roy Billington and Ronald N. Allan [16].

4.3.3 Adequacy Assessment of Composite Generation and Transmission Systems Containing Wind Power

Today there is no consensus on how to treat wind power in composite adequacy evaluations. Wind power cannot be treated the same as conventional generation in these methods due to its intermittent nature. Considerable work has been done on developing methods for generating capacity adequacy evaluations and reliability assessment of conventional generating systems

incorporating wind power. But these studies focus on HL-I, the ability to supply the total system load, and not HL-II and BES [4]. Relatively little work has been done on the integration of wind power in composite generation and transmission system reliability analysis [4].

Generation system reliability results for wind power, e.g. ELCC, cannot be directly integrated into composite power systems. Therefore, in order to include the mechanical failure and outages of wind turbines as well as unavailability due to wind speed, other methodologies to model wind power need to be used for the analyses. The wind model methodologies used are explained in the theory section 4.4 Modelling of Wind Power in Adequacy Assessments and in the methodology section 5.1 Wind Power Modelling.

4.4 Modelling of Wind Power in Adequacy Assessments

Wind energy conversion systems (WECS) behave differently compared to conventional generating units. This needs to be considered when modelling and incorporating wind power in adequacy evaluations of both generation systems and composite systems [26]. An applicable model should be able to incorporate the randomness and the intermittent characteristics of the wind speed for any wind unit. Probabilistic reliability techniques are required to model the impacts of wind power on system reliability and adequacy[27].

One of the simplest wind turbine generator (WTG) model is a multi-state capacity outage probability table (COPT) that can portray the variability and the intermittency of the WTG power output[26]. The capacity state probability model of intermittent generation has been developed by Billington and Harrison (1978) and Billington and Allan (1996) for probabilistic reliability evaluation. In this model, wind generation output is dependent on wind turbine outage and wind speed [27]. A multi-state WTG COPT is made by combining the wind speed with the power curve of the WTG unit to calculate the capacity probability of wind power, depicted in Figure 15. The wind speed is measured by collecting hourly mean data and the probability density of the wind is then found for different wind speeds. This is then compared with the power curve of the specific wind turbine, calculating the probability of different power outputs.

In the literature, most methods used to include wind power in reliability assessment assume the wind turbines to have high availability, causing the FOR to have no major effect on the reliability indices. However, these assumptions may not be supported by field statistics and measurements for WTG outage [15]. At a particular geographical site of a wind farm, the power output is dependent on the wind speed and if the WTG are technical available. Therefore both the forced outage rate (FOR), including mechanical failures and scheduled maintenance, and the wind speed need to be considered when realistically representing the output power of WTG [28] [15]. With zero WTG FOR, the multi-state model is based on wind speed probabilities and output. To include outage of one wind turbine, a FOR can be included in the COPT of a single unit by multiplying the availability of the wind turbine with the capacity probability of different derated states and adding the FOR to the down state where the generating unit has zero capacity in. The resulting WTG COPT for one unit and several FOR values can be found in Table 15.

Using multi-state generating unit models will increase the number of generation contingency states and can cause a considerable increase of the computation time. To solve this issue, a derated adjusted forced outage rate (DAFOR) or equivalent forced outage rate (EFOR) is calculated. Using DAFOR in adequacy assessment can give more pessimistic appraisals compared to using multi-state models. The DAFOR of a generating unit is obtained using Equation 4.16 [29, 30].

$$DAFOR = P_{DN} + \sum_{i=1}^{n} \frac{Cap.Curi}{Cap} \times P_{DEi} \tag{4.16}$$

- DAFOR is the derated-adjusted forced outage rate
- P_{DN} is the probability of the generating unit being in the down state (=U)
- Cap.Curi is the curtailed capacity of the generating unit in the ith derated state (MW)
- Cap is the full capacity of the generating unit (MW)
- P_{DEi} is the probability of the generating unit in the ith derated state
- n is the number of generating unit derated states

The derated states in the DAFOR equation is the different states in the multi-state model obtained for the wind farm or wind turbine, illustrated in Figure 15. The calculated DAFOR value is used as a forced outage rate or unavailability for a generating unit representing the wind farm or wind turbine. This can be used as an input in a conventional two-state COPT illustrated in Table 2, where the DAFOR equals U and A equals 1-DAFOR.

4.5 Challenges of Overlapping and Unforeseeable Faults

The different operating states with different contingencies do not take into consideration that different weather events could cause simultaneously outages. In the generation system adequacy assessment, the COPT consider each contingency and outage as independent events. The COPT groups together events that cause the same amount of power outage and adds together the probabilities of the different events. The contingency list of the COPT used in the generation adequacy assessment includes all possible contingencies, including all units being unavailable simultaneously. The contingency enumeration method used in the composite analysis uses the same algorithm as the COPT to list all possible contingencies and the combinations of these. However, the contingencies are not grouped according to the power outage, to be able to separate which generating unit or cable is out. A maximum of two simultaneously contingencies are considered.

5 Methodology

5.1 Wind Power Modelling

One of the wind turbine generator (WTG) model used in this thesis, is a multi-state capacity outage probability table (COPT) that includes both the technical unavailability and the intermittency of the WTG output. For one single WTG unit, or a wind farm with a WTG forced outage rate of 0%, the multi-state model is created by taking the wind speed measured by collecting hourly mean data. The probability density of the wind is then found for different wind speeds and calculating the wind speed probability using Equation 3.5, combining the wind speed probability with the power curve of the WTG, the capacity output and the appurtenant probabilities is calculated. The process of creating the multi-state COPT model for one Hywind wind turbine at Utsira High area is illustrated in Figure 15. The capacity probability of the wind power in Figure 15 and Figure 28 assumes that the wind turbine is available when needed, hence a FOR of 0%. This model can be put into a table with available and unavailable capacity for the wind farm with probabilities for each state, creating a zero FOR multi-state COPT model of the wind farm.

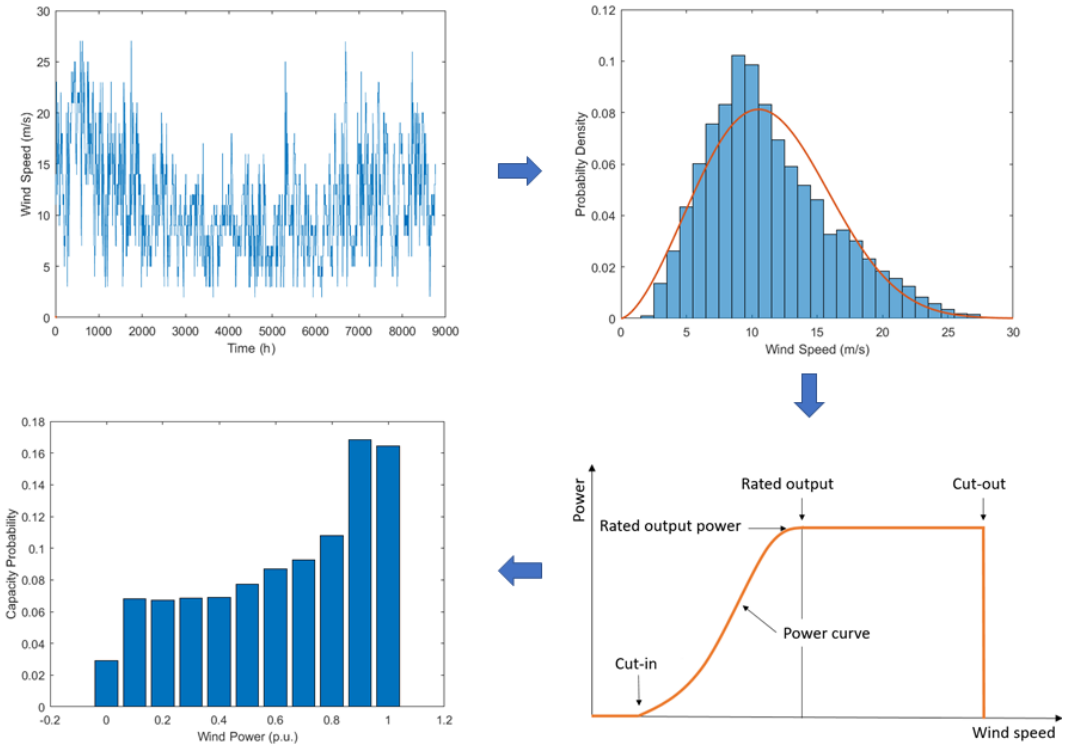

Figure 15: Multi-state model for a wind unit

The capacity probability of the wind power in Figure 15, Figure 28 and Table 11 is only for one unit, but a larger wind farm usually consists of several wind turbine generators. To create a COPT for one complete wind farm with both the wind speed and the individual technical availabilities for the WTG incorporated, the individual multi-state COPT of all units need to be combined into one. For conventional generation, this is straight forward due to independent failures and capacity distribution. For the WTG units, the capacity distribution is highly dependent on each other due to the individual generation output is dependent on the wind speed. When WTG units are placed in one area, the wind speed at each WTG is dependent and almost equal. Because the statistical independence is not satisfied, as it is with conventional generation, the recursive convolution method illustrated in Table 2 cannot be used on the conventional generation to create a COPT consisting of multiple WTG [28].

The basic wind farm multi-state model is the same as that of a single WTG unit as shown in Figure 28 and Figure 15 if the wind farm consists of identical WTG units with zero FOR [26]. To create a multi-state model of the whole wind farm with FOR values higher than zero, both a COPT that represents all possible technical availabilities and capacities and a COPT that represent possible capacities based on wind speed are needed. The COPT based on technical outages is created using the conventional two-state methodology to create a COPT explained in section 4.2, where all the individual wind turbines in the wind farm are included in the model with rated power and the corresponding availability based on the chosen FOR for each turbine. The COPT based on wind speed is created with a FOR of 0%, and is created using the methodology depicted in Figure 15. These COPTs are combined into one COPT with different capacity states and corresponding probabilities based on both the combined technical wind turbine availability for the whole wind farm and the wind energy availability from the wind speed. This is done by creating a matrix with the number of available wind turbines on one side and the available wind power per turbine on the other side, the probability of each combination is calculated using MatLab and the COPT for technical availability and the COPT for wind power availability. The capacity outputs are grouped into power outputs of 6 MW (10% of the installed capacity), and the probabilities of the states that result in the same group output are summarised and put into the multi-

state COPT. This COPT is a multi-state model for the whole wind farm with several derated states. A multi-state model is created for each forced outage rate that are investigated. In this thesis, four multi-state models for the same wind farm is created. The zero FOR multi-state model for the wind farm is the same as the one for one WTG unit only based on wind speed. Further the FOR of 4%, 5% and 10% multi-state models are created using the methodology explained above.

To calculate the adequacy indices in the analyses, the multi-state model of the wind farm need to be combined with the model of the conventional generation in the system. The capacity outage probability table (COPT) with one multi-state generating unit representing the wind farm and several two-state conventional generation is created by using the same principle as when the table only consists of two-state units. The table includes the capacity that is available in the system, the capacity outage, the individual probability for each state and the cumulative probability. The different states are all the possible operating states with different combinations of generating units either functioning, not functioning, or operating in one of the other derated states. Each state in the COPT is made from one or multiple combinations of different generator states that combined supply the same amount of electric power. If only one combination of generator states give one power output, the probability of that state in the COPT equals the combination probability, the probability of each generator operating state multiplied by each other. If more combinations of generator operating states supply the same power, the COPT state probability equals the sum of the combination probabilities. The reliability indices, i.e. LOLE and EENS, of the generation system, can be derived from this COPT and the load data.

As mentioned, using multi-state generating unit models may cause a considerable increase of the computation time. In order to solve this issue, a derated adjusted forced outage rate (DAFOR) is calculated to model the wind farm as a two-state generating unit. The DAFOR of the wind farm is obtained using Equation 4.16 and the multi-state model. The two-state model of the wind farm using DAFOR is added as an input to the COPT the same way as a conventional generator is. The wind farm is added as a generator, with a power rating of 60 MW, an availability (A) equal to 1-DAFOR, and an unavailability (U) equal to DAFOR. The COPT is created using the

conventional methodology with two-state units as explained in section 4.2. From the four different multi-state models, four DAFOR values corresponding to the different FOR values are obtained and studied in this thesis.

5.2 Generation System Adequacy Analysis

5.2.1 Calculating the LOLP and the LOLE

To calculate the LOLP and LOLE, the generation model and load model is used as input to compute the COPT for the system. When wind is modelled as negative load, the hourly wind power is subtracted from the original load demand, and the new load model is used as input. When wind power is modelled as a two-state generating unit. The unit is included in the COPT using the same methodology as for conventional two-state generating units illustrated in Table 2. When the wind power is modelled as a multi-state model, the different wind power capacities are incorporated into the COPT by combining the different combinations that result in operating states with given available capacities and capacity outages. To calculate the loss of load probability (LOLP), the COPT is used as a look-up table for each hour throughout the year to find the probability for outages larger than the load demand at each hour. Further, the loss of load expectation (LOLE) can be computed by summarising the LOLP for the whole year using Equation 4.6.

5.2.2 Calculating the EENS

The EENS is found by using the different capacity outage states in the capacity outage probability table (COPT), checking for each hour the difference between supply and demand, as described mathematically in Equation 4.7. The flowchart in Figure 16 depicts the method of calculating the EENS of a system. It uses some of the same methodologies as calculating the LOLE and is based on the system COPT and load model. A more mathematically flowchart depicting the methodology of obtaining the EENS can be found in Appendix D.

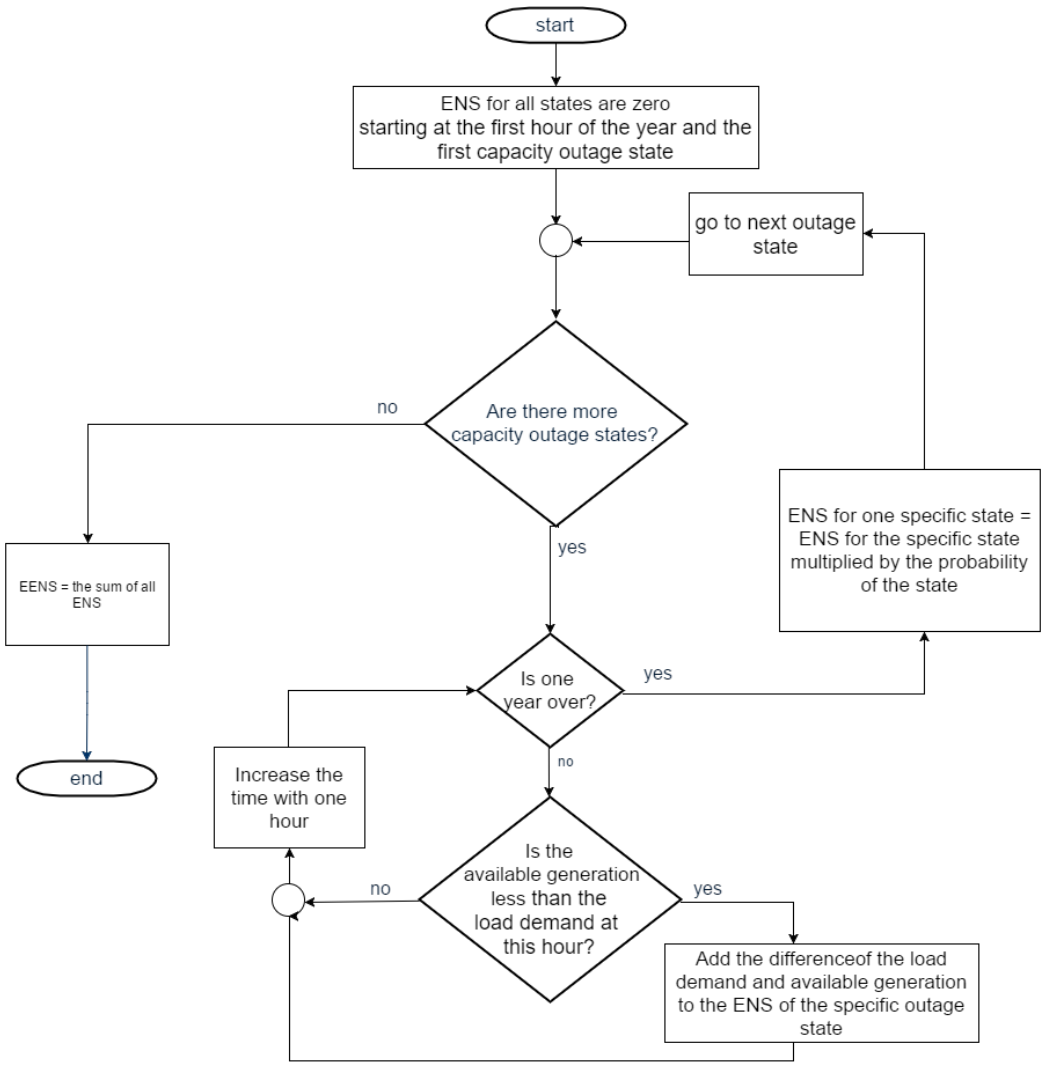

Figure 16: Finding the expected energy not served (EENS)

5.2.3 Calculating the ELCC

The effective load carrying capability (ELCC) is a measure of how much the wind farm contribute to the reliability of the system, and is a derated power rating of the wind farm. The ELCC of the wind power generation is computed by using the COPT of the power system together with hourly load duration curve and time series of wind power output. First, the LOLPs without the contribution of the wind power is calculated by using the COPT of the generation system and hourly load time series. Then, the annual LOLE is computed and compared with the target reliability level. If the calculated LOLE does not meet the target reliability level, the load can be adjusted until it reaches that level. Secondly, the time series of wind power

output is considered as negative load and added to the load time series to get the net load time series. In order to calculate the ELCC the wind power is modelled as negative load and used as an input in the model. The COPT is created by using the installed conventional generation, and the new varying hourly load demand is calculated by subtracting the hourly wind power from the original load demand. A new annual LOLE for the system containing wind is then computed, which will be lower than the former LOLE.

The load time series, both with and without wind power, more and more load is iteratively added for all hours until the LOLE calculated for the increment has reached the target LOLE. The load difference between the two intersection points where the two LOLE curves intersect the target LOLE line is the ideal load carrying capability (ILCC). This is the load carrying capability of the wind power plant if compared to a generator with an availability of 100%. However, because zero FOR is not possible, a different method is used to find the ELCC of the wind power plant.

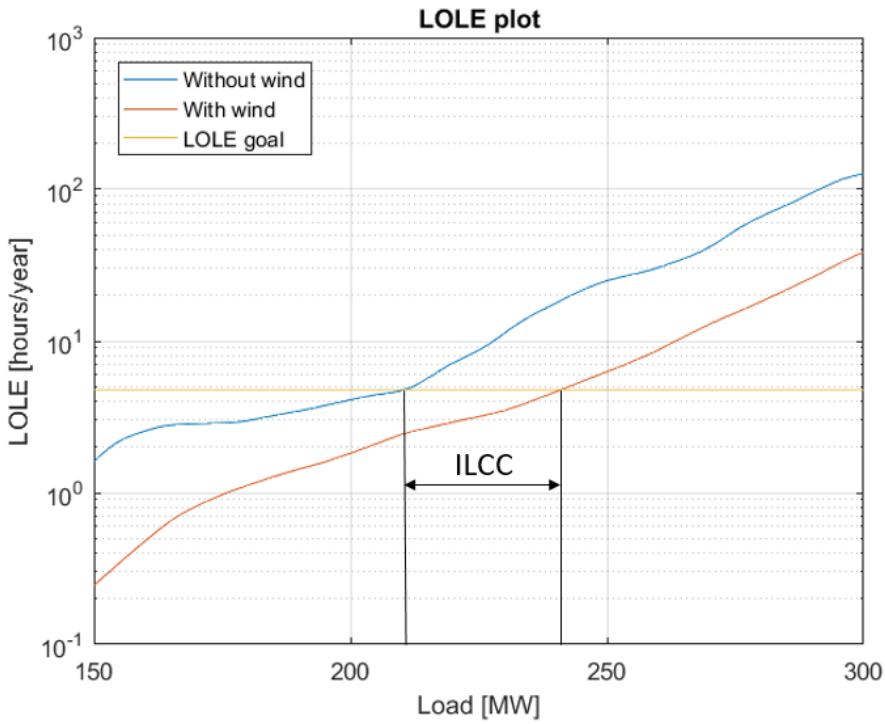

Figure 17: ILCC for the generation system with 50 MW wind

A new generator with the power rating of the obtained ILCC and availability equal to that of the other gas generators in the system is added to the system without wind, adding iteratively more and more power until the LOLE curve with the new generator intersects the target LOLE at the same load level as the system with wind. The total amount of added power from the new gas generator is the ELCC, the derated capacity of the wind power plant [12].

5.2.4 Methodology for the HL-I Analysis of Utsira High

In the HL-I analysis, two different generation models are studied. One with only the planned generation, and one with 60 MW wind power in addition to the planned generation. The planned generation consists of three gas turbines rated at 33 MW and two HVDC-connections to shore that combined can draw a maximum of 300 MW. The HVDC connections are assumed to have some losses, hence the first connection is rated at 100 MW and the second at 180 MW in the model. These two systems are illustrated in 7.1 Generation Adequacy Test Systems.

The system load demand is the same for both models, and is based on a reference platform with hourly load data and scaled to fit the estimated load demand for Utsira High at different years. The wind data input is hourly measures from the Utsira High area, and a more detailed description can be found in section 2.4 Wind Data.

For the model without wind power, a COPT consisting of the five different generating units are computed. And based on the load data and the COPT, EENS and LOLE is calculated for different load levels. The step-by-step methodology used to calculate the LOLE and EENS from a COPT and load data is described in sections 5.2.1 and 5.2.2. These methodologies are applicable to generation systems with or without wind power. With wind power, the analysis becomes more complex due to the intermittent nature of wind. To calculate the adequacy indices of the generation system with wind power, different wind modelling methodologies are used to compare the methodologies and the results. The wind-integrated adequacy analysis is first performed with wind modelled as a negative load to calculate the effective load carrying capability (ELCC) the LOLE values, and the EENS for different load values. The step-by-step methodology of calculating the ELCC

is given in section 5.2.3. This value is used to compare with the results from the specialisation project, to compare with the other methodologies to model a wind farm in generation system adequacy analysis, and to see how much conventional generation the wind farm can replace. The ELCC is then included in the COPT as a gas generator with the ELCC as a power rating and the EENS and LOLE are calculated.

To include the mechanical failure and downtime of the individual wind turbines, the multi-state model of the wind farm with different forced outage rates are computed. Wind turbine generator forced outage rates (WTG FOR) of 0%, 4%, 5%, and 10% are studied, causing four different multi-state models for the wind farm. This is performed as explained in the theory section 4.4 Modelling of Wind Power in Adequacy Assessments and in the methodology section 5.1 Wind Power Modelling. The multi-state model of the wind farm is incorporated into the COPT consisting of the conventional generating units. The other conventional generators are still modelled as two-state generating units, with 100% capacity (up-state) and 0% capacity (down-state), where the availability is the probability for the up-state and the unavailability is the probability for the downstate. The wind farm is modelled with 11 capacity states, from 0% to 100% with increments of 10%, each capacity state with a probability. Due to the multi-state COPT for the wind farm, this causes longer computational time and a high increase the number of operating states. Four different combined conventional generation and wind power COPTs are calculated, based on the four different multi-state wind models. Using these final combined COPTs and the methodology described in section 5.2.1 and 5.2.2 to calculate the LOLE and the EENS.

Following the adequacy analyses with the wind farm as a multi-state model, a two-state wind farm model is investigated. How the wind is modelled as a two-state model is explained in sections 4.4 and 5.1. From the multi-state wind model, the derated adjusted forced outage rate (DAFOR) of the wind farm is calculated, providing four different DAFOR values for the wind farm corresponding to the wind turbine FOR values of 0%, 4%, 5%, and 10%. The two-state model of the wind farm using DAFOR is added as an input to the COPT the same way as a conventional generator is. The wind farm is added as a generator, with a power rating of 60 MW, and an availability equal to 1-DAFOR. Four different COPTs are created, one for each DAFOR

value, to obtain the adequacy results for the different FOR values. The combined COPTs are used to calculate the LOLE values and the EENS, using the same basic methodology that is explained in the theory and in sections 5.2.1 and 5.2.2.

Finally, all these different results with the wind power modelled as negative load, wind power modelled as a multi-state generating unit, and wind power modelled as a two-state generating unit are compared to observe the effect of different FOR values and different wind model methodologies.

5.3 Composite Generation and Transmission System Adequacy Analysis

5.3.1 Methodology for the HL-II Analysis of Utsira High

In a HL-II adequacy evaluation of the system consisting of both generation and transmission, the model is more complex compared to looking at generation and transmission separately. For example, Case 2, consisting of four cables and 5 conventional generating units, is a system with 9 elements resulting in 512 different capacity states in a two-state model. This causes increased calculation time and may make it a necessity to limit the number of states by selecting the contingencies to be included in the model [16]. Events with three or more individual failures are negligible due to the low probability of the events. Due to this, only up to two simultaneously outages are evaluated in this thesis. Hence, only N-1 and N-2 events are included in the HL-II assessment.

If the largest HVDC connection to shore is lost, the power demand is larger than the available power. For this incident, the system would collapse without a protection system. With a smart protection system, parts of the system could be isolated during the event, preventing collapse and provide power to the most important loads. Such a system assumes a priority order for the different load points. Which loads that during a contingency should be prioritised and supplied, and which loads that will be curtailed during the event.

For the analytical assessment of the composite systems in this thesis, Matlab is used to create a contingency list consisting of N-1 and N-2 contingencies

and calculating the state probability for each outage state. To limit the computational time and due to the data acquired only provided a probability for either 100% or 0% available capacity, the two-state model for all generating units and cables, including wind power, is used in the composite assessments. The wind farm is modelled as a two-state generating unit using the DAFOR values as the generator unavailability. How the wind power is modelled as a two-state model is explained in the theory section 4.4 Modelling of Wind Power in Adequacy Assessments and in the methodology section 5.1 Wind Power Modelling. The DAFOR values are calculated using Equation 4.16 and based on the multi-state model obtained for the generation adequacy analysis. The same DAFOR values are also used in the generation system adequacy analysis and the composite generation and transmission reliability analysis. A contingency list is created using the same algorithm as the COPT, but only one or two simultaneously contingencies are included. Contingencies that result in the same capacity outage are not grouped together. The outages are not grouped together in order to be able to separate the consequences of different cables and generating units being out. Microsoft Excel is used to create a spreadsheet to manually insert the resulting load curtailment at the different load points for the different outages. For each contingency, the resulting load curtailment (LC) at each load point is calculated and multiplied by the state probability, P_j, resulting in expected load curtailment (ELC). After all the possible capacity outage states, contingency combinations, the ELC for each load point from all states are summarized to a total ELC for each load point (bus), and Equation 4.14 is used to calculate the EENS at each load point and total for the whole system. In Equation 4.14, the ELC is the $L_{Kj}P_j$. The process is repeated for all the different cases, different load demands and different DAFOR values from the various FOR values of the wind turbines. An extract of the excel sheet for one case and only one load point is found in Apendix B. How the method is performed in the excel sheet is depicted in a flowchart in Appendix F.

The methodology used requires a constant load demand, hence in this thesis, the composite generation and transmission adequacy analysis is only performed with a constant load demand. The load demand at the different load points (platforms) is taken into consideration. Different load demand values are used in the analysis, the estimated load value for the year of 2028 and

2023. The load demand in 2028 is the peak demand for the whole system, in 2023 the load demand is higher at platforms 2, 3 and 4 and with still a high demand at platform 1.

5.4 Cost of energy not served

The price of energy not served in the O&G-sector is high, and a decrease in the expected energy not served (EENS) is money saved. Kvalitetsjusterte Inntektsrammer ved ikke Levert Energi (KILE) is a Norwegian acronym and can be translated to Quality Adjusted Income Framework for Energy Not Served. From the KILE-prices, there is no listed estimated cost of ENS for offshore O&G-installations, but the prices for the gas and refinery section can be used as an indicator. In this thesis, the smallest resolution of load and generation is one hour. Hence the cost estimation of losing load for one hour, 56.9 NOK/kW, is used to compare the different cases [31]. This means a cost of 56900 NOK/MWh. When the EENS decrease from adding wind power or an addition cable to the power system at Utsira High, the production time of the platforms increase, causing higher income. The cost of energy not served is calculated by multiplying the cost of 56900 NOK/MWh with the obtained EENS from the adequacy analysis. KILE-prices and calculating the cost of energy not served can be a way to compare the different cases and the effect of different ways of modelling wind.

6 System Components

6.1 Cables

6.1.1 Cable Data

Table 5: Subsea Cable Ratings [1, 32]

Cable	Type	Rating (MV)	Voltage level (kV)	Length (km)	Comment
1-land	HVDC	120	80	200	planned and built
1-land	HVDC	200	80	200	planned, phase 2
1-2 (C1)	HVAC	75	110	20	planned, phase 2
2-3 (C2)	HVAC	30	110	10	Planned, phase 2
1-4 (C3)	HVAC	30	110	60	planned, phase 2
3-4 (C4)	HVAC	not given	110	60	not planned

6.1.2 Cable Rating

In the Base Case and Case 1, the grid topology is radial and the cables have the planned ratings, enough to supply the peak demand of connected platforms. The power flow in this topology is set. In Case 2 and 3, the grid topology is a ring, and the power flow is dependent on the resistance in cables and demand from the different platforms. In the radial grid, the cable rating could be changed to find the optimal cable cross section.

In the radial grid configurations in Case 2 and 3, two different cable ratings are investigated to see the impact on the composite system reliability indices for the whole system and for the different load points. A high rating of 75 MW for all the cables, enough to power platform 2-4, and a low rating of 30 MW for cable 2-4, (C2-C4) are investigated. Cable 1 (C1) will be rated 75 MW for all configurations. This is clearly shown in the case summery in Table 13.

6.1.3 Cable Type

The subsea cables connecting the platforms are using high voltage alternating current (HVAC) technology due to the shorter distance between the platforms compared to the distance to the shore. With HVAC, there is no need for converter stations at each end, hence saving space and money. The

choice of subsea cables for the Utsira High is not available, thus the choice of cable, including manufacturer, transfer method, conducting material and cable insulation are assumed in this thesis.

For the conductor, there are two commonly used materials; copper and aluminium. Copper has a higher conductivity compared to aluminium, hence aluminium needs a larger cross section to transfer the same amount of power. Aluminium is a less expensive material. For an AC-system, one can use one three-core cable or one three-phase group of single-core cables. There are also different materials and ways of insulating the cables, these have different characteristics and benefits. When it comes to dielectric losses in the insulation of the cable, the losses are lower in XLPE cables compared to fluid-filled cables and EPR cables. The dielectric losses in the XLPE cables should be considered for a system operating at about 100 kV. Other losses in XLPE cable are primarily due to ohmic losses in the conductor and the metallic screen [33].

Figure 18: Single-core cables with lead sheath and wire armour and three-core cables with optic fibers, lead sheath, and wire armour, ABB [33]

For this thesis, XLPE insulated submarine cables with copper conductors are chosen. The cross section depends on the current rating, hence cables with a higher power rating will have a larger cross section. Cross section is chosen based on the XLPE Submarine Cable Systems brochure from ABB [33]. The tables used in this thesis are found in Appendix H.

Based on the power ratings of the cables Table I and Table II in Appendix H, the three-core copper conductor cable cross section should be 300 mm^2. For a single-core cable, 185 mm^2 is sufficient, as seen from Table II. This will

be used in calculating transfer losses in the cables. If the rating of cables is increased, the cross-section might have to be increased as well due to higher currents. There are no data for single core cables and 100 kV. Thus, the chosen cables are three-core cables for calculating power flow and losses.

6.1.4 Cable Transfer Losses

When running a power flow simulation, different losses in the cables need to be considered. An equivalent circuit representing a cable can be observed in Figure 19. The different values for conductor resistance, screen resistance, capacitance and inductance are dependent on the manufacturer, and choice of cable cross-section and length.

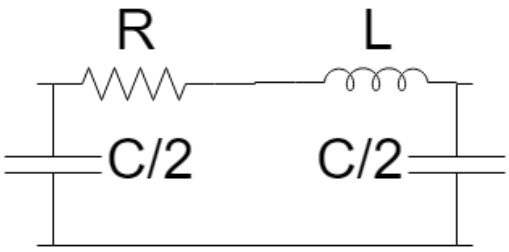

Figure 19: Equivalent circuit for a cable

The data is based on the chosen cables for this thesis. These values are based on Table I, Table II, and Table III in Appendix H. Resistance R is the sum of both the conductor resistance and the screen resistance. The load losses in the XLPE cables are mainly from the ohmic conductor and screen resistance [33].

Table 6: Cable data for power flow analyses, Case 2 and Case 3

Cable	Length (km)	R (ohm/km)	L (mH/km)	C (µF/km)	Power rating (MW)
C1	20	0.10	0.41	0.17	75
C2	10	0.10	0.41	0.17	75/30
C3	60	0.10	0.41	0.17	75/30
C4	60	0.10	0.41	0.17	75/30

Table 7: Cable data for power flow analyses, the Base Case and Case 1

Cable	Length (km)	R (ohm/km)	L (mH/km)	C (µf/km)	Power rating (MW)
C1	20	0.10	0.41	0.17	75
C2	10	0.10	0.46	0.14	30
C3	60	0.10	0.46	0.14	30

6.1.5 Cable Unavailability

From the Cigré report [34] the failure rate of a submarine HVAC XLPE cable is 0.0705 per 100 km per year and have an MTTR (mean time to repair) value of 720 hours. To compare, a submarine HVDC cable has an MTTR of 1368 hours in the same report. It would be reasonable to assume similar repair time of cables. The Cigré report only includes four reported failures for the HVAC XLPE cables, it is therefore assumed that the data basis is insufficient and that the MMTR is equal to that of the HVDC cables [34, 35]. Because of this, the estimated time to repair in this thesis is set to 1368 hours.

Table 8: Cable reliability data

Cable	Length (km)	Failure rate: λ (faults/year)	Repair Time: r hours/fail-ure	Repair rate µ (r/yr)	Unavailability: U
C1	20	0.0141	1368	6.40350877	0.00220191781
C2	10	0.00705	1368	6.40350877	0.0011009589
C3	60	0.0423	1368	6.40350877	0.00660575342
C4	60	0.0423	1368	6.40350877	0.00660575342

The reliability indices of the components, such as failure rate and mean repair time are derived from a collection of data of the components, calculating the statistically mean failure rate and repair time. From these numbers, the unavailability of the component can be found. The availabilities of the offshore cables are high, with less than 1% unavailability throughout the year. Despite the long repair time, the low failure frequency is causing high availability.

6.2 Generating units and power supply

6.2.1 Generation Data and Assumptions

In this thesis, the generation data is not available, hence some assumptions must be made. The assumptions for the planned configuration (the Base Case) are that three gas turbines, two on platform 2 and one on platform 4 will be installed due to platform operations before full electrification from shore. Platform 1 will have one HVDC cable with a rating of 120 MW installed in phase 1 and a second HVDC cable with a rating of approximately 200 MW will be installed in phase 2. In phase 2, all four platforms should be powered from land. The maximum allowable power drawn from the onshore grid is 300 MW. Taking the losses into account, the HVDC cables will have an assumed new derated capacity. These capacity values are presented in Table 9 and are used in the reliability calculations.

Table 9: Power supply from shore and conventional generation

Generation	Capacity (MW)
G1	100
G2	180
G3	33
G4	33
G5	33

In addition, all platforms have small emergency diesel generators installed. Platform 4 has a 1.8 MW diesel generator installed [7]. If the same generator size is assumed for the other platforms, and taking the different load demands into account, six diesel generators can be assumed for the whole system. Platform 1 will be fitted with three diesel generators and the other platforms will have one each. The power contribution from the emergency diesel generators are small, and their main task is to secure the workers and run the most critical equipment. At a large outage, almost all the load at a platform would be curtailed, even if including the emergency generators in the evaluation. For these reasons, and to limit the computational time for both the HL-I and the HL-II assessments, the emergency generators placed on the platforms are neglected in the different cases and in the generation systems.

In the HL-I evaluations from the specialisation project, the system was simulated without backup gas turbines (G3, G4 and G5). This resulted in a less reliable system, even with 50 MW wind power was connected. Due to this and the fact that the gas generators already are installed at the platforms, all cases in this thesis include the backup gas turbines. This is also a motivation for maintaining the gas turbines in good condition.

6.2.2 Gas Turbines

Platform 2 and 4 are fitted with gas turbines type GE LM2500+, each rated 33 MW. Platform 2 has two turbines and is able to supply its own power demand as well as platform 3's in the time before full electrification from shore. Platform 4 is fitted with one gas turbine and is able to supply its own demand [32]. These are considered as backup generators after full electrification from shore, hence all cases evaluated in this thesis assume that the gas turbines are installed.

6.2.3 Wind Turbines

In this thesis, the wind turbines installed is assumed to be the same wind turbines as used in Hywind Scotland Pilot Park, the Siemens SWT 6.0 154, and is the basis for calculating the output wind power [3]. 60 MW (10x6 MW) is the assumed installed wind power capacity at Utsira High. This is the double of the installed capacity at Hywind Scotland Pilot Park [3].

Table 10: Technical Specifications [10]

Turbine Model	SWT-6.0-154
IEC Class	IA
Nominal Power	6,000 kW
Rotor diameter	154 m
Blade length	75 m
Swept area	18,600 m2
Hub height	Site specific
Power regulation	Pitch regulated, variable speed
Cut-in wind speed	3 - 5 m/s
Nominal power at	12 - 14 m/s
Cut-out wind speed	25 m/s
Maximum 3 s gust	70 m/s (IEC version)

6.2.4 Generation Unavailability

From reports [1, 36], it is given that each HVDC power train to land will have a forced outage rate (FOR) of approximately 2.3 non-planned failures per year. Each fault has an estimated duration of 27 hours. In addition, there is one planned day per year for maintenance, but this can coincide with maintenance on platforms. The electric local grid on land is estimated to have a failure rate of 0.3 per year, with only a short duration[36]. This gives an availability for the total HVDC-transfer system, for each cable, of 98.16%[1].

Table 11: Unavailability HVDC power trains [1]

Segment	Frequency per year	Average event down-time (hrs)	Average Production down-time (hrs)	Both power trains unavailable	One power train unavailable
Land grid	0.27	0.13	12.13	0.00 %	
Cable failures	0.016	2190	12		0.40 %
Converter sys-tems	4.66	27	12		1.44 %
Total	4.946	32.53	12.1	0.00 %	1.84 %

As numbers for frequency and average downtime are weighted measures, the total is not the sum of the above numbers. The total unavailability for one powertrain is 1.84%, giving an availability of 98.16%. The availability of each gas turbine on the platforms is provided by the manufacturer, and calculated to be 95.84% [32, 37]. The total failure rate of the HVDC power train, considering it as one single unit, is 4.946 failures/year. The average event downtime gives the total mean time to repair (MTTR) of 32.53 hours. The reason why the repair time is much lower than the cable repair time is due to the shorter repair time of the land grid and converter systems, which have a higher failure frequency than the cable. This gives an expected repair rate, μ, of 269.3 repairs/year.

The HVDC cables are modelled as generators because only the power they supply to the system and their total availability is of importance for the analysis. The total forced outage rate for the "HVDC-generators" includes the availability data for the onshore grid and converters as presented in

Table 11. Hence the whole cable system is included in the FOR, and each HVDC power train can be modelled as a generating unit with one power rating and one availability.

Table 12: Generation availability data [1, 37]

Generating unit	Power rating	Availability	Failure rate: λ (No. faults/year)	Repair Time: r (hours)	Repair frequency μ (r/yr)
HVDC (G1)	100	0.9816	4.946	32.53	269.289886
HVDC (G2)	180	0.9816	4.946	32.53	269.289886
Gas (G3)	33	0.9584	5.4069348	64	136.875
Gas (G4)	33	0.9584	5.4069348	64	136.875
Gas (G5)	33	0.9584	5.4069348	64	136.875

The availability is given for the specific gas turbines that are placed on the platforms, GE LM2500+[37]. Repair time and repair frequency data are taken from Offshore Reliability Data Handbook (OREDA), as these data are not available from GE. OREDA is prepared by SINTEF and distributed by DNV, (now DNV GL) [38]. The repair time data is the mean man-hours needed to repair the units and is based on historical data of installed industrial gas turbines rated 10000-50000 kW. Failure rate and repair time are taken from the critical failures, derated operating states are neglected in this two-state model. The probability for a gas turbine failing to start on demand in critical and failure mode is given to be 0.043 [38].

In this thesis, the technical unavailability of wind turbines (WTG FOR), as well as the unavailability from the intermittent wind speed, will be included in the reliability analysis. The technical unavailability consists of mechanical failure, scheduled maintenance, and other technical downtime. The different models of wind power including WTG FOR is explained in section 4.4 Modelling of Wind Power in Adequacy Assessments and in section 5.1 Wind Power Modelling. Different forced outage rates (FOR) of the individual WTG are used in the assessment to see the consequences of how technical failure of wind turbines in the system reliability. Individual WTG FOR of 0%, 4%, 5% and 10% are investigated. These values are chosen from frequent use of 4% and 5% in other studies [4, 26, 28], and 10% is included to see the effect from high unavailability and is also used in "Wind Models for Large Wind Farms in Generation System Planning" [28]. Finally, 0% is included

to compare the different models with negative load and for comparison within the wind models. Today, WTG FOR are not well defined due to the absence of long operating data. The outage can be caused by electrical and mechanical faults, including failure in the drive train, rotor, nacelle or tower [28].

7 Simulations and Analyses

7.1 Generation Adequacy Test Systems

For the HL-I analysis, the generation system adequacy analysis, the transmission system is neglected and the system can be simplified into the model depicted in Figure 13 and the model at the top of Figure 20. In this thesis, the generation system adequacy is studied with and without wind power, with different system load values and different reliability parameters for the wind farm is in addition, modelled using different methodologies.

7.1.1 Generation System Model Without Wind Power

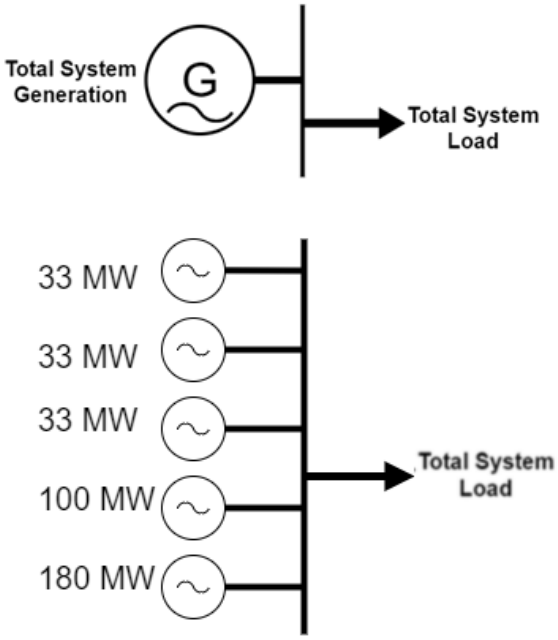

Figure 20: Generation system model without wind power

In the HL-I analysis, the system without wind power can be illustrated as the model depicted at the bottom of Figure 20. Only the total system generation and the total system load is included in the model and the grid topology and how loads and generating units are interconnected are not relevant in a generation system adequacy assessment.

7.1.2 Generation System Model With Wind Power

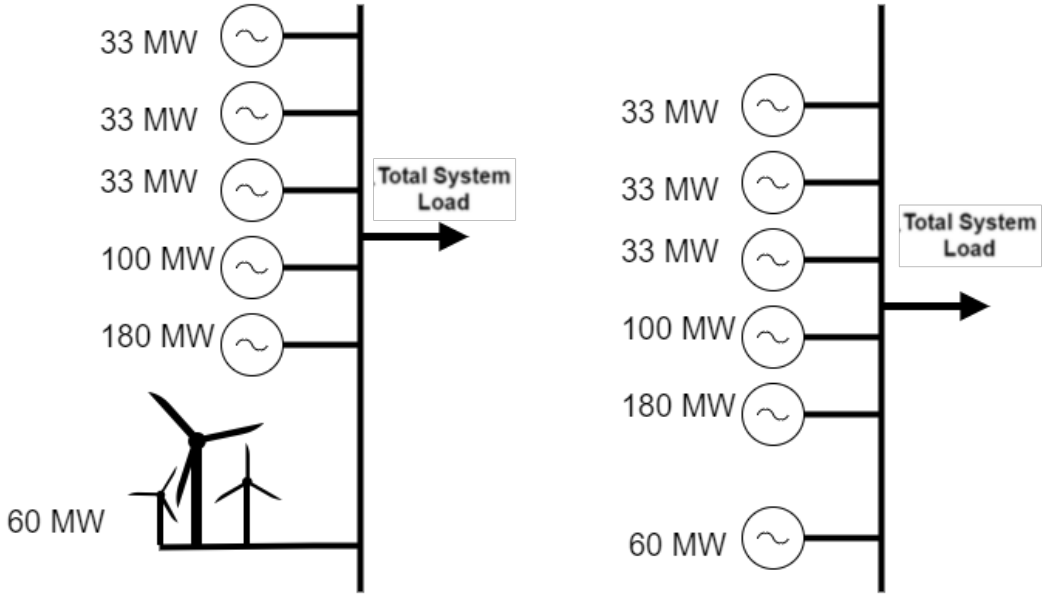

Figure 21: Generation system model with wind power

In the HL-I analysis, the system with wind power can be illustrated as the model depicted in Figure 21. The wind turbines are modelled as one wind farm, i.e. one generating unit. The wind farm "generator" is modelled in the HL-I analysis as a two-state model with different DAFOR as equivalent forced outage rate, and as several multi-state models based on the wind speed and on different individual forced outage rate of the wind turbines.

7.2 Composite Adequacy Test Systems

The Base Case is the planned power solution and configuration of Utsira High. In Case 1, 60 MW of wind power is added to the Base Case and connected to platform 1 as a power supply for the whole area. In Case 2, a cable between platform 3 and 4 is connected to the Base Case, creating a ring grid topology. In Case 3, both wind power and the cable is added to the Base Case configuration. For all four cases, both connections from shore to platforms 1 are installed, platform 2 has two gas generators installed and platform 4 has one gas generator installed.

The connections to shore are modelled in the power system adequacy analysis as generators supplying the area. The generators are modelled with the total reliability of the HVDC cables, including failures in the land grid and conversion system, this is presented in Table 11.

All cases are modelled under different operating states, which includes different load profiles, with different system peak demands and different load distributions between the platforms based on yearly power demand estimations provided by Lundin [1, 6-8].

7.2.1 Base Case

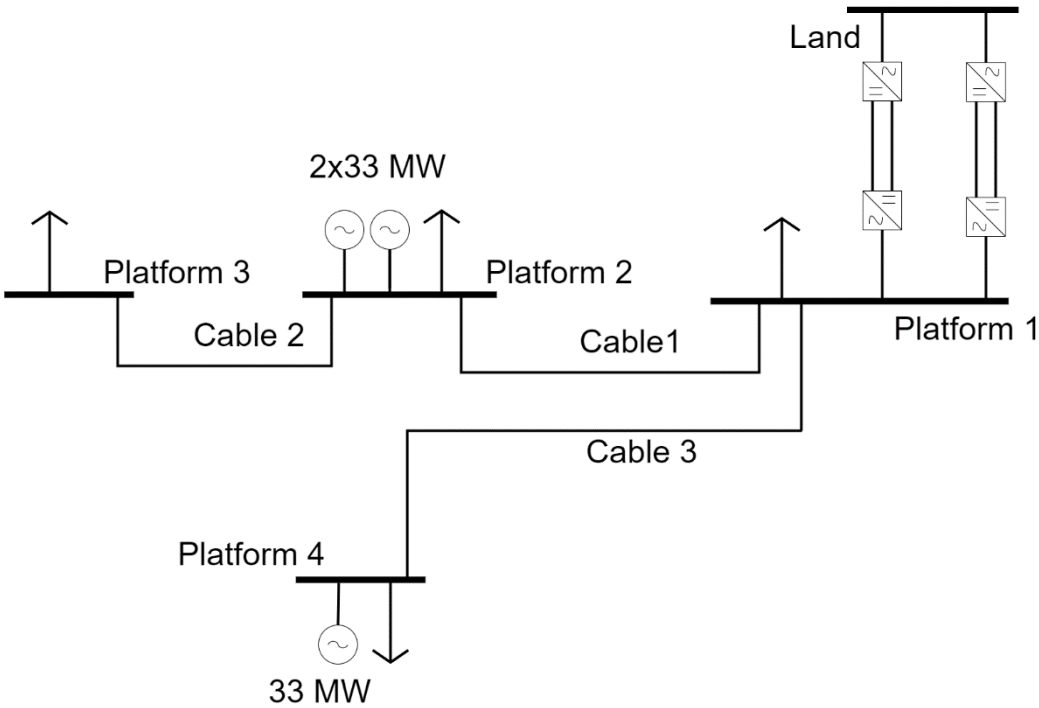

Figure 22: Base Case

Figure 22 illustrates the planned electrification outline of the area with electrification from shore and backup gas turbines. The system consists of two gas turbines on platform 2, one gas turbine on platform 4, and two HVDC connections to shore. The generation data can be found in section 6.2.1 Generation Data and Assumptions. Cable 1 is rated at 75 MW, Cable 2 and 3 are rated at 30 MW. This case is used as a basis to observe the benefits from the additional elements that are included in the other cases.

7.2.2 Case 1

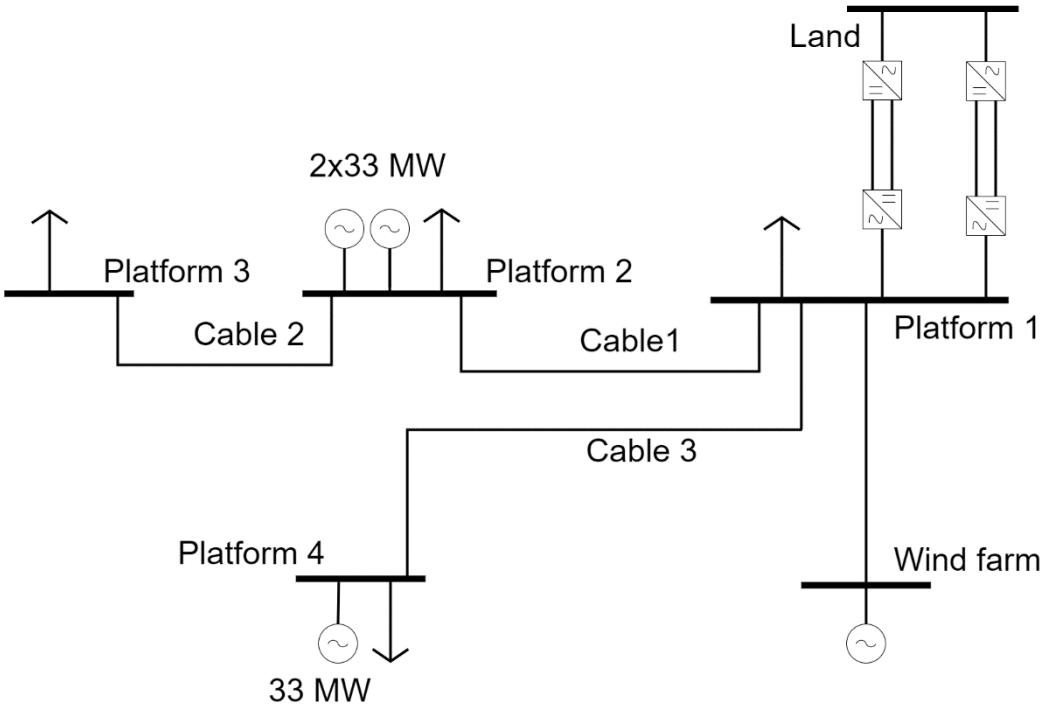

Figure 23: Case 1

Case 1 has the same grid configuration and the same power supply as the Base Case, but with a wind farm as an additional power supply. The wind turbines are modelled as one wind farm (one unit) with one connection to platform 1. The wind power is modelled using the two-state DAFOR model including the technical availability of the wind turbines as well as the power availability from the wind speed. The other generating units are modelled the same way as in the Base Case.

7.2.3 Case 2

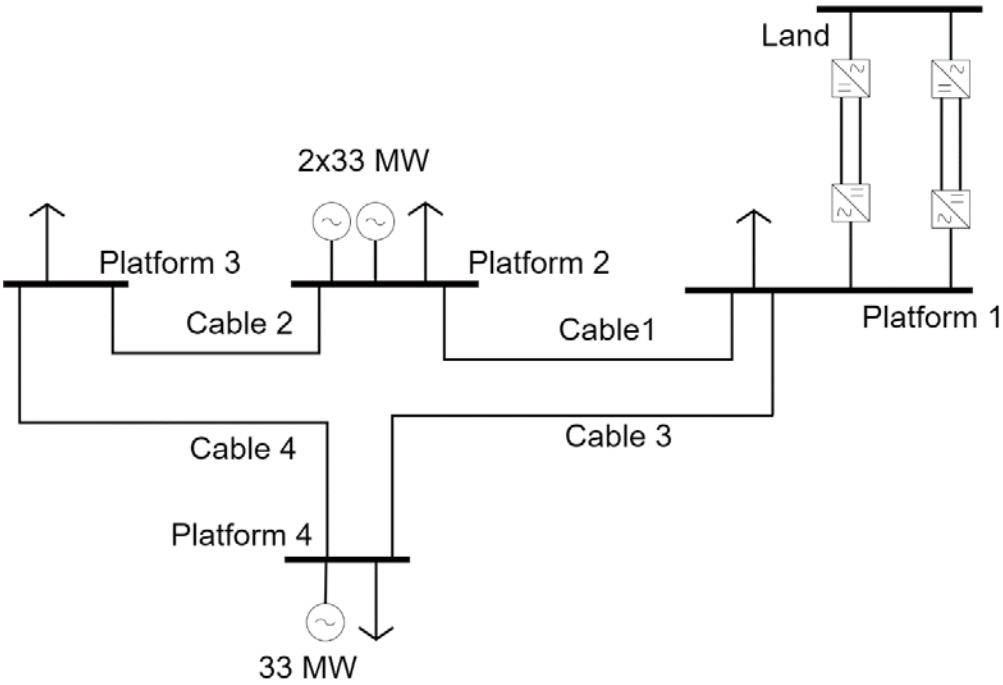

Figure 24: Case 2

Case 2 has the same power supply as the Base Case, but the grid topology is changed to a ring grid configuration. This case is used to study the impact a grid improvement, creating a ring or meshed grid, has on a small system. The impact is studied both on a system level and for the different load points (platforms). The additional cable, cable 4 (C4), will have the same reliability parameters per km as the other cables in the system. The cables are investigated with both high ratings of 75 MW and low ratings of 30 MW. Cable 1 is kept at the planned 75 MW rating for all configurations.

7.2.4 Case 3

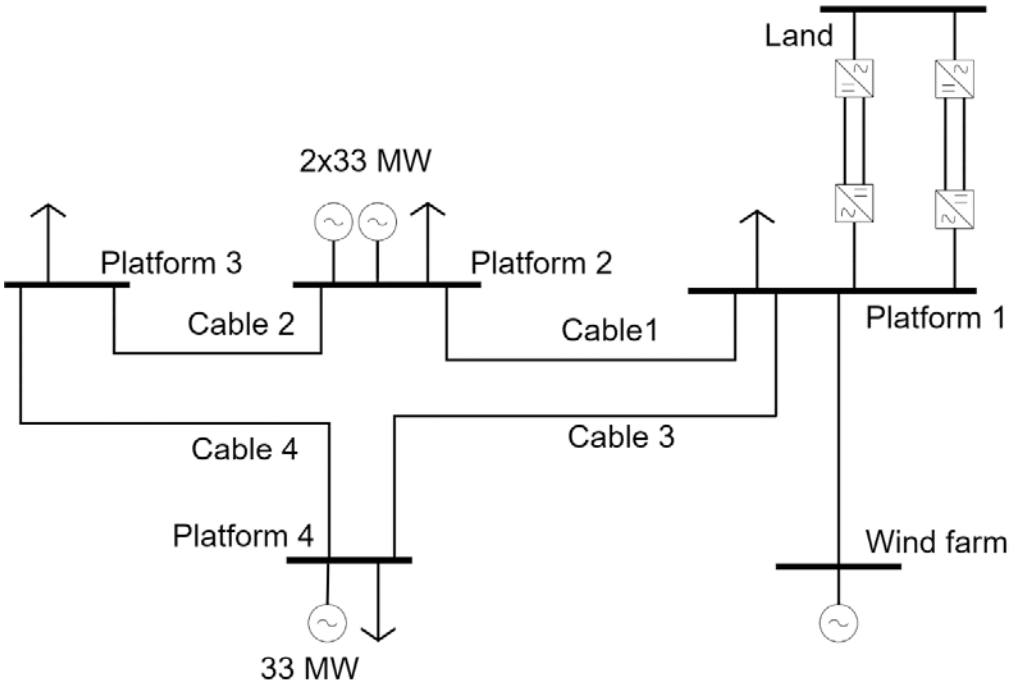

Figure 25: Case 3

Case 3 is the planned configurations with both the wind power and an additional cable added. The different cable ratings will be investigated in Case 3 in the same way as in Case 2, and the wind farm is modelled in the same way in Case 3 as in Case 1. This case is used to investigate how the system is affected by adding both improvements to the system compared to the individual improvements. The effect on the reliability of both the system and the load points is studied.

7.2.5 Composite Case Summary

Table 13: Case Summary

Case	Generation/Power Supply				Grid topolog	Cables	
	Name	Type	Platform	Power Rating		Name	Power Rating
Base case	G1	HVDC	1	100	Radial	C1	75
	G2	HVDC	1	180		C2	30
	G3	Gas	2	33		C3	30
	G4	Gas	2	33			
	G5	Gas	4	33			
Case 1	G1	HVDC	1	100	Radial	C1	75
	G2	HVDC	1	180		C2	30
	G3	Gas	2	33		C3	30
	G4	Gas	2	33			
	G5	Gas	4	33			
	G6	Wind	1	60			
Case 2	G1	HVDC	1	100	Ring	C1	75
	G2	HVDC	1	180		C2	30/75
	G3	Gas	2	33		C3	30/75
	G4	Gas	2	33		C4	30/75
	G5	Gas	4	33			
Case 3	G1	HVDC	1	100	Ring	C1	75
	G2	HVDC	1	180		C2	30/75
	G3	Gas	2	33		C3	30/75
	G4	Gas	2	33		C4	30/75
	G5	Gas	4	33			
	G6	Wind	1	60			

7.3 Assumptions and Simplifications

In both the HL-I and HL-II analyses, several assumptions and simplifications are made. In the analytical composite adequacy assessment, the load level is considered to be constant in order to calculate the load curtailment and expected energy not served. The priority of the different load points (platforms) are not given, and assumed in this thesis. The priority order is from highest to lowest as follows, platform 1, platform 2, platform 4 and platform 3, based on the load demand and production. In the analytical assessment in the composite generation and transmission system, the transfer losses in the cables between the platforms are not considered.

Failure in circuit breakers and other components in the system is not included in this analysis. The effect of these components is neglected to limit

the number of states in the HL-II analysis. The reliability of these components can in later studies be included into the reliability of the cables, as it is done with the HVDC-connections to shore.

The wake effect of the wind turbines and their relative placing to each other is not included. The correlation of wind speed and wind power production is included in all wind power modelling, and it is assumed that if wind power is available for one turbine, it is also available for the neighbouring turbines. Mechanical faults of the turbines are considered as independent events. The effect of bad weather causing multiple simultaneous failures are not taken into consideration in this thesis, and outages are calculated based on the assumption that the events are not connected.

7.4 Input and System Parameters

7.4.1 Load

Table 14: Load Profiles

Year	Power Demand (MW)			
	Utsira	Platform 2 and platform 3	Platform 4	Platform 1
2028	281	33	11	237
2023	268	35	25	208

The year 2028 is peak production year for platform 1. This is also the year with the highest total system demand of the area and the peak demand at platform 1. The other platforms have peak production and demand at other times. The year 2028 is used as a basis worst case for the total power demand. How the load demand is divided between platform 2 and 3 is unknown, and in the composite analysis, the load is assumed to be 11 MW at platform 3 and 22 MW at platform 2 [1, 6-8]. To get a better understanding of how the load variation at different load points affects the total load curtailment in the composite system, different load values are used in the assessment. The load profile of 2023 is the estimated load demands at the platforms in the year 2023. In 2023, the load demand, and hence production, at platform 2 and 3 is high, platform 4 is estimated to operate at peak power demand, and platform 1 has a high and increasing power demand and production. Due to the high total power demand and higher demands at platforms 2-4 compared

to the 2028 load profile, the load profile of the year 2023 is included in the composite adequacy assessments. In the HL-I analysis, the load profile of 2023 is not studied. This is due to the load distribution between the platform is not relevant for the generation system. In the generation system adequacy analysis, only the total system load is considered. Load values lower than the 2028 load value of 281 MW, will give lower EENS and LOLE values and hence higher reliability due to higher reserve capacity. 250 MW and 200 MW is included in the HL-I analysis because of the this is the previous low and high load estimation.

For the composite HL-II analysis the different load values at the platforms are taken as the constant load throughout the year. For the generation HL-I analysis, only the total system load is considered, the different load demand at the platforms are irrelevant. The total system loads for 2028 and 2023 is assumed to be the system peak load and equal to 1 per unit (pu) in the HL-I analysis, the loads follow the hourly variations illustrated in Figure 26. The load variation for one year from the reference platform is assumed to be for the whole system in the generation adequacy analysis.

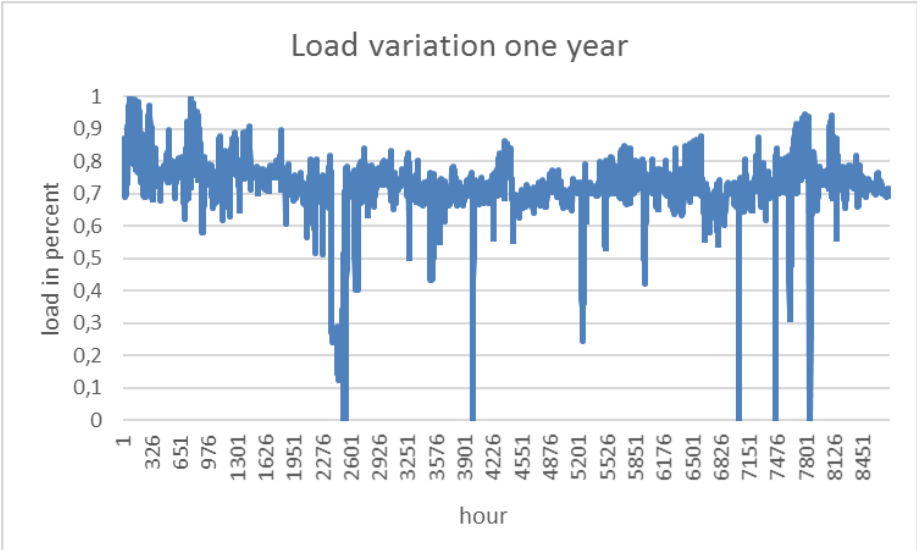

Figure 26: Load from a reference platform

7.4.2 Wind Power

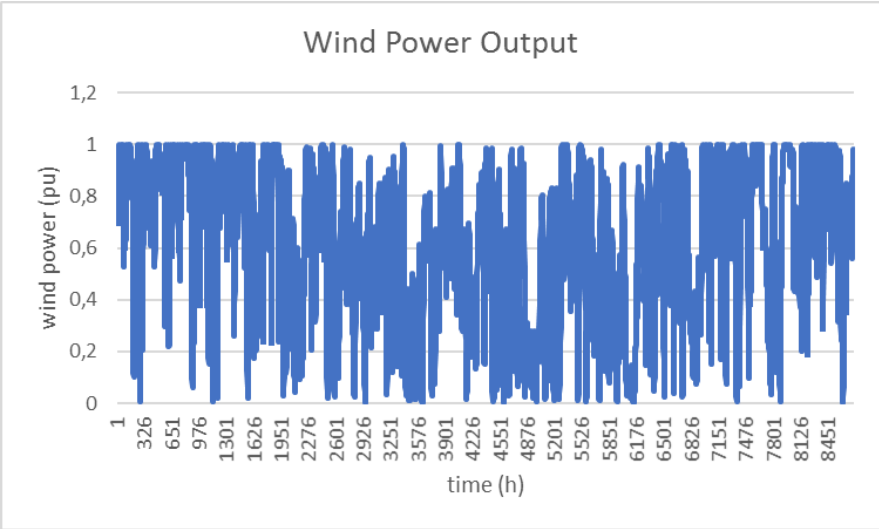

Figure 27: Power output wind turbine in per unit of rated power, one year

Figure 27 illustrates the power output of a wind turbine based on the wind speed data from Utsira High area. This data is used as input for the reliability assessments with wind power as negative load and used for the calculation of the multi-state model and DAFOR representation of the wind farm.

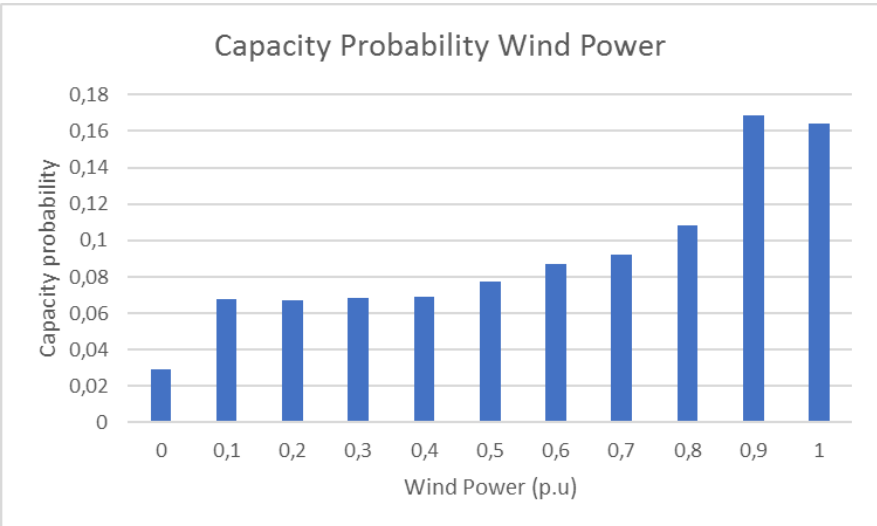

Figure 28: Capacity probability wind power

Figure 28 depicts the multi-state model of a wind turbine or a wind farm with a zero FOR at Utsira High. The model is derived using the methodology illustrated in Figure 15. The capacity table for different wind turbine forced outage rates are found in Table 15.

Table 15: WTG Capacity Probability Table, one unit

CAPACITY IN %	CAPACITY OUT %	PROBABILITY			
		FOR = 0%	FOR= 4%	FOR= 5%	FOR= 10%
0	100	0.02922374	0.06805479	0.07776256	0.12630137
10	90	0.06792237	0.06520548	0.06452626	0.06113014
20	80	0.06712329	0.06443836	0.06376712	0.06041096
30	70	0.06872146	0.0659726	0.06528539	0.06184932
40	60	0,06917808	0.06641096	0.06571918	0.06226027
50	50	0.07751142	0.07441096	0.07363584	0.06976027
60	40	0.0869863	0.08350685	0.08263699	0.07828767
70	30	0.09246575	0.08876712	0.08784247	0.08321918
80	20	0.10810502	0.10378082	0.10269977	0.09729452
90	10	0.168379	0.16164384	0.15996005	0.1515411
100	0	0.16438356	0.15780822	0.15616438	0.14794521

Table 16: Wind Farm Capacity Probability Table for WTG FOR

CAPACITY IN %	CAPACITY IN MW	PROBABILITY		
		FOR= 4%	FOR= 5%	FOR= 10%
0	0	0.00000000	0.00000000	0.00000000
10	6	0.00000000	0.00000000	0.00000001
20	12	0.00000000	0.00000000	0.00000036
30	18	0.00000002	0.00000008	0.00000875
40	24	0.00000073	0.00000267	0.00013778
50	30	0.00002104	0.00006094	0.00148803
60	36	0.00042081	0.00096481	0.01116026
70	42	0.00577112	0.01047506	0.05739563
80	48	0.05194005	0.07463480	0.19371024
90	54	0.27701360	0.31512470	0.34867844
100	60	0.66483264	0.59873694	0.38742049

Table 15 and Table 16 is input data for the COPT which combined gives the technical unavailability and unavailability due to wind speed for the whole wind farm. Combining the column with a zero FOR from Table 15 (the multi-state model of the wind turbine generator) and Table 16 gives the COPT for the wind farm where both wind speed and technical availability of the different turbines are considered. The resulting capacity outage probability table (COPT) for the whole wind farm, found in Table 17, are used in the adequacy assessment and later combined with the COPT for the conventional generation to create a COPT of the whole generation system.

Table 17: COPT for one wind farm based on both technical and wind availability

CAPACITY IN %	CAPACITY IN MW	CAPACITY OUT MW	PROBABILITY WIND FARM			
			FOR = 0%	FOR = 4%	FOR = 5%	FOR = 10%
0	0	60	0.02922374	0.02922437	0.02922758	0.02927153
10	6	54	0.06792237	0.06834583	0.06871418	0.07279222
20	12	48	0.06712329	0.07064082	0.07220855	0.08109493
30	18	42	0.06872146	0.06912098	0.06946044	0.07288032
40	24	36	0.06917808	0.08877264	0.09104923	0.09825632
50	30	30	0.07751142	0.09901731	0.10201679	0.10550697
60	36	24	0.08698630	0.09200447	0.09439449	0.10868684
70	42	18	0.09246575	0.09242482	0.09238253	0.09128263
80	48	12	0.10810502	0.10743328	0.10687263	0.10051703
90	54	6	0.16837900	0.15858712	0.1538984	0.12394359
100	60	0	0.16438356	0.10928755	0.09846575	0.06368556
DAFOR=			0.37340	0.40028	0.40530	0.42574

Table 17 is the input data for the multi-state representation of the whole wind farm. Here both the technical unavailability due to mechanical failure, scheduled maintenance and other outages in the individual wind turbines, and the unavailability due to wind speed are taken into account. This multi-state model is used as an input to create a multi-state COPT, combined with conventional generation and used in the calculation of adequacy indices in the generation capacity adequacy assessment. The combined COPT consisting of both multi-state wind and conventional generation, and a small extract can be found in Appendix A2.

The DAFOR values, representing the equivalent forced outage rate of the whole wind farm for the different individual WTG FOR, are used to create a two-state COPT in combination with conventional generation. Here the input for the wind farm to the total system COPT is a generating unit rated at 60 MW and has an availability equal to 1-DAFOR. This input into the COPT calculation is the same as for the other conventional generating units, with a power rating and an availability, found in Table 18. This input is also used to compute the contingency list and state probability for the HL-II analysis.

7.4.3 Generation

Table 18: Two-state generation input to the COPT

Generation	Capacity (MW)	Availability (WTG FOR=0%)	Availability (WTG FOR=4%)	Availability (WTG FOR=5%)	Availability (WTG FOR=10%)
1	100	0.9816	0.9816	0.9816	0.9816
2	180	0.9816	0.9816	0.9816	0.9816
3	33	0.9584	0.9584	0.9584	0.9584
4	33	0.9584	0.9584	0.9584	0.9584
5	33	0.9584	0.9584	0.9584	0.9584
6	60	0.62660	0.59972	0.59470	0.57426

The data from Table 18 are used in input to calculate the COPT in the generation adequacy assessment when the wind power is modelled as a two-state generating unit with DAFOR used as an equivalent forced outage rate. For the multi-state model, the data input for conventional generation 1-5 is the same as in Table 18, while the wind farm input equals that of Table 17.

7.4.4 Cables

The cable data from Table 6 and Table 7 are used in PowerFactory to calculate power flow and losses. The reliability data from Table 8, are used as input in PowerFactory, but also used in MatLab to calculate the different possibilities for the different outage states.

7.4.5 KILE Costs

Table 19: KILE cost [31]

Voltage dip and loss of load	2010 Gas and Refinery (NOK/kW)
Voltage dip	31.8
1 sec	31.8
1 min	53.3
3 min	53.4
1 hour	56.9
4 hours	67.8
24 hours	200.1

7.5 Simulation Programs

7.5.1 Matlab

For the calculation of the generation adequacy and the capacity outage tables, Matlab is used. The reliability simulations using Matlab is an analytical method of obtaining reliability indices, which is pure calculations. In the analytical method, using the probability of different operating states, the same input will always result in the same output. Matlab is used to create the COPT and contingency lists from the generator input, load data and wind data. From this, Matlab is used to calculate the LOLE and EENS for a varying load for one year.

7.5.2 PowerFactory

To run power flow simulations and obtain reliability indices for the composite system, but also the generation system, DIgSILENT PowerFactory is used. In this thesis, this program is referred to as PowerFactory. This program allows the generators to have a multi-state operation with different probabilities for each operating state and to enter availability on cables and other components in the system. In PowerFactory, the wind farm can be modelled as a multi-state or two-state generator with the states given in the COPT found in Table 17. The DAFOR from the same table can be given as input to PowerFactory in a two-state model of the wind farm. The DAFOR is used as the forced outage rate (FOR) or unavailability (U) for the wind farm. The wind farm will be modelled as a typical PQ-bus.

8 Results

This section presents the results obtained in the analyses. The results are presented to show the differences between the cases, the impact of different wind modelling methodologies, and the impact of different reliability parameters. Different load levels are also included in the results as a sensitivity analysis to illustrate the effect of system and load point indices.

For the generation system reliability assessments, the results are presented by wind model methodology, before the results are combined and compared based on wind turbine forced outage rate and methodology. The results are presented both graphically and in tables, comparing the results of different load levels, wind model methodologies, and wind turbine forced outage rate.

In the composite system reliability assessments, the results are presented both graphically and in tables, comparing the results of different cases, load profiles and wind turbine forced outage rate. The results are first presented for the whole system, and then for the different load points. The axes of the graphical representations only stretch over the span relevant to view the differences between the cases. This is done because the differences are relatively small. For this reason, the axes are not the same in each figure, and the different simulations cannot be compared at a glance.

Lastly, the results from the composite generation and transmission system and the generation system with constant load are compared to observe the difference and possible benefits from the different analyses.

All of the analyses spring out from the input values, as given in section 7.4 Input and System Parameters. As illustrated in in 7.2 Composite Adequacy Test Systems, there are four different that are studied in the composite analysis. In the composite analysis, which one of these is the best option based on reliability was found. Case 3 proved to be the best option reliability when focusing on the improved reliability. However, the additional cable separating Case 1 from Case 3 contributed little to the reliability. The increase of the reliability was shown to rely more on the additional wind power than the additional cable, hence Case 1 would be a preferable solution.

8.1 Generation System

This section presents the results of the HL-I generation system analysis, focusing on the expected energy not served (EENS) and the loss of load expectation (LOLE). The results include the analyses with different load levels, different wind model methodologies, and different wind turbine generator forced outage rates (WTG FOR). The system is studied both with and without 60 MW of wind power. Concerning the results presented in this section, the load is assumed to follow the hourly variation from the reference platform, scaled to the yearly estimated peak demand.

The cases are not specified in these results because only the generation adequacy is evaluated. The different cases differ from each other based both grid configurations and generation, and in the HL-I assessments, only the generation and load is relevant. The generation system is evaluated based on peak load, load duration curve and the generation system with and without wind power. The HL-I systems that are studied in this section are illustrated and presented in section 7.1 Generation Adequacy Test Systems.

8.1.1 Wind Modelled as Negative Load

From the specialisation project, the results from the analyses are that a wind farm with an installed capacity of 50 MW has an effective load carrying capability (ELCC) of approximately 32 MW at Utsira High. In this thesis, 60 MW is the chosen installed wind capacity. With the increase of 10 MW of wind power, the values of LOLE, EENS, LOLP and ELCC will differ from the specialisation project.

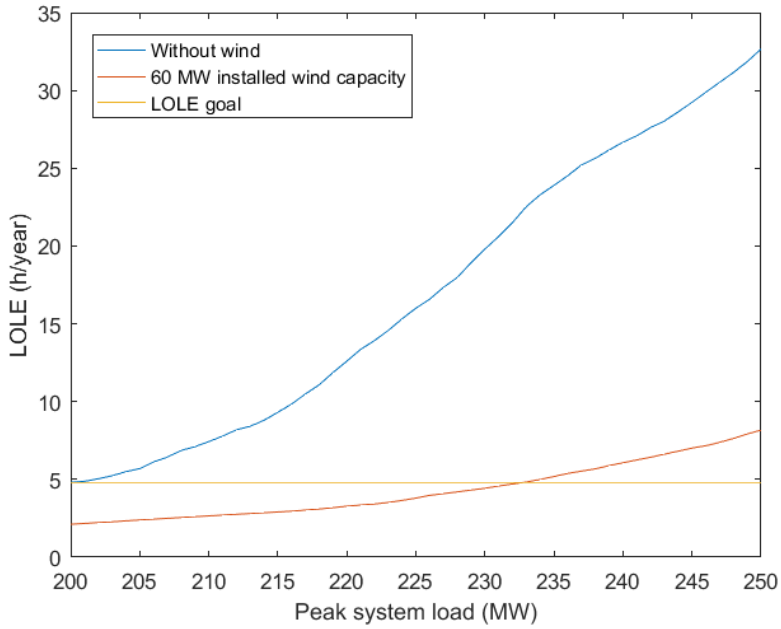

Figure 29: LOLE with 60 MW of installed wind power as negative load

Using the same ELCC methodology as in the specialisation project which is explained in 5.2.3. The ELCC of the 60 MW wind farm is calculated to be 33 MW when losses in the WTG are included, and 34 MW when the losses are not included. This is for the system at Utsira High only and with a LOLE goal of 4.8 hours/year. Other systems could get a different ELCC for the same wind turbines and wind conditions. An ELCC of 33 MW is equivalent to one gas turbine generator, causing the reliability of the system to be unchanged if 60 MW of wind is connected to the system and one gas generator is removed [39]. The ideal load carrying capability (ILCC) can be observed in Figure 29 and is the distance in MW between the two intersection points of the LOLE goal. The LOLE goal is the reliability target and is the LOLE-value obtained with the planned generation units installed and with the minimum load estimate of 200 MW.

Using the negative load modelling approach, the HL-I results from the specialisation project with 50 MW of wind power are found in Table 20. Table 21 presents the HL-I LOLE and EENS results with 60 MW of wind power as negative load. The load level of 200 MW and 250 MW is used due to the previous low and high peak load estimates for the area [1]. Newly provided information estimate the peak system load to be 281 MW in 2028 and is

therefore included in the reliability assessment for both HL-I and HL-II evaluations in this thesis but not in the specialisation project.

Table 20: Reliability results from specialisation project with wind as negative load

Peak Load (MW)	LOEP	EENS (MWh/year)	Total Energy Demand (MWh)	LOLE (hours/year)
200	0.000141	177.04	1257806.06	4.81
250	0.000548	861.56	1572257.57	32.67
200 w/ wind	0.000063	61.70	976178.06	2.59
250 w/ wind	0.000192	248.05	1290629.58	9.39

Table 21: LOLE with 60 MW of wind as negative load

Peak Load (MW)	Total Energy Demand (MWh)	LOLE (hours/year)	EENS (MWh/year)
200	1257806.06	4.81	177.041
250	1572257.57	32.67	861.559
281	1767412.33	112.906	2412.544
200 w/ wind	976178.06	2.117	51.997
250 w/ wind	1290629.58	8.603	216.904
281 w/ wind	1439651.68	26.321	594.694

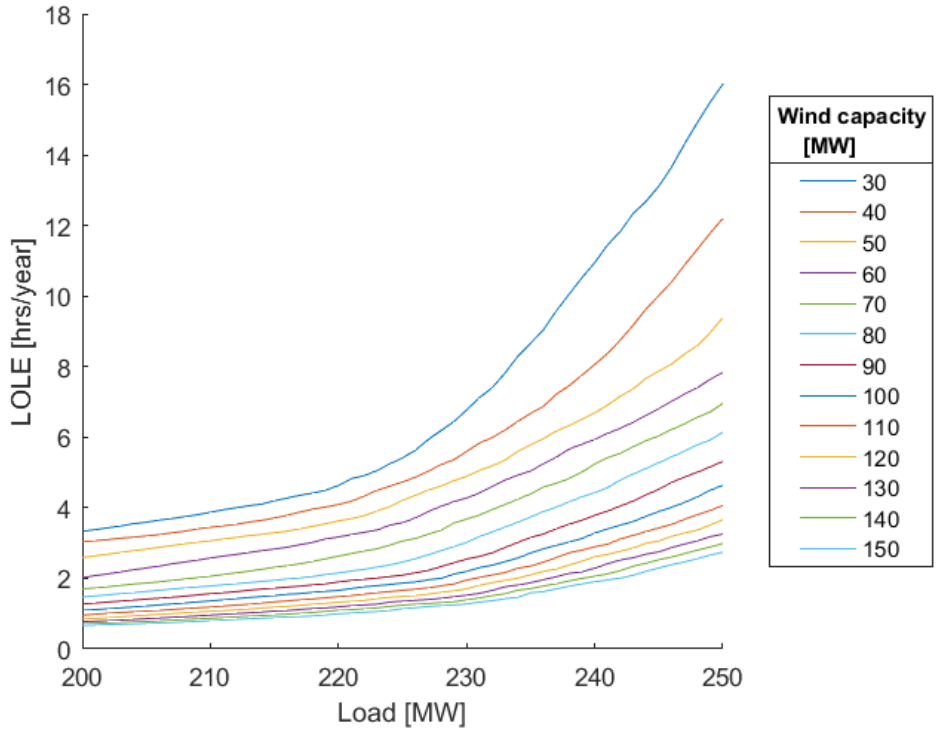

Figure 30: Generation adequacy LOLE with different wind capacities

Figure 30 portrays the generation system adequacy impact of different installed wind power capacities. The wind power input in this simulation is negative load. When more wind power is added to the system, the total system load decreases. The loss of load expectation (LOLE) decrease as more wind power is added, however, the difference in the improvement of the LOLE also decreases as more wind is added. Hence at a certain point, adding more wind power to the system does not increase or influence the reliability of the system anymore.

8.1.2 Wind Modelled as Multi-State Generating Unit

The multi-state representation of the wind farm is found in Table 17 and is based on both wind speed and technical availably of the wind turbines. Table 22 present the energy demand for different system loads, and corresponding LOLE for different WTG forced outage rates when 60 MW of wind power is included in the system.

Table 22: Reliability results multi-state COPT

Peak Load (MW)	Total Energy Demand (MWh)	LOLE (hours/year)	WTG FOR (%)
200	1257806.06	4.81	NA
250	1572257.57	32.67	NA
281	1767412.33	112.91	NA
200 w/ wind	1257806.06	2.36	0
250 w/ wind	1572257.57	10.75	0
281 w/ wind	1767412.33	29.82	0
200 w/ wind	1257806.06	2.48	4
250 w/ wind	1572257.57	11.16	4
281 w/ wind	1767412.33	30.92	4
200 w/ wind	1257806.06	2.50	5
250 w/ wind	1572257.57	11.24	5
281 w/ wind	1767412.33	31.15	5
200 w/ wind	1257806.06	2.99	10
250 w/ wind	1572257.57	14.68	10
281 w/ wind	1767412.33	41.40	10

Table 23: Loss of load expectation results using multi-state COPT

Load (MW)	LOLE (negative load) (hours/year)	LOLE (FOR=0%) (hours/year)	LOLE (FOR=4%) (hours/year)	LOLE (FOR=5%) (hours/year)	LOLE (FOR=10%) (hours/year)
200	4.810	4.810	4.810	4.810	4.810
250	32.670	32.670	32.670	32.670	32.670
281	112.906	112.906	112.906	112.906	112.906
200 w/ wind	2.117	2.3636	2.479	2.500	2.989
250 w/ wind	8.603	10.7513	11.160	11.242	14.681
281 w/ wind	26.321	29.8192	30.924	31.151	41.393

Table 23 presents the LOLE for different system loads and different forced outage rate for the individual wind turbines, compared with the results from modelling the wind power as negative load. For all load levels and different wind turbine forced outage rates, the LOLE values are lower in all cases where wind power is added. Higher FOR values results in higher LOLE values, and the multi-state model results in higher LOLE values compared to wind modelled as negative load.

Table 24: Expected Energy Not Served using multi-state COPT

Load (MW)	EENS (negative load) (MWh/year)	EENS multi-state (FOR=0%) (MWh/year)	EENS multi-state (FOR=4%) (MWh/year)	EENS multi-state (FOR=5%) (MWh/year)	EENS multi-state (FOR=10%) (MWh/year)
200	177.041	177.041	177.041	177.041	177.041
250	861.559	861.559	861.559	861.559	861.559
281	2412.544	2412.544	2412.544	2412.54	2412.544
200 w/ wind	51.997	55.502	58.473	59.0399	61.560
250 w/ wind	216.904	258.558	267.455	269.073	276.579
281 w/ wind	594.694	690.616	716.801	721.601	743.525

Table 24 present the expected energy not served from the HL-I analysis modelling wind as one multi-state generating unit, compared with the results of wind modelled as negative load. For all load levels and different wind turbine forced outage rates, the EENS decrease when wind power is added to the system. Higher FOR values results in higher EENS values, and the multi-state model results in higher EENS values compared to wind modelled as negative load.

8.1.3 Wind Modelled as a Two-state Generating Unit (DAFOR)

Table 25: Loss of load expectation results using equivalent forced outage rate

Load (MW)	LOLE (DAFOR=0.3734) (hours/year)	LOLE (DAFOR=0.40028) (hours/year)	LOLE (DAFOR=0.4053) (hours/year)	LOLE (DAFOR=0.42574) (hours/year)
200 w/ wind	2.162	2.274	2.295	2.381
250 w/ wind	14.399	15.166	15.312	15.909
281 w/ wind	47.255	50.013	50.537	52.681

Table 25 presents the obtained LOLE from the HL-I analysis, using a two-state model of the wind farm with different DAFOR values to represent an equivalent forced outage rate corresponding to WTG FOR of 0%, 4%, 5%, and 10% in addition to unavailability due to wind speed.

Table 26: Loss of load expectation results using DAFOR and constant load

Case	Analytical method (COPT and MatLab)		PowerFactory	
	LOLE (h/yr)	average LOLP (%)	LOLE (h/yr)	average LOLP (%)
no wind	320.010	3.653	358.800	4.096
wind (DAFOR=0.37340)	220.990	2.523	243.966	2.785
wind (DAFOR=0.40028)	225.241	2.571	248.784	2.844
wind (DAFOR=0.40530)	226.031	2.580	244.842	2.795
wind (DAFOR=0.42574)	229.261	2.617	249.572	2.849

To compare and confirm the analytical methodology used in the HL-I analysis, a generation adequacy analysis using Monte Carlo simulations (MCS) is run in PowerFactory. The simulations are performed with constant load levels throughout the year and the load profile of 2028. The DAFOR values are used as input in a two-state model of the wind farm in PowerFactory. The results from both using both the analytical approach and the PowerFactory simulation are presented in the table over. The PowerFactory simulation result in higher values compared to the analytical approach for all DAFOR values and for the system without wind. The LOLE values derived from the analysis with constant load are not realistic values due to the constant load, but can be used to compare the analytical method and the MCS method.

Table 27: Expected Energy Not Served using DAFOR and varying load

Peak Load (MW)	EENS (DAFOR=0.3734) (MWh/year)	EENS (DAFOR=0.40028) (MWh/year)	EENS (DAFOR=0.4053) (MWh/year)	EENS (DAFOR=0.42574) (MWh/year)
200	177.041	177.041	177.041	177.041
250	861.559	861.559	861.559	861.559
281	2412.544	2412.544	2412.544	2412.544
200 w/ wind	73.438	77.791	78.618	82.001
250 w/ wind	378.594	398.885	402.743	418.512
281 w/ wind	1041.616	1099.213	1110.163	1154.926

Table 27 presents the obtained EENS from the HL-I analysis with varying load, using a two-state model of the wind farm with different DAFOR values to represent an equivalent forced outage rate. For all peak load levels and different wind turbine forced outage rates, the EENS is decreased in all cases where wind power is added. Higher FOR values results in higher EENS values, and the two-state DAFOR model results in higher EENS values compared to wind modelled as negative load and wind modelled as a multi-state model that is presented in Table 24.

8.1.4 Combined Results for Different Wind Models

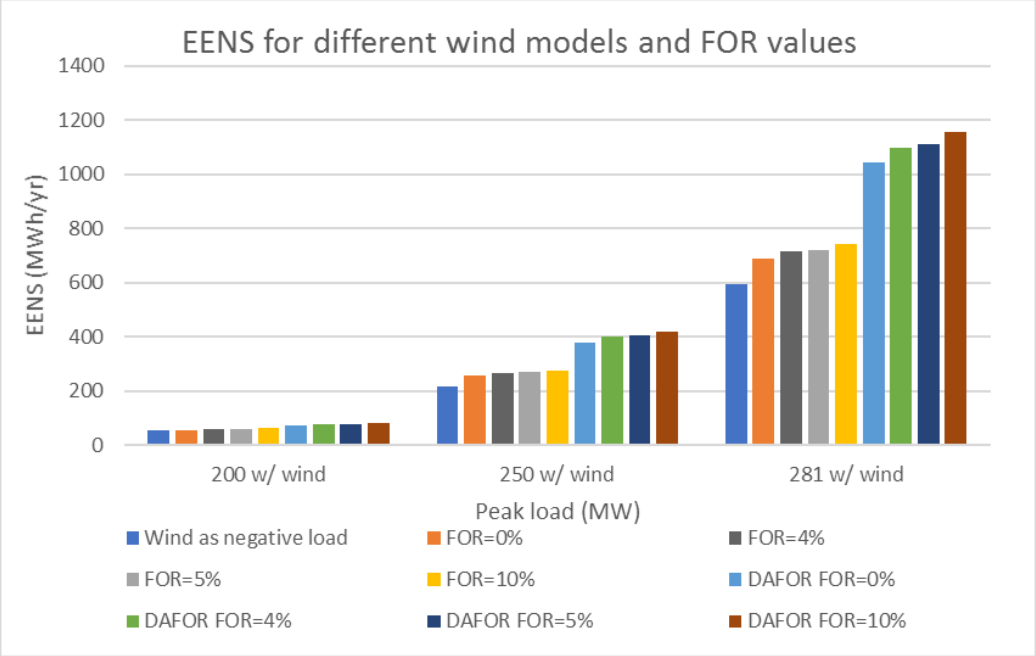

Figure 31: EENS for different wind models, load values and WTG FOR values

Figure 31 shows the HL-I results for the system with wind power and for three different system load levels, different methods of model wind power and different individual forced outage rates for the wind turbines (WTG). From the figure above, it is clear that a higher system load increases the EENS of the system, higher WTG FOR values increase the EENS for both the two-state and the multi-state wind farm model, and the two-state DAFOR wind farm model results in the most pessimistic results. From Figure 31 one can also observe that with low system load values, the impact of using different methodologies and FOR values is small. For low load demands, the resulting EENS and LOLE are low, due to the higher reserve capacity causing higher reliability of the system. When the load demand is increased, the difference between using different methodologies and FOR values increase, and the EENS values for all configurations increase. When the system is strained with high load demands, the effect from using different models is higher.

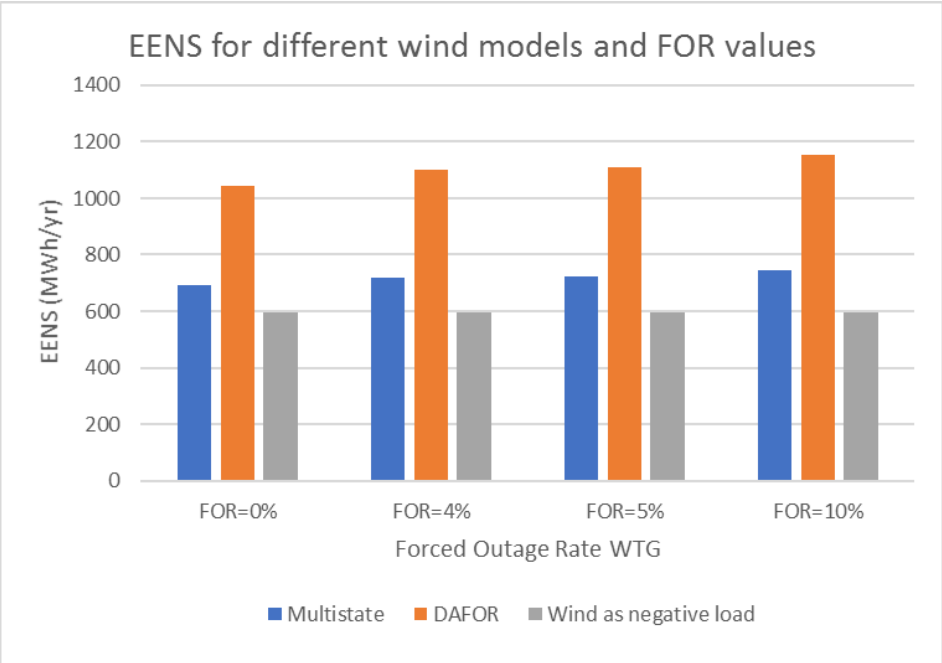

Figure 32: EENS for different wind models and FOR values

Figure 32 shows the different results when the wind farm is modelled as negative load, as a multi-state generating unit, and a two-state generating unit using DAFOR, for different WTG FOR values and the same system load of 218 MW (the load profile of the year 2028). When the wind power is modelled as negative load, the wind turbines are assumed available at all times, hence zero FOR for all the "wind as negative load" results presented in Figure 32 for the estimated system load of 281 MW in 2028.

Table 28: Increase in EENS from increase of WTG FOR

FOR	Increase in EENS from increase of WTG FOR			
	Multi-state		DAFOR	
	(MWh)	(%)	(MWh)	(%)
0% --> 4%	26.186	3.792	57.596	5.530
0% --> 5%	30.986	4.487	68.546	6.581
0% --> 10%	52.909	7.661	113.310	10.878
negativ load --> FOR 4%	122.107	20.533	504.519	84.837
negativ load --> FOR 5%	126.907	21.340	515.468	86.678
negativ load --> FOR 10%	148.831	25.026	560.232	94.205

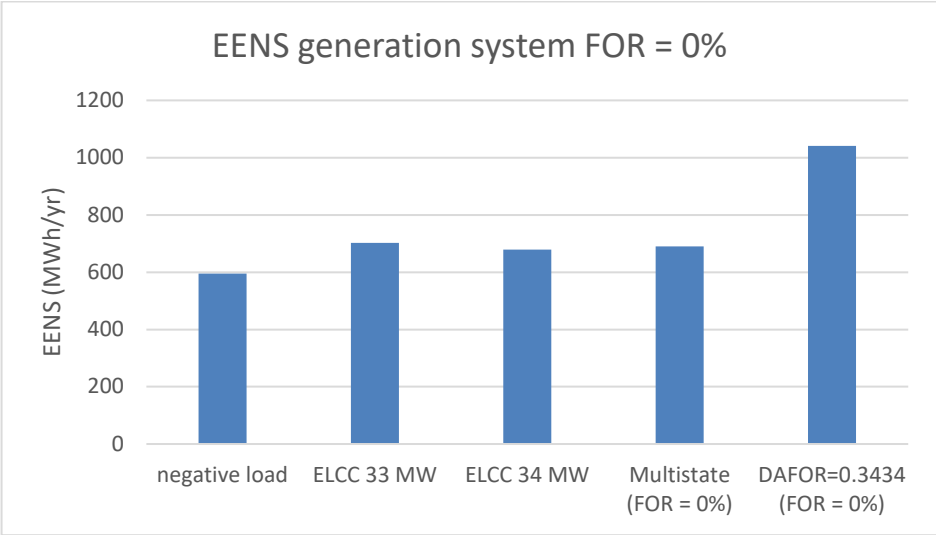

Figure 33: EENS, all wind models and FOR= 0%

Figure 33 illustrates the different results obtained in the HL-I analysis with different wind farm modelling methodologies and the same wind turbine forced outage rate of 0% and the same system load profile of 2028 (281 MW). This is the same as all wind turbines being available at all time, no down time to maintenance or mechanical failure, availability of wind power is only based on the wind speed when FOR=0%. In Figure 33, the obtained effective load carrying capability (ELCC) are used to compare more methodologies with a FOR of 0%. Due to the uncertainty of calculating the EENS using the obtained capacity value of wind, the EENS values obtained using ELCC are not used further in this thesis. The results are, however, used here to compare with the other zero FOR results. The negative load clearly results in the most optimistic appraisals, while DAFOR results in the most pessimistic appraisals of the generation system adequacy.

Under, Figure 34 to Figure 37, depicts the different LOLE values for different system load levels, comparing the results from using the multi-state and two-state DAFOR methodologies. Figure 34 present the results for both DAFOR and multi-state with FOR=0%, 4%, 5%, and 10%. Figure 35, present the same results as Figure 34, but focuses on higher load values and at a smaller load range to differentiate between the results. Figure 36 presents the results with FOR values of 4% and 5%, for both DAFOR and multi-state. Figure 37 presents the results with FOR values of 0% and 10%, for both DAFOR and multi-state. These figures illustrate the effect of

increased system load and forced outage rate, and how the different methodologies affects the results.

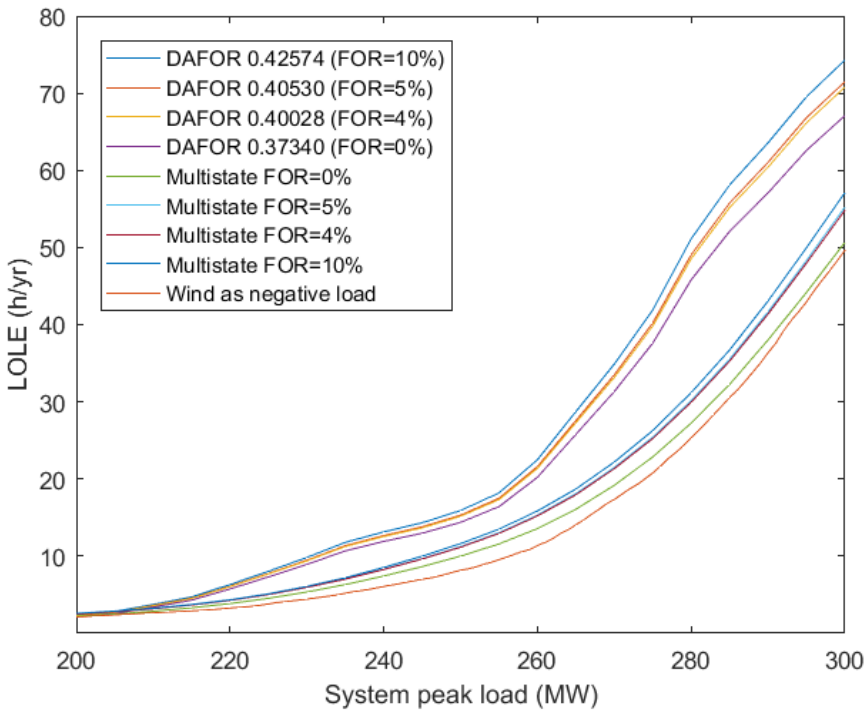

Figure 34: LOLE with different load levels and different wind models

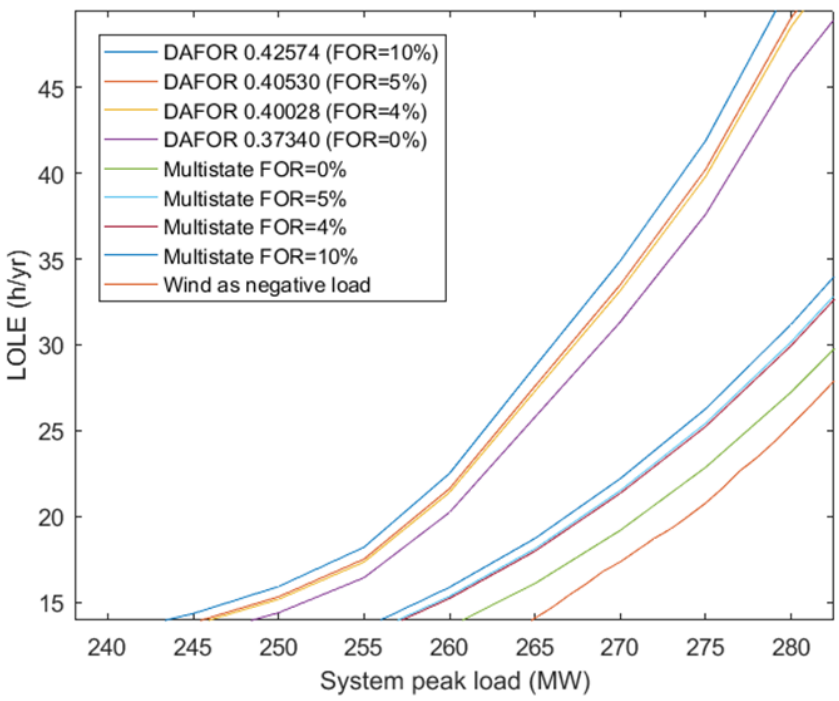

Figure 35: LOLE with different load levels and different wind models

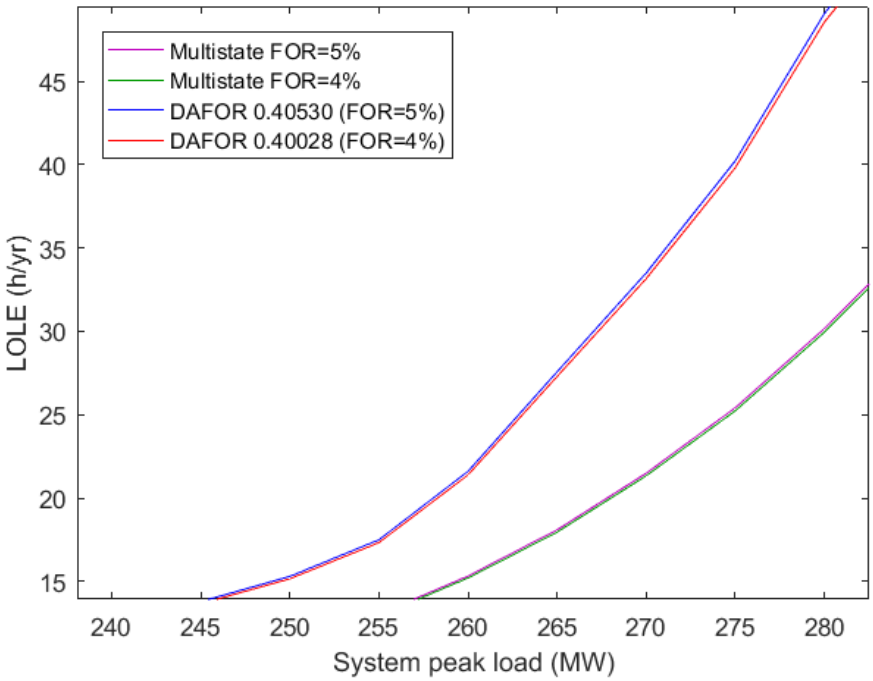

Figure 36: LOLE with different load levels and different wind models with forced outage rates of 4% and 5%

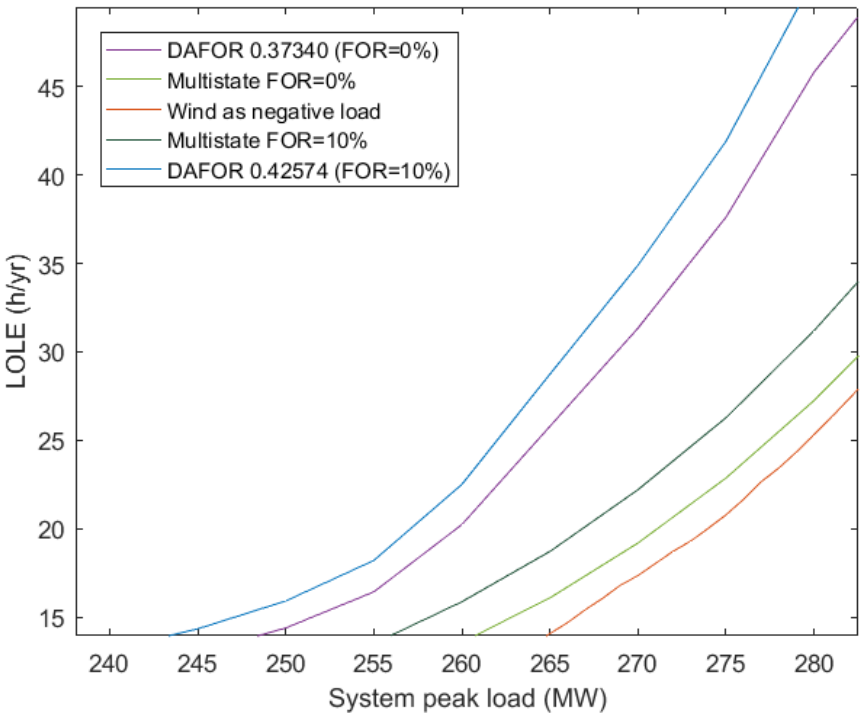

Figure 37: LOLE with different load levels and different wind models with forced outage rates of 0% and 10%

From Figure 34 to Figure 37, it can be observed that on low system load levels, the difference between the different methodologies and forced outage rates are insignificant, while when the load is increased, the difference between the results from the different methodologies different FOR values increase. The choice of methodology has the largest impact on the results when the load level is high, and the results differ more between the methodologies than between the different outage rates within one model. The gradient of the obtained LOLE graph is increasing with the load level. The increase of LOLE and EENS is higher when the load is increased from 250 MW to 300 MW compared to when the load is increased from 200 MW to 250 MW.

8.1.5 Cost of Energy Not Served

The cost of expected energy not served (EENS) is based on the KILE-price estimation from the gas and refinery section. The estimated price is 56.9 NOK/kWh energy not served.

Table 29: Cost reduction and cost of Expected Energy Not Served, Generation System

Forced Outage Rate WECS	Cost from EENS (mill NOK)		Cost reduction of adding wind (mill NOK)	
	Multi-state	DAFOR	Multi-state	DAFOR
FOR=0%	39.296	59.268	97.978	78.006
FOR=4%	40.786	62.545	96.488	74.729
FOR=5%	41.059	63.168	96.215	74.105
FOR=10%	42.307	65.715	94.967	71.558

Table 29 presents the estimated cost reduction and estimated cost of expected energy not served from the generation system reliability analysis. The multi-state model resulted in the least estimated cost and the highest estimated cost reduction.

8.2 Composite Generation and Transmission System

This section presents the results from the HL-II composite generation and transmission system analysis, focusing on the expected energy not served based on load curtailment at the different load points. The results are from the evaluation of the four different cases that is presented in section 2.2 Different Power Solutions and Layouts and described in section 7.2 Composite Adequacy Test Systems.

Base Case: Radial grid, no connected wind power
Case 1: Radial grid, 60 MW connected wind power
Case 2: Ring grid, no connected wind power
Case 3: Ring grid, 60 MW connected wind power

The results include the analyses with different load levels, different WTG FOR values, and the four cases. The wind farm is modelled as one generating unit with a derated adjusted forced outage rate (DAFOR) to represent the unavailability of the unit in a two-state model. Different individual wind turbine FOR cause different DAFOR values for the whole wind farm. In this thesis, 0%, 4%, 5%, 10% WTG FOR are studied and the resulting DAFOR values are used in the wind farm model. Two different load profiles are also investigated in order to observe how the load distribution impact the reliability of the load points and the system. The load in all different load profiles are assumed to be constant throughout the year.

8.2.1 Analytical Analysis - System Results

The composite HL-II assessments are performed using state probabilities and load curtailment and maximum two simultaneously independent contingencies. MatLab is used to create the contingency list with coherent probabilities, the cases are manually investigated to determine the load curtailment for each contingency in Excel. The load is considered to be constant for the composite analysis.

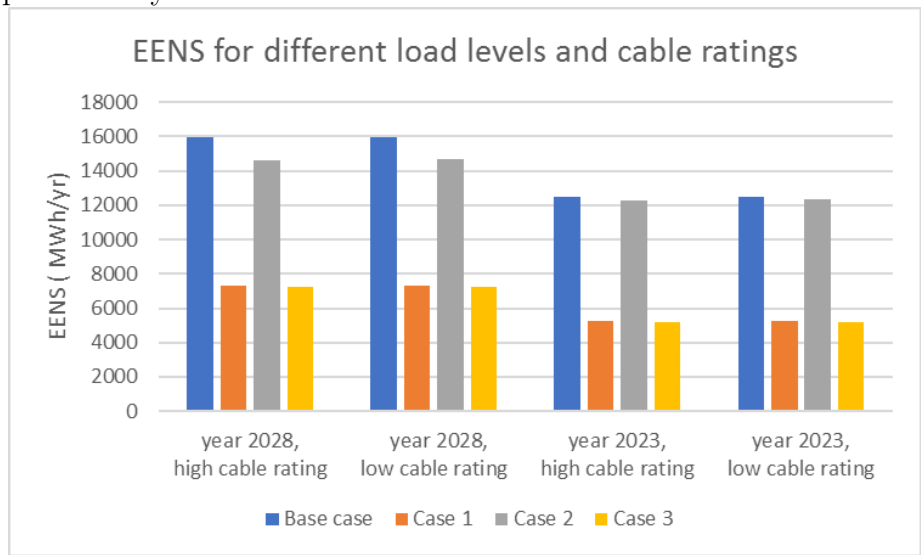

Figure 38: EENS for different load levels and cable rating, DAFOR = 0.40028

Table 30: EENS composite systems, load profile of 2028, high cable rating

	EENS (MWh)			
DAFOR	Base Case	Case 1	Case 2	Case 3
0.37340	15959.729	7103.878	14647.839	7027.891
0.40028	15959.729	7296.071	14647.839	7220.061
0.40530	15959.729	7331.965	14647.839	7255.950
0.42574	15959.729	7478.111	14647.839	7402.079

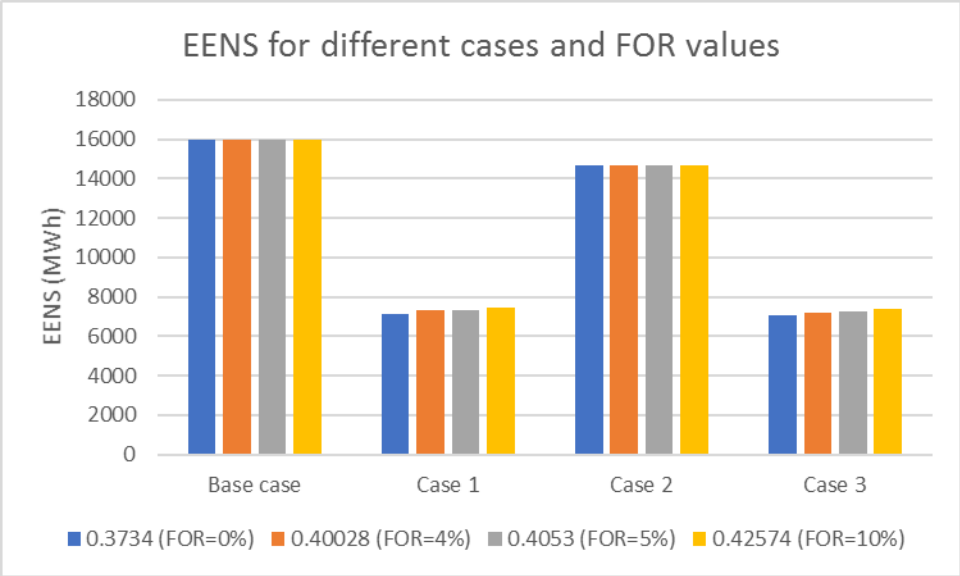

Figure 39: EENS for composite systems, comparing different cases and DAFOR values for 2028 load profile

Table 30 and Figure 39 present the same results for the composite analysis for a system load of 281 MW, the estimated load in 2028, and all four cases. The analysis is performed with different DAFOR values corresponding to a forced outage rate of the individual wind turbines at 0%, 4%, 5%, and 10%. These results are from analyses in which the cable rating is assumed to be high enough to transfer the power needed in Case 2 and Case 3, estimated to be around 75 MW.

Table 31: EENS composite systems, load profile of 2023, high cable rating

	EENS (MWh)			
DAFOR	Base Case	Case 1	Case 2	Case 3
0.37340	12490.661	5040.734	12255.671	4959.884
0.40028	12490.661	5235.418	12255.671	5152.615
0.40530	12490.661	5271.245	12255.671	5188.609
0.42574	12490.661	5417.122	12255.671	5335.165

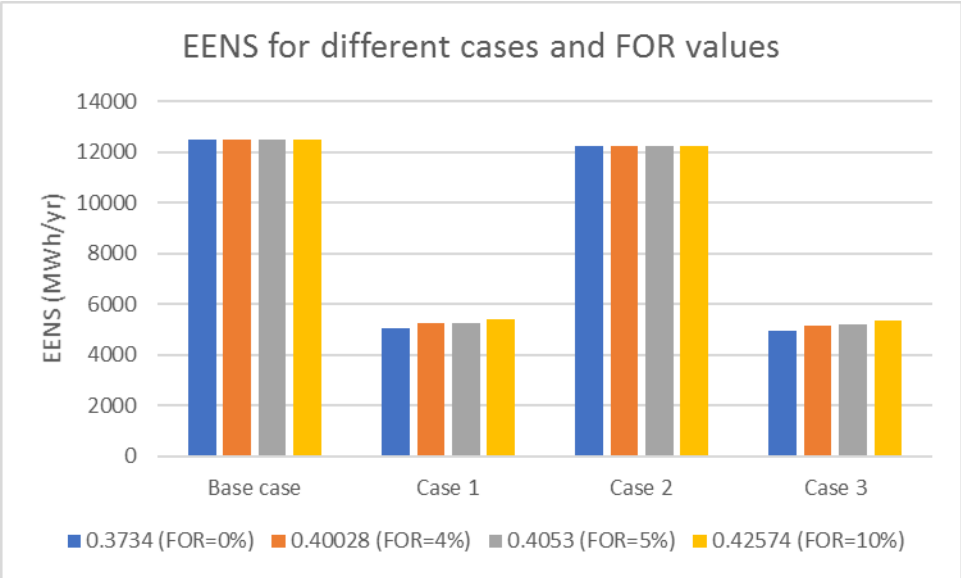

Figure 40: EENS for composite systems, comparing different cases and DAFOR values for 2023 load profile

Table 31 and Figure 40 present the same results for the composite analysis for a system load of 281 MW, the estimated load in 2023, and all four cases. The analysis is performed with different DAFOR values corresponding to a forced outage rate of the individual wind turbines at 0%, 4%, 5%, and 10%. These results are from analyses in which the cable rating is assumed to be high enough to transfer the power needed in Case 2 and Case 3, estimated to be around 75 MW. Notice that the y-axis on Figure 39 and Figure 40 stretches over different EENS spans.

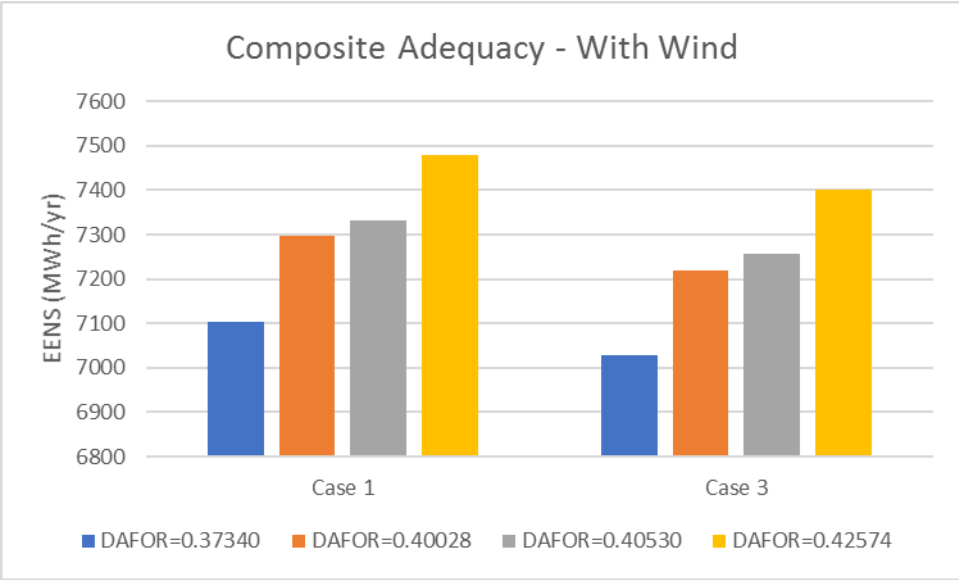

Figure 41: **Composite adequacy with wind power, 2028 load profile**

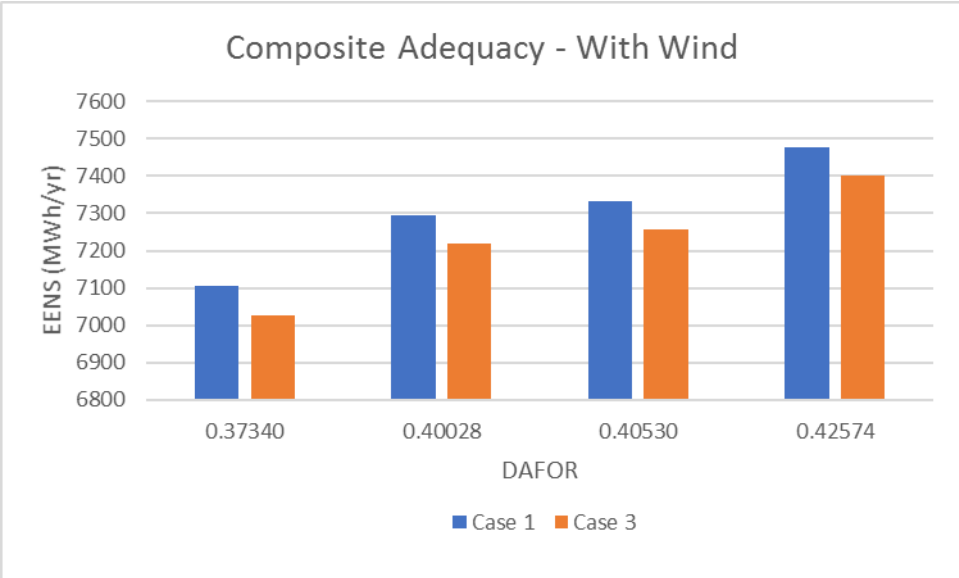

Figure 42: Composite adequacy with wind power, 2028 load profile

Figure 41 and Figure 42 present the composite adequacy results for Case 1 and Case 3, these are the two cases with a wind-integrated composite system. In the two graphs, the effect of increased forced outage rate is observable. In Figure 41 the increase in the expected energy not served (EENS) for both the cases when the forced outage rate is increased is illustrated, but the difference between Case 1 and 3 is not that evident. In Figure 42, the difference between the two cases is more observable.

Table 32: EENS reductions for 2028 load profile

DAFOR	Reduction EENS (MWh/yr)		
	Improvement from adding wind	Improvement from adding cable	Improvement from adding both
0.37340	8855.851	1311.890	8931.839
0.40028	8663.658	1311.890	8739.669
0.40530	8627.765	1311.890	8703.780
0.42574	8481.619	1311.890	8557.650

The improvement of adding wind power is found by comparing the results from Case 1 to the Base Case, the improvement from adding the cable between platform 3 and 4 is found by comparing the results from Case 2 to the Base Case, and the improvement of adding both wind power and the extra cable is found by comparing the results from Case 3 to the Base Case. The EENS reduction of adding the cable is the same for all values of DAFOR as the improvement is not dependent on the forced outage rate of the wind turbines. The improvement of the EENS from adding both wind power and the extra cable to the system does not equal to the sum of both individual improvements.
Table 32 show that the EENS reduction from both wind power and the cable is almost equal to that of wind power alone.

8.2.2 Analytical Analysis - Load Point Results

To evaluate the adequacy of a BES, both load point indices and system indices are needed. The load point indices provide information for each major load point in the system, and indices provides information on the overall system performance. The different load point indices are dependent on the priority and the load curtailment system, due to different load bus priorities in the actual system[4]. The assumed supply priority of the load points in this thesis is first platform 1, then platform 2, platform 4, and lastly platform 3 last. The load at platform 3 will be curtailed first during a contingency if possible. The load point results from three different loads and two different cable ratings can be found in Appendix C.

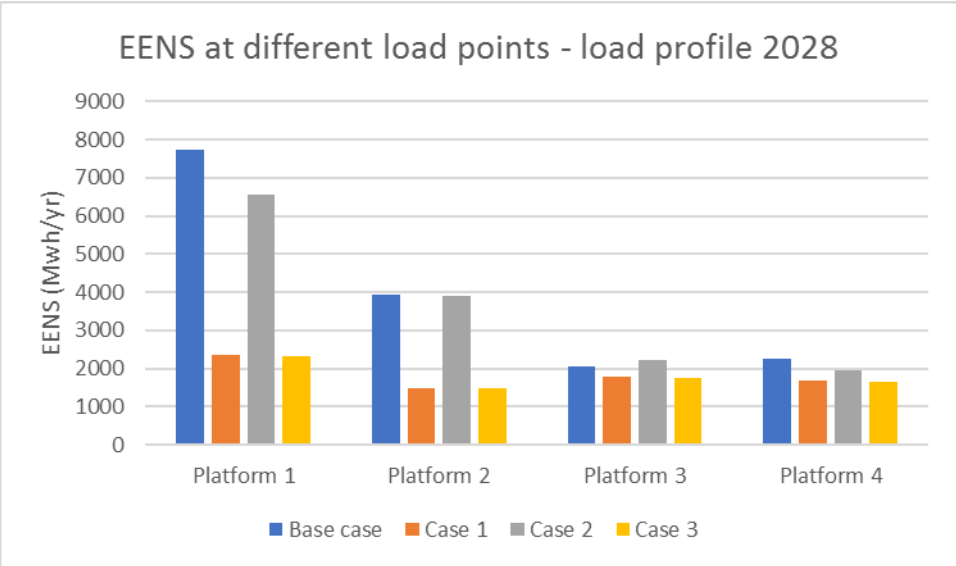

Figure 43: Load point indices, load profile of 2028, high cable rating

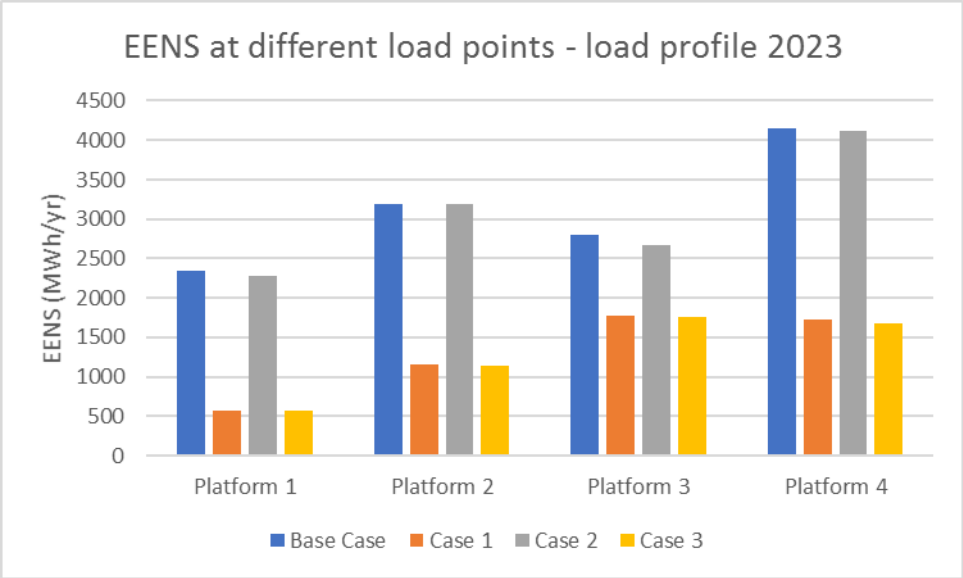

Figure 44: Load point indices, load profile of 2023, high cable rating

Figure 43 and Figure 44 depict the load point results for the estimated load values of the year 2028 and 2023 respectively, and high cable rating in all four cases. Both figures only include the results with a WTG FOR of 4%.

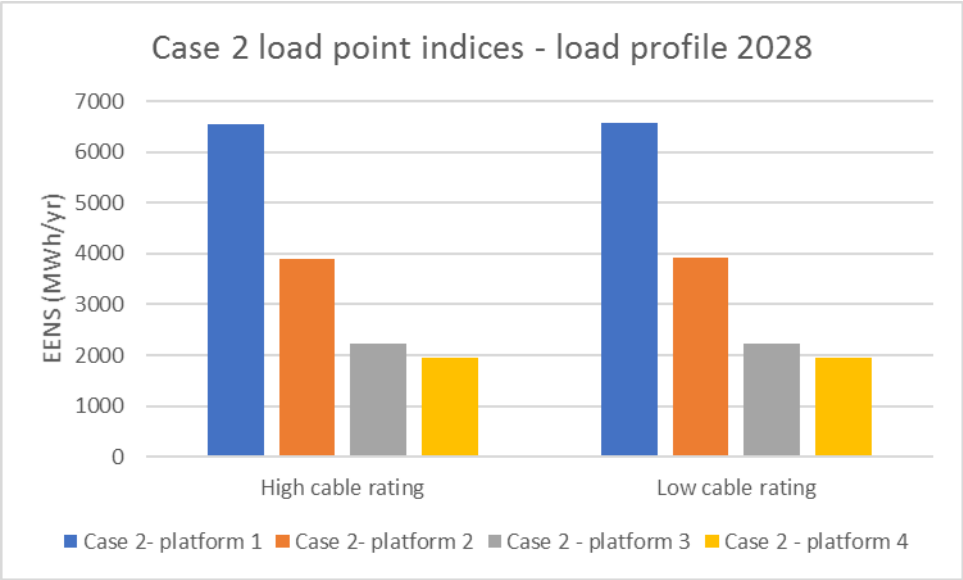

Figure 45: Case 2 load point indices, load profile of 2028, comparing high and low cable rating

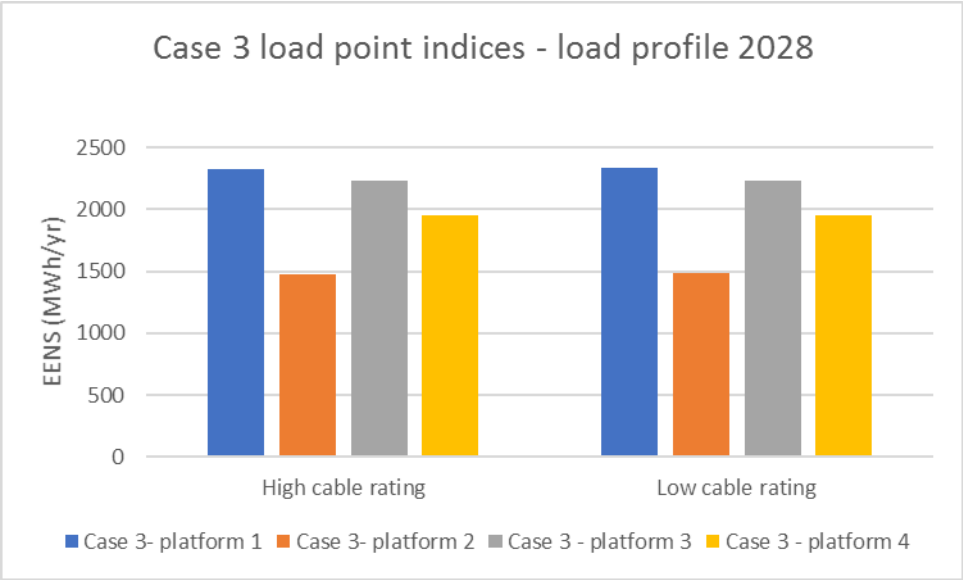

Figure 46: Case 3 load point indices, load profile of 2028, comparing high and low cable rating

Figure 45 and Figure 46 depict the load point results for the estimated load values of the year 2028, a FOR of 4% for Case 2 and 3, comparing high and low cable rating. Notice that the y-axis on the two figures stretches over different EENS spans.

8.2.3 Cost of Energy Not Served

The cost of energy not served is based on the KILE-price estimation from the gas and refinery section. The estimated price is 56.9 NOK/kWh energy not served and is the same as used in the generation adequacy assessment. The load profile used in the cost calculations is the 2028 load profile with the highest total system load. This also causes the highest EENS values and the highest costs from ENS.

Table 33: Cost of Energy Not Served, Composite System

DAFOR	EENS (MWh)	Cost of EENS (mill NOK)
Base case		
NA	15959.729	908.109
Case 1		
0.37340	7103.878	404.210
0.40028	7296.071	415.146
0.40530	7331.965	417.189
0.42574	7478.111	425.505
Case 2		
NA	14647.839	833.462
Case 3		
0.37340	7027.891	399.887
0.40028	7220.061	410.821
0.40530	7255.950	412.864
0.42574	7402.079	421.178

Table 34: Cost reduction due to reduction in Energy Not Served, Composite System

DAFOR	Cost reduction EENS (mill NOK)		
	Improvement from adding wind	Improvement from adding cable	Improvement from adding both
0.37340	503.898	74.647	508.222
0.40028	492.962	74.647	497.287
0.40530	490.920	74.647	495.245
0.42574	482.604	74.647	486.930

The cost reduction of adding the cable is the same for all values of DAFOR because the improvement is independent of the forced outage rate of the wind turbines. The improvement of the EENS of the system from adding both wind power and the extra cable to the system do not equal the sum of both individual improvements.

8.2.4 Load Flow and Losses

Load flow results from PowerFactory for Case 2 and Case 3 with a ring grid are presented in Table 35 and Table 36. The different cases are tested with the load profile of 2023 and the load profile for the year 2028. Load flow from when the platforms are powered from shore and wind power, and when all generating units are feeding power into the system are presented in the tables. The Base Case and Case 1 are not included due to the radial grid.

Table 35: Load flow with 2023 load profile, 268 MW

Case 3 - Only powered from platform 1				
Cable	From	to	P (MW)	Losses (MW)
C1	Platform 1	Platform 2	40	0.5
C2	Platform 2	Platform 3	19.5	0.2
C3	Platform 1	Platform 4	21.4	0.7
C4	Platform 4	Platform 3	-4.3	0
Case 3 - all generators feeding				
Cable	From	to	P (MW)	Losses (MW)
C1	Platform 1	Platform 2	-13.7	0.4
C2	Platform 2	Platform 3	16.3	0.1
C3	Platform 1	Platform 4	-1.1	0.4
C4	Platform 4	Platform 3	-1.2	0.1
Case 2 - Only powered from platform 1				
Cable	From	to	P (MW)	Losses (MW)
C1	Platform 1	Platform 2	40.3	0.7
C2	Platform 2	Platform 3	19.6	0.2
C3	Platform 1	Platform 4	21.5	0.9
C4	Platform 4	Platform 3	4.4	0
Case 2 - All generators feeding				
Cable	From	to	P (MW)	Losses (MW)
C1	Platform 1	Platform 2	13.7	0.5
C2	Platform 2	Platform 3	16.3	0.1
C3	Platform 1	Platform 4	-1.1	0.7
C4	Platform 4	Platform 3	-1.2	0.1

Table 36: Load flow with 2028 load profile, 281 MW

Case 2 - Only powered from platform 1				
Cable	From	to	P (MW)	Losses (MW)
C1	Platform 1	Platform 2	-37.8	0.6
C2	Platform 2	Platform 3	6.2	0.2
C3	Platform 1	Platform 4	-7	0.8
C4	Platform 4	Platform 3	5	0
Case 2 - All generators feeding				
Cable	From	to	P (MW)	Losses (MW)
C1	Platform 1	Platform 2	-20.8	0.5
C2	Platform 2	Platform 3	7.2	0.1
C3	Platform 1	Platform 4	-10	0.7
C4	Platform 4	Platform 3	4	0.1
Case 2 - Only powered from platform 1				
Cable	From	to	P (MW)	Losses (MW)
C1	Platform 1	Platform 2	-37.8	0.6
C2	Platform 2	Platform 3	6.2	0.2
C3	Platform 1	Platform 4	-17	0.8
C4	Platform 4	Platform 3	5	0
Case 2 - All generators feeding				
Cable	From	to	P (MW)	Losses (MW)
C1	Platform 1	Platform 2	-20.8	0.5
C2	Platform 2	Platform 3	7.2	0.1
C3	Platform 1	Platform 4	-10	0.7
C4	Platform 4	Platform 3	4	0.1

Only the active power transfer is included in this thesis, the reactive power flow is included in the PowerFactory simulations, but due to lacking data of generated reactive power and reactive load demand, these results are not included. The results indicate that even with different load profiles with higher demand at the platforms that is not directly connected to shore, cable 4 (C4) is transferring the lowest amount of power and is excessive in most operating states.

8.3 Combined Composite and Generation System Results

In the generation adequacy analysis, using a varying load will give more accurate results. In order to compare generation system adequacy to the composite generation and transmission system adequacy, both adequacy assessments need to be performed using the same load profile. Henceforth, the results from the constant load generation adequacy analysis will need to be used to compare to the composite adequacy results, and all the results presented in this section assume constant load throughout the year. Table 37 present the results from the composite analysis, with high and low cable rating, and from the generation analysis, for different DAFOR values and a system load value of 281 MW, the estimated load demand of 2028. Table 38 present the same results, using the load level of 2023, 268 MW. These two tables are presented graphically in Figure 47 and Figure 48, the systems without wind are placed to the left and the wind-integrated systems are placed to the right. For the composite system, Base Case and Case 2 are without wind power, and Case 1 and Case 3 are with wind power.

Table 37: EENS for composite and generation system with 2028 load profile (281 MW)

DAFOR	EENS (MWh)			
	Without Wind		With Wind	
	Base Case	Case 2	Case 1	Case 3
	Composite, load year 2028, high cable rating			
0.37340	15959.729	14647.839	7103.878	7027.891
0.40028	15959.729	14647.839	7296.071	7220.061
0.40530	15959.729	14647.839	7331.965	7255.950
0.42574	15959.729	14647.839	7478.111	7402.079
	Composite, load year 2028, low cable rating			
0.37340	15959.729	14677.252	7103.878	7034.142
0.40028	15959.729	14677.252	7296.071	7226.044
0.40530	15959.729	14677.252	7331.965	7261.883
0.42574	15959.729	14677.252	7478.111	7407.808
	Generation, load year 2028			
0.37340	15146.136		8483.546	
0.40028	15146.136		8769.359	
0.40530	15146.136		8822.736	
0.42574	15146.136		9040.073	

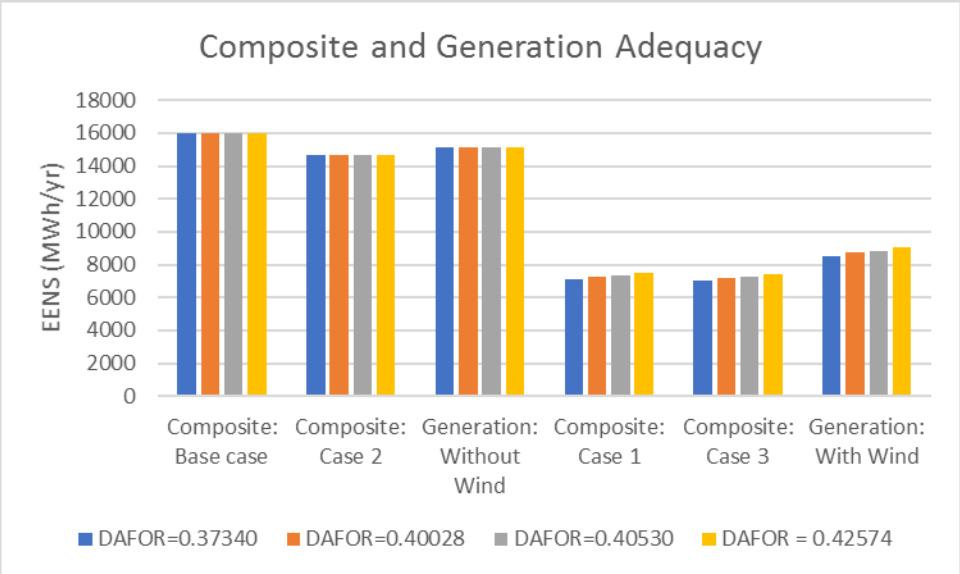

Figure 47: Composite and Generation Adequacy, 2028 load profile

Table 38: EENS for composite and generation system with 2023 load profile (268 MW)

DAFOR	EENS (MWh)			
	Without Wind		With Wind	
	Base case	Case 2	Case 1	Case 3
	Composite, load year 2023, high cable rating			
0.37340	12490.661	12255.671	5040.734	4959.884
0.40028	12490.661	12255.671	5235.418	5152.615
0.40530	12490.661	12255.671	5271.245	5188.609
0.42574	12490.661	12255.671	5417.122	5335.165
	Composite, load year 2023, low cable rating			
0.37340	12490.661	12315.263	5040.734	4969.042
0.40028	12490.661	12315.263	5235.418	5161.381
0.40530	12490.661	12315.263	5271.245	5197.301
0.42574	12490.661	12315.263	5417.122	5343.559
	Generation, load year 2023			
0.37340	12525.409		6187.954	
0.40028	12525.409		6459.820	
0.40530	12525.409		6510.592	
0.42574	12525.4089		6717.323	

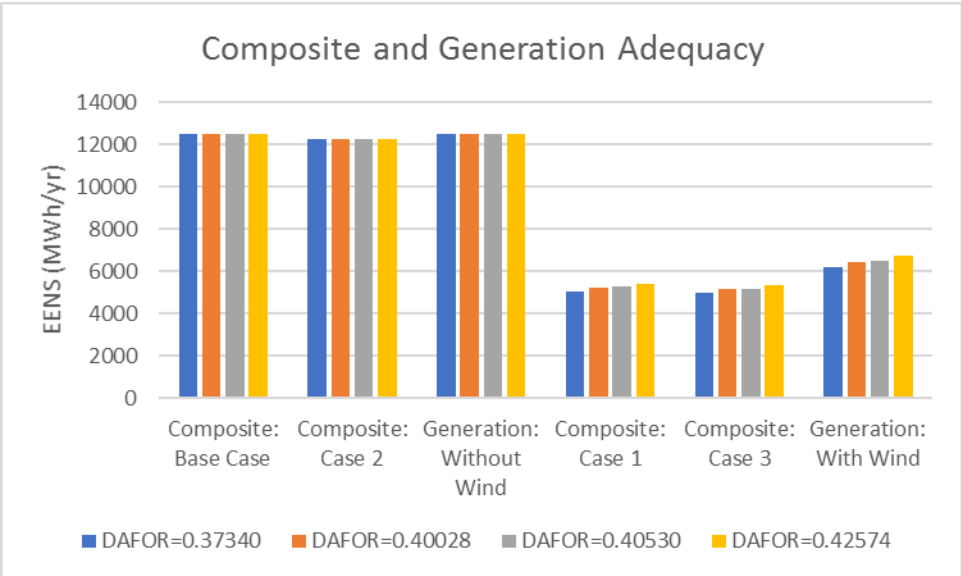

Figure 48: Composite and Generation Adequacy, 2023 load profile

In both the composite and the generation adequacy analysis, the wind-integrated systems have a lower value of the expected energy not served (EENS) than the systems without wind. When wind power is included, the generation system analysis with the constant estimated load profile of 2028 have a higher EENS value compared to both Case 1 and Case 3. When wind power is not included, the generation system analysis with the constant estimated load profile of 2028 have a lower value of EENS compared to the Base Case and a higher value compared to Case 2. This can be seen in Figure 47, but is more observable in Figure 49 and Figure 50. With the estimated load profile of 2023, the generation system analysis with constant load resulted in higher EENS values compared to the composite systems, both with and without wind power included. The latter be seen in Figure 48.

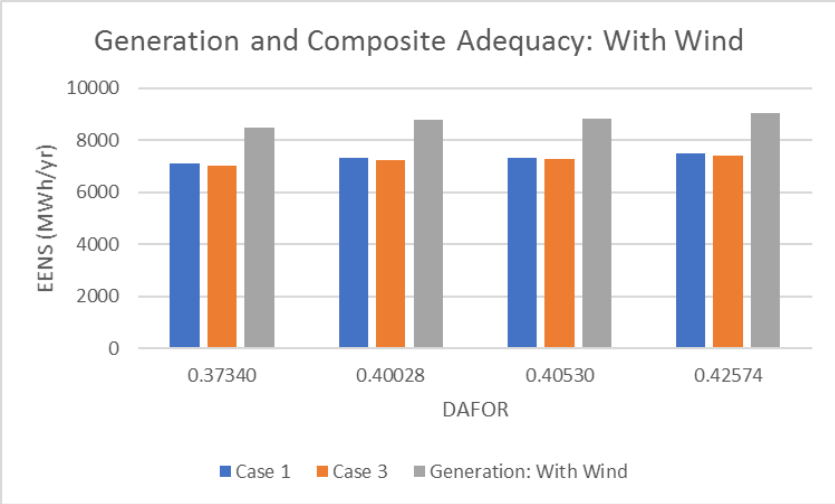

Figure 49: Composite and Generation Adequacy with wind, 2028 load profile

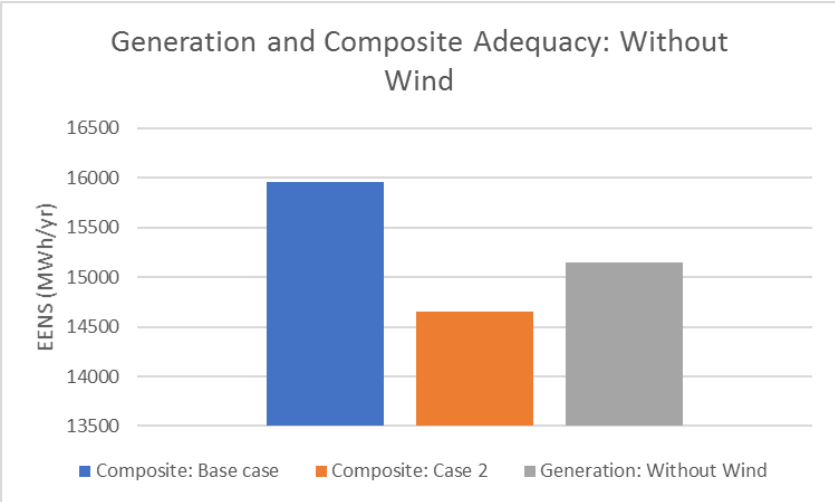

Figure 50: Composite and Generation Adequacy without wind, 2028 load profile

Table 39 and Table 40 present the increase in EENS (MW) from the increase of WTG FOR, when the estimated system load profile of 2028 (281 MW) is used and the load is constant for both the generation system and the composite system. The load estimation for 2028 is used in the comparison of WTG FOR in both the generation and composite system because it is the worst-case for the generation system. A two-state DAFOR wind model is used and the cables have high enough rating to transfer the necessary power.

Table 39: Change in the system EENS (MW) from change in WTG FOR, 2028 load profile

FOR	Increase in EENS from increase of WTG FOR		
	Generation system	Composite System Case 1	Composite System Case 3
0% --> 4%	285.813	192.193	192.170
0% --> 5%	339.190	228.086	228.059
0% --> 10%	556.527	374.233	374.189

Table 40: Change in the system EENS (%) from change in WTG FOR, 2028 load profile

FOR	Percentage increase in EENS due to increase of WTG FOR		
	Generation system	Composite System Case 1	Composite System Case 3
0% --> 4%	3.369	2.705	2.734
0% --> 5%	3.998	3.211	3.245
0% --> 10%	6.560	5.268	5.324

When the forced outage rate of the wind turbine increase, the generation system EENS values increases the most compared to the composite systems. Looking at the percentage EENS increase, Case 1 is least affected by the increase of WTF FOR.

8.3.1 Cost of Energy Not Served

The cost of energy not served is based on the KILE-price estimation from the gas and refinery section. The estimated price is 56.9 NOK/kWh energy not served. The load profile used in the cost calculations is the 2028 load profile with the highest total system load. This also caused the highest EENS values, hence the highest costs from ENS. Table 41 present the cost reduction from EENS reduction using the 2028 load profile and constant load for the generation system and composite system.

Table 41: Cost reduction EENS from adding wind, 2028 load profile

	Cost reduction EENS from adding wind (mill NOK)	
DAFOR	Composite System	Generation System
0.37340	503.898	379.101
0.40028	492.962	362.839
0.40530	490.920	359.801
0.42574	482.604	347.435

The improvement in the expected energy not served (EENS) for the composite system is higher than in the generation system with a constant load. This causes the cost reduction of adding wind power to be higher in the composite system. For the composite system, the improvement of adding wind power is calculated by comparing the EENS for the Base Case with the EENS for Case 1.

9 Discussion

9.1 Generation System

With 60 MW installed (10x6 MW Hywind turbines), the wind farm has an effective load carrying capability (ELCC) of 33 MW when losses in the wind turbine generator (WTG) are included, and 34 MW when the losses are not included. This corresponds to one additional gas turbine generator of the same type that is already installed on platform 2 and 4, hence the windfarm can replace one gas turbine without lowering the reliability of the system. The simulations performed with wind power modelled as negative load indicate that the improvement in loss of load expectation (LOLE) and ELCC decrease as more wind power is added, resulting in that after a certain point adding more wind to the system will not improve the reliability anymore.

The gradient of the obtained LOLE graph is increasing with the load level, hence the increase of LOLE and expected energy not served (EENS) is higher when the load is increased from 250 MW to 300 MW compared to when the load is increased from 200 MW to 250 MW. When including wind power, the LOLE of the system for both the multi-state and the two-state model is close to or under the standard LOLE target for power systems at 2.4 hour/year at the lowest load estimate of 200 MW [16]. Without wind power the LOLE value is double the standard LOLE target.

As mentioned, using multi-state generating unit models will increase the number of generation contingency states and can cause a considerable increase of the computation time. To solve this issue, a derating adjusted forced outage rate (DAFOR) is calculated, replacing the multi-state model. Using DAFOR in adequacy assessment can give more pessimistic results with higher risk estimates compared to using multi-state models [29, 30]. From the results, this can clearly be seen in Figure 31 and Figure 34, where the obtained EENS and LOLE have significantly higher values using DAFOR compared to a multi-state model. Using the estimated cost of energy not served, the multi-state model resulted in the least cost and the highest estimated cost reduction, thus proving that DAFOR is more pessimistic and produce higher risk estimates.

The PowerFactory simulations result in more pessimistic values compared to the analytical approach for all DAFOR values and for the system without wind. The LOLE values derived from the analysis with constant load using both the analytical approach and Monte Carlo simulation (MCS) in PowerFactory are not realistic values due to the constant load, but can be used to compare the analytical method and the MCS method. The methods did not obtain identical adequacy indices, but the results are close, causing the analytical approach to be credible.

Wind modelled as negative load gives the most optimistic results, this is because when the wind power is modelled as negative load, all wind turbines are assumed to be available 100% of the time. This is equivalent to a wind turbine generator forced outage rate (WTG FOR) of 0%. Multis-state model with FOR =0% still have more pessimistic results compared to negative load, this could be because the power output of the wind is grouped together into different wind outputs consisting of 10% of the total rated power, where the small power outputs are rounded down.

Looking at the expected energy not served (EENS) for the different wind modelling methodologies and different forced outage rates, the results show that using a WTG FOR value of 4%, and a multi-state wind farm model, the EENS will increase by approximately 20% compared to when the wind is modelled as negative load. Looking at the results a two-state wind farm model with DAFOR, and the same WTG FOR value of 4%, the EENS will increase by approximately 85% compared to when the wind is modelled as negative load. This is expected from use of DAFOR, where the results are more pessimistic, but faster to compute. These results are presented in Table 28. Within the wind models, the increase of the wind turbine FOR cause a percentage increase of the EENS in the system equal to a little under the FOR increase for the multi-state model, and a little over the FOR increase for the DAFOR model. Changing the WTG FOR from 0% to 4%, by changing the wind model from negative load to a two-state or multi-state model with FOR=4%, cause a higher EENS increase compared to increasing the FOR from 0% to 4% within the wind models. Even when taking the technical availability of the wind turbines into consideration with different WTG FOR, the generation system still results in higher reliability and lower EENS and LOLE values compared to the generation system without wind power. This

can clearly be seen in Table 23 and Table 24 for the multi-state model, and in Table 27 for the two-state DAFOR model.

Different forced outage rates of the wind turbine were tested to see the effect of the different outage rates within the different modelling methodologies, and to see the effect on the adequacy of the system when technical outages of wind turbines are included. From Figure 31 one can observe that with low system load values, the impact of using different methodologies and FOR values is small. For low load demands, the resulting EENS and LOLE are low, due to the higher reserve capacity causing higher reliability of the system. When the load demand is increased, the difference between using different methodologies and FOR values increase, and the EENS values for all configurations increase. From Figure 34 to Figure 37, it can be observed that on low system load levels, the difference between the resulting EENS from assessing different methodologies and forced outage rates are insignificant and that the differences increase with the load. When the system is strained with high load demands, the effect from using different models is higher. The choice of methodology has the largest impact on the results when the load level is high, where the results differ more between the methodologies than between different forced outage rates. Thus, the generation adequacy results indicate that the choice of wind model methodology has a higher impact on the reliability of the system compared the FOR values of the wind turbines.

The difference of the results using different modelling methodologies show the importance of using a good wind model. The DAFOR can be used when looking at a worst-case scenario and is faster and easier to use. A multi-state model will be more correct, but the computational time will be longer.

9.2 Composite Generation and Transmission System

From the composite analysis, Case 3 has the highest reliability compared to the other cases, and the Base Case has the lowest reliability results. As expected, the case where both the installed generation capacity is increased and the network has an additional cable, has the highest reliability and most optimistic appraisals of the composite adequacy. The Base Case with the radial grid and no additional power generation has, as expected, the lowest reliability.

The results also indicate that the improvement of the system EENS, from adding both wind power and the extra cable to the system does not equal the sum of the individual improvements. The EENS reduction from both wind power and the cable, found by comparing Case 3 to the Base Case, is almost equal to that of wind power alone. Accordingly, the impact from the additional cable is higher when the wind power is not added to the system. Individually, wind power has a larger positive impact on the reliability of the system compared to the cable. As seen from the results, changing the cable rating has little impact on the reliability of the system. The additional cable improved the reliability in the analyses, but increasing the cable rating over 30 MW had little impact. Due to the constant load, the actual EENS values are not realistic, but the values are beneficial when comparing different cases and to see the impact of different reliability variables.

The system EENS values are higher for the load profile of 2028 compared to the load profile of 2023. This is expected due to the higher system load in 2028, however, the load profile and how the load is divided between the platforms has a larger influence on the different load point adequacy indices compared to the system adequacy indices. The expected load curtailment and expected energy not served at the different load points varied greatly between the different load distributions through the years of operation at Utsira High. Examining Figure 43 and Figure 44, the different values of the EENS at the different load points (platforms) for the different cases, greatly depends on the load profile. Even though the total estimated system load is lower in 2023, the load at especially platform 4 is much higher, creating a higher amount of energy not served at that load point. In the load profile of 2028, platform 1 benefits the most from adding cable 4 (C4), while in 2023 with a higher load demand at platform 3, platform 3 benefits the most. All load points, for both load profiles investigated, benefits more from adding wind power than adding cable 4. This can be observed in Figure 43 and Figure 44, by comparing the difference between Case 1 and the Base Case, where only wind power is added, and the difference between Case 2 and the Base Case, where only cable 4 is added.

Load flow simulations from PowerFactory indicate that cable 4 is excessive in most operating states and is only needed during the operating states in

which the power supply from shore is unavailable. During normal operational conditions, cable 4 transfer a small amount of active power compared to the other cables. In this thesis, reactive power is not included which can be a source of error for the transfer capacity of the cables and benefits of the additional cable.

9.3 Comparing Generation and Composite System

The EENS obtained from the different composite analyses are higher compared to the EENS values obtained from the generation adequacy analyses. This is because the composite analyses assumed a constant load, causing more load to be curtailed during outages. When comparing the reliability results for the generating system and the generation and transmission system, the load need to be kept constant for both analyses. Comparing constant load analysis of the composite system to varying load analysis of the generation system would be unrewarding and unnecessary. The results with constant load is discussed below.

With wind power, Case 1 and Case 3 in the composite analysis is compared to the generation system with wind power. One can observe that the EENS is higher for the generation system compared to the two composite systems for both load levels investigated. Increasing the forced outage rate of the wind turbine generators, caused an increase of the EENS in both the composite systems and the generation system. This can be observed in Figure 49. When the WTG FOR is increased, the generation system has the highest increase of EENS, and Case 1 has the lowest increase. Hence, the generation system is the most negatively affected and Case 1 the least negatively affected by an increase of WTG FOR. The increase of the WTG FOR have a higher impact on the generation system compared to both the wind-integrated composite systems, as shown in Table 39 and Table 40. This can be due to the number of outage states where the generation system includes all possible combinations of contingencies, while the composite system only includes maximum two overlapping contingencies. When wind power is included in the generation system as one generating unit, the number of outage states in the COPT for the system increase from 32 to 64. While the generation system doubles the number of outage states, the composite system increases by 9 or 10 depending on if cable 4 is included.

Without wind power, the Base Case and Case 2 in the composite analysis is compared to the generation system without wind power. The correlation between composite and generation systems differs from the results with wind power. Without wind power, the Base Case has the highest EENS Case 2 has the lowest EENS, and the generation system has an EENS between these two for the 2028 load estimate. For the 2023 load estimate, the generation system has the highest EENS values compared to the composite system both with and without wind power. The obtained adequacy indices for both the generation system and the composite system, studied with both load profiles, are similar when separating the wind-integrated systems and the systems without wind power.

The reduction in the EENS when wind power is added is higher for the composite system than for the generation system with a constant load. This causes the cost reduction of adding wind power to be higher for the composite generation and transmission system. In other words, the composite system seems to benefit the most from adding wind power. The generation adequacy indices and the composite adequacy indices are obtained using different methodologies and with simplified approaches, hence the comparison is subject of uncertainty.

9.4 Validity of Results

Analytical methods represent the system by mathematical models and usually involve some form of contingency enumeration. This method frequently requires assumptions to simplify the overall problem and direct numerical analysis is used to derive the reliability indices [4]. For this thesis, the generation system adequacy indices were obtained using both analytical method and Monte Carlo simulation (MCS) run in PowerFactory. The MCS results are not identical to the analytical results, but they are close enough to confirm the analytical method of the generation system. The composite adequacy indices were obtained using only analytical methods by contingency enumeration and mathematical models. This required several simplifications of the system, e.g. the load curtailment, a constant load demand throughout the year, and only up to two overlapping contingencies. This causes the reliability results in the composite analyses to be subject to uncertainty due to the simplified approach, but the tendencies observed from the results

regarding the importance of wind model methodology, and the wind turbine forced outage rate, as well as the improvement of reliability of the system, should be weighted and considered.

The wind data should be used with reservations regarding the accuracy. In this thesis, the assessments of different methodologies and the benefits from connecting wind power are the main focus areas, and for this purpose, the accuracy of the hourly wind data is less important. One weakness in the wind data is that the sample is for one year only, treating the output wind power as fixed values and effectively assuming that every year is the same. Using multiple historical data would give a better estimation [12]. Because the program calculates the power output based on the power characteristics of a chosen turbine and measured wind speed, the effect of wind turbine placement and wind wake from other turbines are not considered [12].The reliability results for the wind-integrated systems are not completely accurate, but what the results indicate regarding the importance of wind model methodology and the wind turbine forced outage rate, as well as the improvement of reliability of the system, should be weighted and considered.

In this thesis, many simplifications have been made, most importantly in terms of electric losses, reactive power, cable reliability, not including circuit breakers or emergency generators as independent components in the analyses, KILE-costs and neglecting how weather could cause multiple outages at the same time. The impact of the simplifications needs to be examined in order to evaluate the real value of added interconnections.

10 Conclusion

Looking at the capacity value of wind power, the effective load carrying capability (ELCC) of the 60 MW wind farm connected to the system at Utsira High was found be equal to 33 MW when losses in the wind turbine generators (WTG) are included and 34 MW when the losses are not included. This corresponds to one additional gas turbine generator of the same type that is already installed on platform 2 and 4. Based on this analysis, it is fair to conclude that the wind farm can replace one gas turbine, but it is not sufficient to replace all the gas turbine generators or one of the HVDC-connection to land without drastically lowering the reliability of the system.

The analysis methodology is not accurate enough to determine the best power system solution at Utsira High, but the indication that wind power will greatly improve the adequacy of the system is strong. Comparing the different cases in the composite analysis, it is clear that adding wind power to the system has a larger impact on the reliability compared to the impact from creating a ring grid. The results show that Case 3 is the best option among the four when focusing on improved reliability. However, the additional cable separating Case 1 from Case 3 contributes little to the reliability of the system. The improvement from adding both wind power and the extra cable proved to be less than the combined improvement of adding the cable and the wind farm individually, and is almost equal to the improvement from wind alone. From the composite reliability analysis, it was also revealed that the cable ratings have little impact on the reliability of the system when they were rated higher than 30 MW. From the load flows and reliability results, the improvement from cable 4 is not sufficient to make a decision to connect the cable. Cable 4 is excessive in most operating states and is only needed during the operating states in which the power supply from shore is unavailable. The composite analysis indicates that the increase of the reliability relies more on the additional wind power than the additional cable and that the additional cable is excessive in most operating states, hence Case 1 would be a preferable solution.

Including the mechanical faults and outages of all the individual wind turbines in a wind farm by using the derated adjusted forced outage rate (DAFOR) and the multi-state methodology, causes more pessimistic results

compared to treating wind power as negative load and assuming 100% technical availability. By taking the forced outage rate of the wind turbines into consideration, the calculated expected energy not served (EENS) increases for both the multi-state and two-state wind power representation. The results from the adequacy analysis still indicates a high increase in the reliability from adding wind power. The analysis using a two-state model with DAFOR for the wind farm gave more pessimistic results compared to the multi-state model. The DAFOR methodology is an easy way to integrate technical failure of wind turbines and gives a worst-case scenario, while the multi-state model gives more realistic result, but the computational time is higher. In the adequacy results obtained in the generation system analysis, it was clear that the choice of the wind model, i.e. negative load, DAFOR, and multi-state, has a higher impact on the reliability indices than the wind turbine generator forced outage rate (WTG FOR). From this, it is fair to conclude that the wind model methodology has a higher impact of the reliability indices of the generation system than the WTG FOR and that connecting wind power will improve the reliability of the system at Utsira High even when taking the technical availability into consideration.

10.1 Further Work

In this thesis, many simplifications have been made, most importantly in terms of electric losses, cable reliability, excluding circuit breakers and emergency generators as independent components in the analyses, KILE-costs and neglecting how weather could cause multiple outages at the same time. Assumptions regarding the priority order of the platforms (load buses) are likely to have a strong impact on the load point indices in the composite generation and transmission analysis. The impact of the simplifications and assumptions needs to be examined in order to evaluate the real value of added interconnections. There are several other continuations to this thesis that also can be investigated.

The methodology from the composite analysis is too simplistic to draw clear conclusions. Using different simulation programs meant for composite analysis could provide more confident results. Several research papers used for the literature review for this thesis, used Monte Carlo simulation software, such as MECORE and RapHL-II, to obtain system and load point reliability

indices for the wind-integrated composite generation and transmission systems[4, 26, 29, 30]. These programs were not available at NTNU for this thesis, but the use of these or similar programs could provide more accurate analyses and results using Monte Carlo simulation, calculating both load point and system reliability indices.

Even if the results are subject to uncertainty from simplified approached, the analysis still provided beneficial information and is important in the planning of cable ratings, and the decision to create a more robust grid by creating a ring topology. Simulating the composite system for each year during the lifetime and operation of the platforms would provide more accurate results due to the changing load profile of the system through the years. In addition, a varying hourly load should be investigated for the composite analysis. In this thesis, only the estimated load for the year 2028 and 2023 distribution with an assumed constant load demand throughout the year is evaluated.

Other possible layouts could also be explored, e.g. investigating how the composite reliability would respond to the wind turbines being distributed and connected to different platforms. Doing a full economic analysis of the different cases, including investment costs and the levelized cost of energy, cost of imported/exported energy, and externality costs in addition to the cost of unsupplied energy would be beneficial. An economic analysis and calculating other benefits from the addition of wind power, i.e. decrease in CO_2 - emission, would provide a better foundation for the choice of generation and transmission system.

Bibliography

1. Statoil, *Power solutions for Johan Sverdrup field in phase 1 and for full field, RE-PM312-00137*. 2014, Statoil.
2. Statoil. *Hywind Demo*. [cited 2017 30 April]; Available from: https://www.statoil.com/no/what-we-do/new-energy-solutions/our-offshore-wind-projects.html?gclid=CKLIrImmptQCFQncGQodeagDPg.
3. Statoil. *Hywind Scotland Pilot park*. [cited 2017 30 April]; Available from: https://www.statoil.com/en/news/hywindscotland.html.
4. Roy Billington, Y.G., Dankge Huang, Rajesh Karki, *Adequacy Assessment of Wind-Integrated Composite Generation and Transmission Systems*, in *Innovations in Power System Reliability*, G.A.a.A. Vaccaro, Editor. 2011, Springer-Verlag London Limited 2011.
5. Samuelsen, H.J., et al. *Statusrapport "Utsirahøyden Elektrifiseringsprosjekt" Etablering av infrastruktur for kraft fra land til felt på Utsirahøyden*. [Report] 20.12.2012.
6. Lundin, W., RWE, *Plan for utbygging, anlegg og drift av Luno, 23380-LUNAS-RA-0024, Rev.01*. 2011.
7. Det norske, *Plan for utbygging og drift av Ivar Aasen-feltet Del 2: konsekvensutredning September 2012*, in *Lisensene PL001B, PL028B og PL242*. 2012, Det norske oljeselskap ASA , Statoil, Bayerngas Norge.
8. Det norske, T., Exxon Mobil, Statoil, *Plan for utbygging, anlegg og drift av Dagny og Eirin*. 2012.
9. Staffell, I. and S. Pfenninger, *Using bias-corrected reanalysis to simulate current and future wind power output.* Energy, 2016. **114**: p. 1224-1239.
10. Siemens, *Wind Turbine SWT-6.0-154 Techinical specifications*. 2016, Siemens AG.
11. Siemens, *Wind Turbine SWT-3.6-107 Techinical specifications*. 2015, Siemens AG.

12. Mads Bjørkeland, I.D.V., Zaw Win Htun, Marius Holt, *Generation System Reliability*, in *ELK-16 Advanced Power System Analysis*. 2016, NTNU.
13. Toftevaag, T., *Presentation in the course ELK 12 Wind power in electric power systems*. 2016.
14. J.F. Manwell, J.G.M., A.L. Rogers, *Wind Energy Explained Theory, Design and Application*. second ed. 2009: Wiley.
15. Sulaeman, S., et al. *An analytical method for constructing a probabilistic model of a wind farm*. in *2014 IEEE PES General Meeting | Conference & Exposition*. 2014.
16. Billington, R. and R.R. Allan, *Reliability evaluation of power systems*. 2013: Springer Science & Business Media.
17. Vadlamudi, V.V., *Advanced Power System Analysis, presentation on Generation System Reliablility in subject ELK-16*. NTNU, 2016.
18. Kundur, P., et al., *Definition and classification of power system stability IEEE/CIGRE joint task force on stability terms and definitions*. IEEE Transactions on Power Systems, 2004. **19**(3): p. 1387-1401.
19. Mosadeghy, M., *Reliability Impacts of Increased Wind Generation in the Australian National Electricity Grid*, in *School of Information Technology and Electrical Engineering*. 2015, The University of Queensland.
20. James McCalley, I.S.U. *Illustration of Computation of LOLE*. slides 31 to 39]. Available from: http://home.engineering.iastate.edu/~jdm/wind/Wind&Markets.ppt.
21. Keane, A., et al., *Capacity Value of Wind Power*. IEEE Transactions on Power Systems, 2011. **26**(2): p. 564-572.
22. Vadlamudi, V.V., *How to compute LOLE for constant peak load curve*.
23. Li, W., *Risk assessment of power systems: models, methods, and applications*. 2014: John Wiley & Sons.
24. Gao, Y., *Adequacy Assessment of Coposide Generation and Transmission Systems Incorporating Wind Energy Conversion Systems*. 2010, University of Saskatchewan.
25. Vadlamudi, V.V., *Lekcture in course ELK-10 at NTNU: RELRAD Methodology for Distribution System Reliability*. 2016.

26. Roy Billington, R.K., Yi Gao, Dange Huang, Po Hu,, Wijarn Wangdee, *Adequacy Assessment Considerations in Wind Integrated Power Systems.* IEEE Transactions on Power Systems, 2012. **27**(4).
27. Mostafa Hosseinpour, H.R.M., Mohammad Ebrahim Hajiabadi, *A probabilistic model for assessing the reliability of wind farms in a power system.* Journal of Zhejiang University- SCIENCE C, 2013.
28. Chowdhury, A.A. *Reliability models for large wind farms in generation system planning*. in *IEEE Power Engineering Society General Meeting, 2005*. 2005.
29. Li, Y., *Bulk System Reliability Evaluation in a Deregulated Power Industry*, in *Department of Electrical Engineering*. 2003, University of Saskatchewan.
30. Roy Billington, Y.L., *Incorporating multi-state unit models in composite system adequacy assessment.* EUROPEAN TRANSACTIONS ON ELECTRICAL POWER, 2007.
31. Line Furseth Bjørk, E.B., Ulf Møller. *Samfunnsøkonomiske kostnader ved avbrudd, spenningsforstyrrelser og rasjonering-bedrifter med eldrevne prosesser*. 2012; Available from: https://www.nve.no/Media/3197/350_2012-bedrifter-med-eldrevne-prosesser.pdf.
32. Oljedirektoratet. *Elektrifiseringsvurderinger av området midtre Nordsjø*. [Report] 2012 29.06.2012 [cited 2017 29 May]; Available from: http://www.npd.no/Global/Norsk/3-Publikasjoner/Rapporter/Elektrifiseringsvurderinger%20for%20midtre%20nordsj%C3%B8/Endelig-rapport.pdf.
33. ABB. *XLPE Submarine Cable Systems: Attachment to XLPE Land Cable Systems - User´s Guide*. [Brochure] [cited 2017 March]; Available from: http://www05.abb.com/global/scot/scot245.nsf/veritydisplay/2fb0094306e48975c125777c00334767/$file/XLPE%20Submarine%20Cable%20Systems%202GM5007%20rev%205.pdf.
34. B1.10, W.G., *Update of Service Experience of HV Underground and Submarine Cable Systems*, ed. CIGRÉ. 2009: CIGRÉ publications.
35. Veila, S., *Impacts of Interconnecting the Wind Farm Project within the Dogger Bank Zone*, in *Department of Electric Power Engineering*. 2013, Norwegian University of Science and Technology.

36. Statoil, *Johan Sverdrup, Kraft fra land konsekvensutredning*, in *PL265,PL501,501B,PL502*. 2014, Statoil.
37. Badeer, G.H., *GE's LM2500+G4 Aeroderivative Gas Turbine for Marine and Industrial Applications.* 2005.
38. SINTEF, *OREDA Offshore Reliability Data ISBN: 978-82-14-04830-8*. 5th ed. Vol. 1 -Topside Equipment. 2009: OREDA Participants.
39. Vetvik, I.D., *Reliability study of offshore wind connected to multiple oil and gas platforms*. 2016, NTNU.

Appendix A: COPT

A1: Conventional generation

CAPACITY AVAILABLE	CAPACITY UNAVAILABLE	STATE PROBABILITY	CUMULITIVE PROBABILITY
379	0	0.84822197	0.15177803
346	33	0.11045294	0.04132509
313	66	0.00479428	0.03653081
280	99	0.00006937	0.03646144
279	100	0.01589984	0.02056160
246	133	0.00207043	0.01849117
213	166	0.00008987	0.01840130
199	180	0.01589984	0.00250146
180	199	0.00000130	0.00250016
166	213	0.00207043	0.00042973
133	246	0.00008987	0.00033986
100	279	0.00000130	0.00033850
99	280	0.00029804	0.00004052
66	313	0.00003881	0.00000171
33	346	0.00000168	0.00000002
0	379	0.00000002	0.00000000

A2: Conventional generation and multi-state wind generation with FOR=5%

CAPACITY AVAILABLE	CAPACITY UNAVAILABLE	STATE PROBABILITY	CUMULITIVE PROBABILITY
439	0	0,08352082	0,9786905
433	6	0,13054001	0,89516965
427	12	0,09065171	0,76462964
421	18	0,0783609	0,67397793
415	24	0,08006748	0,59561703
409	30	0,08653289	0,51554955
406	33	0,01087583	0,42901667
403	36	0,07722996	0,41814084
400	39	0,01699852	0,34091088
397	42	0,05891787	0,32391236
394	45	0,01180439	0,26499449
391	48	0,06124888	0,25319009
388	51	0,01020392	0,19194121
385	54	0,05828488	0,18173729
382	57	0,01042615	0,12345242
379	60	0,02479148	0,11302627
376	63	0,01126805	0,08823479
373	66	0,00047207	0,07696674
370	69	0,01005665	0,07649467
367	72	0,00073784	0,06643802
364	75	0,00767211	0,06570018
361	78	0,00051238	0,05802807
358	81	0,00797564	0,05751569
355	84	0,00044291	0,0495401
352	87	0,00758968	0,04909714
349	90	0,00045256	0,04150746
346	93	0,00322827	0,04105491
343	96	0,0004891	0,03782663
340	99	6,8335E-06	0,03733753
339	100	0,00156559	0,0373307

Appendix B: Composite Load Point Analysis, Platform 3, Case 1

COPT				Platform 3			
State	*Outage*	*Capacity Outage*	*State Probability DAFOR= 0,40028*	P1j	Probability Pj	LC	ELC
1	*-*	*0*	*0,503667523*	0	0	0	0
2	*C3*	*30*	*0,003349227*	0	0	0	0
3	*C2*	*30*	*0,000555128*	1	0,000555128	11	0,006106413
4	*C2,C3*	*60*	*3,69E-06*	1	3,69143E-06	11	4,06057E-05
5	*C1*	*75*	*0,001111482*	0	0	0	0
6	*C1,C3*	*105*	*7,39E-06*	0	0	0	0
7	*C1,C2*	*105*	*1,23E-06*	1	1,22504E-06	11	1,34755E-05
8	*G6*	*60*	*0,336170273*	0	0	0	0
9	*G6,C3*	*90*	*0,002235424*	0	0	0	0
10	*G6,C2*	*90*	*0,000370518*	0	0	0	0
11	*G6,C1*	*135*	*0,000741853*	0	0	0	0
12	*G5*	*33*	*0,021862029*	0	0	0	0
13	*G5,C3*	*63*	*0,000145375*	0	0	0	0
14	*G5,C2*	*63*	*2,41E-05*	1	2,40957E-05	11	0,000265053
15	*G5,C1*	*108*	*4,82E-05*	0	0	0	0
16	*G5,G6*	*93*	*0,014591698*	0	0	0	0
17	*G4*	*33*	*0,021862029*	0	0	0	0
18	*G4,C3*	*63*	*0,000145375*	0	0	0	0
19	*G4,C2*	*63*	*2,41E-05*	1	2,40957E-05	11	0,000265053
20	*G4,C1*	*108*	*4,82E-05*	0	0	0	0
21	*G4,G6*	*93*	*0,014591698*	0	0	0	0
22	*G4,G5*	*66*	*0,000948936*	0	0	0	0
23	*G3*	*33*	*0,021862029*	0	0	0	0
24	*G3,C3*	*63*	*0,000145375*	0	0	0	0
25	*G3,C2*	*63*	*2,41E-05*	1	2,40957E-05	11	0,000265053
26	*G3,C1*	*108*	*4,82E-05*	0	0	0	0
27	*G3,G6*	*93*	*0,014591698*	0	0	0	0
28	*G3,G5*	*66*	*0,000948936*	0	0	0	0
29	*G3,G4*	*66*	*0,000948936*	0	0	0	0
30	*G2*	*180*	*0,009441201*	1	0,009441201	11	0,103853206
31	*G2,C3*	*210*	*6,28E-05*	1	6,2781E-05	11	0,00069059

32	G2,C2	210	1,04E-05	1	1,04058E-05	11	0,000114464
33	G2,C1	255	2,08E-05	0	0	0	0
34	G2,G6	240	0,00630148	1	0,00630148	11	0,069316283
35	G2,G5	213	0,000409802	1	0,000409802	11	0,004507819
36	G2,G4	213	0,000409802	1	0,000409802	11	0,004507819
37	G2,G3	213	0,000409802	1	0,000409802	11	0,004507819
38	G1	100	0,009441201	0	0	0	0
39	G1,C3	130	6,28E-05	0	0	0	0
40	G1,C2	130	1,04E-05	1	1,04058E-05	11	0,000114464
41	G1,C1	175	2,08E-05	0	0	0	0
42	G1,G6	160	0,00630148	0,181818182	0,00630148	2	0,002291447
43	G1,G5	133	0,000409802	0	0	0	0
44	G1,G4	133	0,000409802	0	0	0	0
45	G1,G3	133	0,000409802	0	0	0	0
46	G1,G2	280	0,000176974	1	0,000176974	11	0,001946719
						ELC =	0,192645788
						EENS=	1687,577105

Appendix C: Composite Load Point Results

EENS (MWh)

Load year 2028, high cable rating

DAFOR	Base case				Case 1				Case 2				Case 3			
	Platform 1	Platform 2	Platform 3	Platform 4	Platform 1	Platform 2	Platform 3	Platform 4	Platform 1	Platform 2	Platform 3	Platform 4	Platform 1	Platform 2	Platform 3	Platform 4
0,37340	7724,25406	3921,88086	2065,58787	2248,00649	2221,60349	1428,6963	1777,23945	1676,33903	6561,90885	3905,35777	2231,21922	1949,3534	2192,31415	1406,70075	1765,59171	1663,28391
0,40028	7724,25406	3921,88086	2065,58787	2248,00649	2351,10538	1497,55788	1777,90596	1669,50216	6561,90885	3905,35777	2231,21922	1949,3534	2321,58749	1475,64616	1766,24986	1656,57722
0,40530	7724,25406	3921,88086	2065,58787	2248,00649	2375,29062	1510,41819	1778,03043	1668,22533	6561,90885	3905,35777	2231,21922	1949,3534	2345,73006	1488,52213	1766,37278	1655,3247
0,42574	7724,25406	3921,88086	2065,58787	2248,00649	2473,76602	1562,78168	1778,53726	1663,02647	6561,90885	3905,35777	2231,21922	1949,3534	2444,03167	1540,94937	1766,87325	1650,22482

Load year 2028, lowcable rating

	Base case				Case 1				Case 2				Case 3			
	Platform 1	Platform 2	Platform 3	Platform 4	Platform 1	Platform 2	Platform 3	Platform 4	Platform 1	Platform 2	Platform 3	Platform 4	Platform 1	Platform 2	Platform 3	Platform 4
0,37340	7724,25406	3921,88086	2065,58787	2248,00649	2221,60349	1428,6963	1777,23945	1676,33903	6585,2315	3910,54943	2235,48784	1945,98368	2200,64915	1412,97972	1763,50796	1657,00495
0,40028	7724,25406	3921,88086	2065,58787	2248,00649	2351,10538	1497,55788	1777,90596	1669,50216	6585,2315	3910,54943	2235,48784	1945,98368	2329,56494	1481,65577	1764,2555	1650,56761
0,40530	7724,25406	3921,88086	2065,58787	2248,00649	2375,29062	1510,41819	1778,03043	1668,22533	6585,2315	3910,54943	2235,48784	1945,98368	2353,64073	1494,48143	1764,39511	1649,3654
0,42574	7724,25406	3921,88086	2065,58787	2248,00649	2473,76602	1562,78168	1778,53726	1663,02647	6585,2315	3910,54943	2235,48784	1945,98368	2451,67045	1546,70385	1764,96355	1644,47033

Fictive Load 275 MW, high cable rating

	Base case				Case 1				Case 2				Case 3			
	Platform 1	Platform 2	Platform 3	Platform 4	Platform 1	Platform 2	Platform 3	Platform 4	Platform 1	Platform 2	Platform 3	Platform 4	Platform 1	Platform 2	Platform 3	Platform 4
0,37340	1061,27677	3987,94092	4675,26026	4101,1929	117,905102	1327,84596	3026,83562	1632,5	1005,16219	3991,9298	4437,90656	4063,28609	117,12625	1319,07454	2994,79055	1587,34562
0,40028	1061,27677	3987,94092	4675,26026	4101,1929	118,763099	1418,78158	3044,88767	1710,36651	1005,16219	3991,9298	4437,90656	4063,28609	117,97858	1409,40946	3013,24029	1666,17219
0,40530	1061,27677	3987,94092	4675,26026	4101,1929	118,923335	1435,76434	3048,25899	1724,90854	1005,16219	3991,9298	4437,90656	4063,28609	118,137757	1426,28004	3016,68589	1680,89352
0,42574	1061,27677	3987,94092	4675,26026	4101,1929	119,575771	1504,9133	3061,98607	1784,11953	1005,16219	3991,9298	4437,90656	4063,28609	129,971292	1494,97221	3030,71539	1740,83456

Fictive Load 275 MW, lowcable rating

	Base case				Case 1				Case 2				Case 3			
	Platform 1	Platform 2	Platform 3	Platform 4	Platform 1	Platform 2	Platform 3	Platform 4	Platform 1	Platform 2	Platform 3	Platform 4	Platform 1	Platform 2	Platform 3	Platform 4
0,37340	1061,27677	3987,94092	4675,26026	4101,1929	117,905102	1327,84596	3026,83562	1632,5	1043,05236	3984,37187	4442,73344	4096,87574	118,452274	1319,07454	2997,2367	1592,08142
0,40028	1061,27677	3987,94092	4675,26026	4101,1929	118,763099	1418,78158	3044,88767	1710,36651	1043,05236	3984,37187	4442,73344	4096,87574	119,24772	1409,40946	3015,58151	1670,70483
0,40530	1061,27677	3987,94092	4675,26026	4101,1929	118,923335	1435,76434	3048,25899	1724,90854	1043,05236	3984,37187	4442,73344	4096,87574	119,396274	1426,28004	3019,00751	1685,38822
0,42574	1061,27677	3987,94092	4675,26026	4101,1929	119,575771	1504,9133	3061,98607	1784,11953	1043,05236	3984,37187	4442,73344	4096,87574	120,001144	1494,97221	3032,95721	1745,17478

Load year 2023, high cable rating

	Base case				Case 1				Case 2				Case 3			
	Platform 1	Platform 2	Platform 3	Platform 4	Platform 1	Platform 2	Platform 3	Platform 4	Platform 1	Platform 2	Platform 3	Platform 4	Platform 1	Platform 2	Platform 3	Platform 4
0,37340	2339,85248	3190,35274	2802,95529	4157,5006	542,829563	1085,93058	1764,59904	1647,37522	2282,57973	3193,54384	2662,74394	4116,8033	539,230104	1077,61556	1744,51432	1598,52358
0,40028	2339,85248	3190,35274	2802,95529	4157,5006	575,510873	1157,66436	1777,63963	1724,60361	2282,57973	3193,54384	2662,74394	4116,8033	568,989605	1148,92446	1757,83031	1676,87064
0,40530	2339,85248	3190,35274	2802,95529	4157,5006	581,082679	1171,06107	1780,07503	1739,02647	2282,57973	3193,54384	2662,74394	4116,8033	574,547369	1162,24182	1760,31715	1691,50242
0,42574	2339,85248	3190,35274	2802,95529	4157,5006	603,769473	1225,60864	1789,99131	1797,75223	2282,57973	3193,54384	2662,74394	4116,8033	597,176991	1216,4663	1770,44286	1751,07882

Load year 2023, high cable rating

	Base case				Case 1				Case 2				Case 3			
	Platform 1	Platform 2	Platform 3	Platform 4	Platform 1	Platform 2	Platform 3	Platform 4	Platform 1	Platform 2	Platform 3	Platform 4	Platform 1	Platform 2	Platform 3	Platform 4
0,37340	2339,85248	3190,35274	2802,95529	4157,5006	542,829563	1085,93058	1764,59904	1647,37522	7691,87376	3187,4975	2663,45373	4131,71702	542,071583	1077,61556	1746,09567	1603,25938
0,40028	2339,85248	3190,35274	2802,95529	4157,5006	575,510873	1157,66436	1777,63963	1724,60361	7691,87376	3187,4975	2663,45373	4131,71702	571,709191	1148,92446	1759,34382	1681,40328
0,40530	2339,85248	3190,35274	2802,95529	4157,5006	581,082679	1171,06107	1780,07503	1739,02647	7691,87376	3187,4975	2663,45373	4131,71702	577,24419	1162,24182	1761,818	1695,99712
0,42574	2339,85248	3190,35274	2802,95529	4157,5006	603,769473	1225,60864	1789,99131	1797,75223	7691,87376	3187,4975	2663,45373	4131,71702	599,781121	1216,4663	1771,89212	1755,41904

Appendix D: EENS Generation Adequacy Flowchart

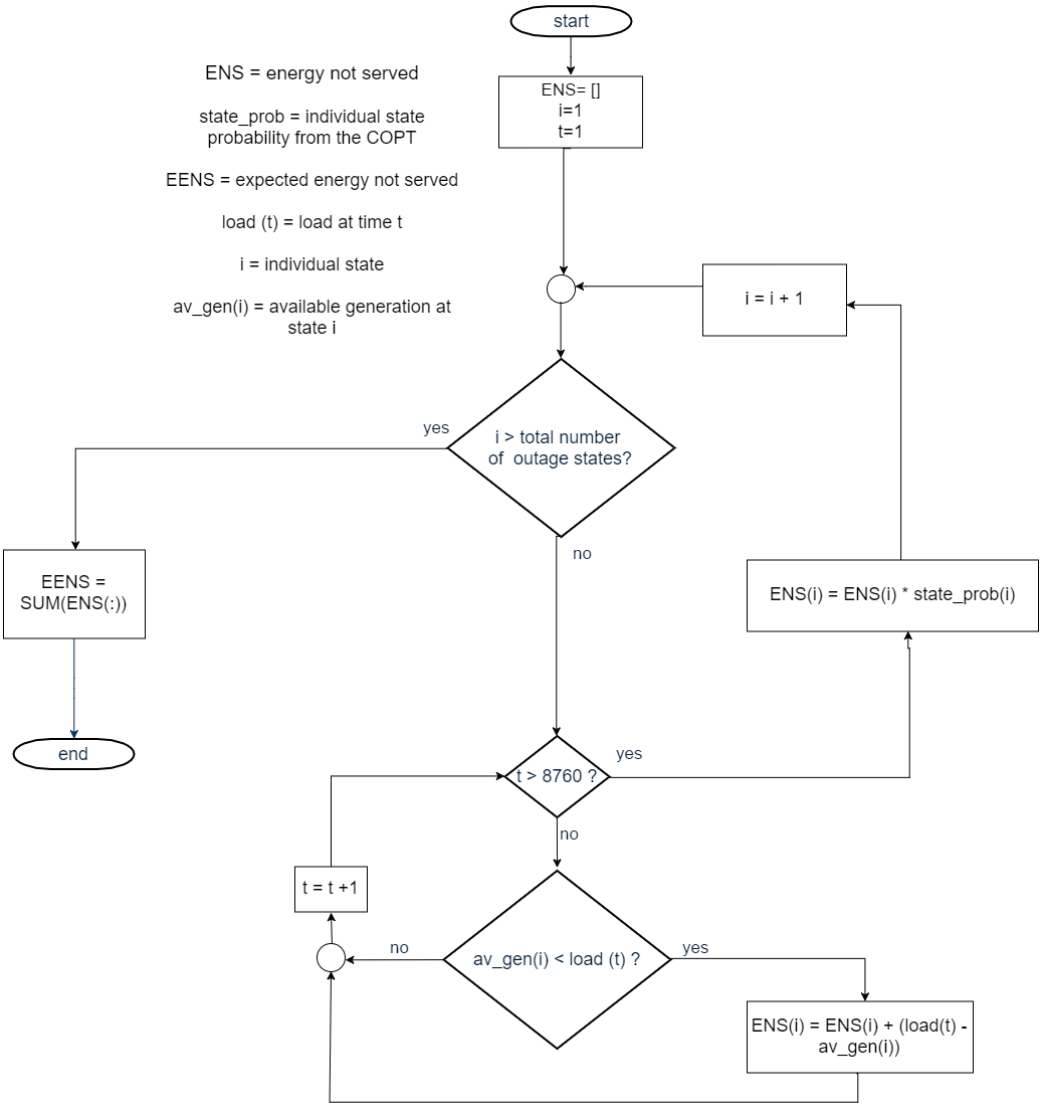

Appendix E: LOLE Flowchart

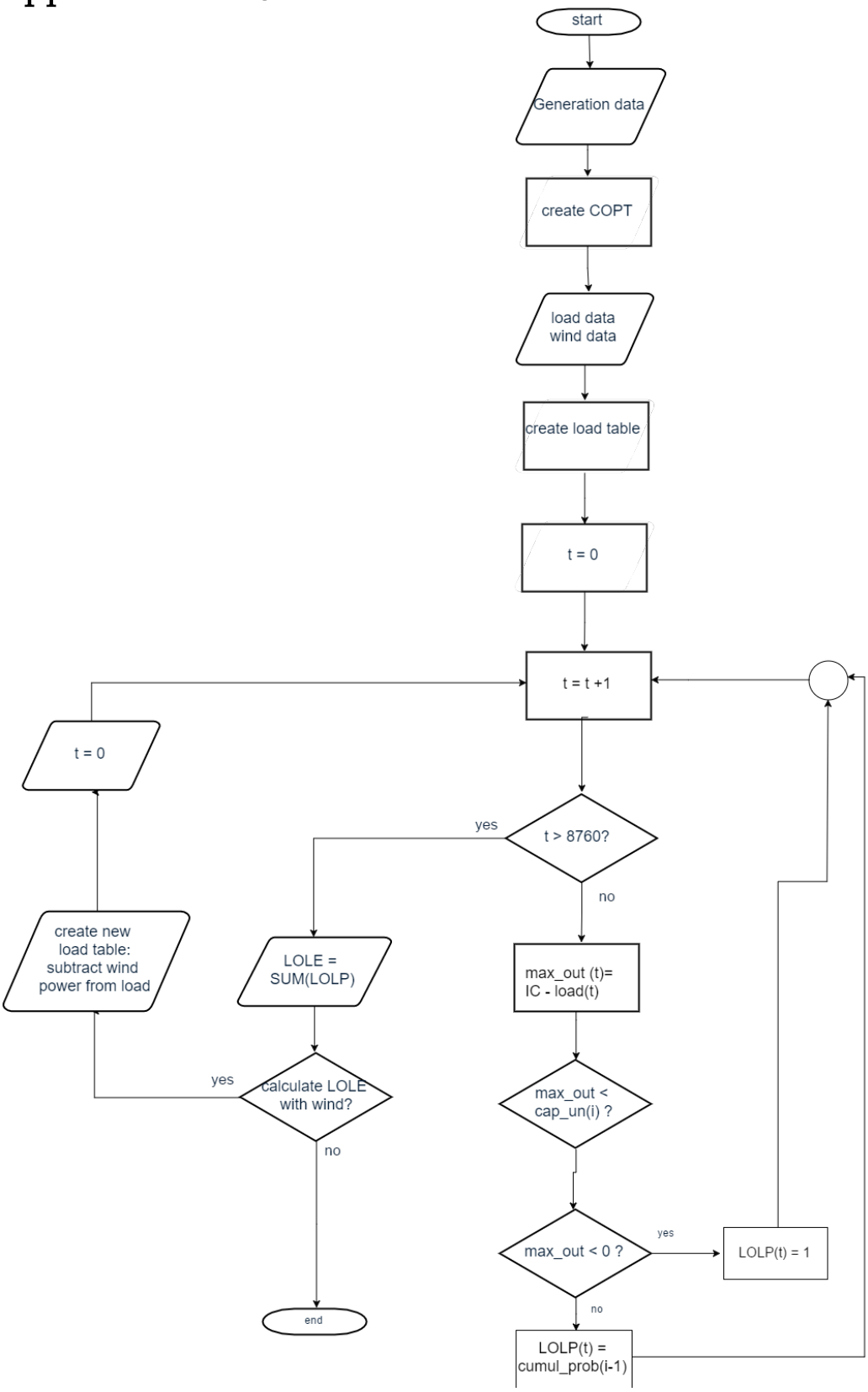

Appendix F: EENS Composite Adequacy Flowchart

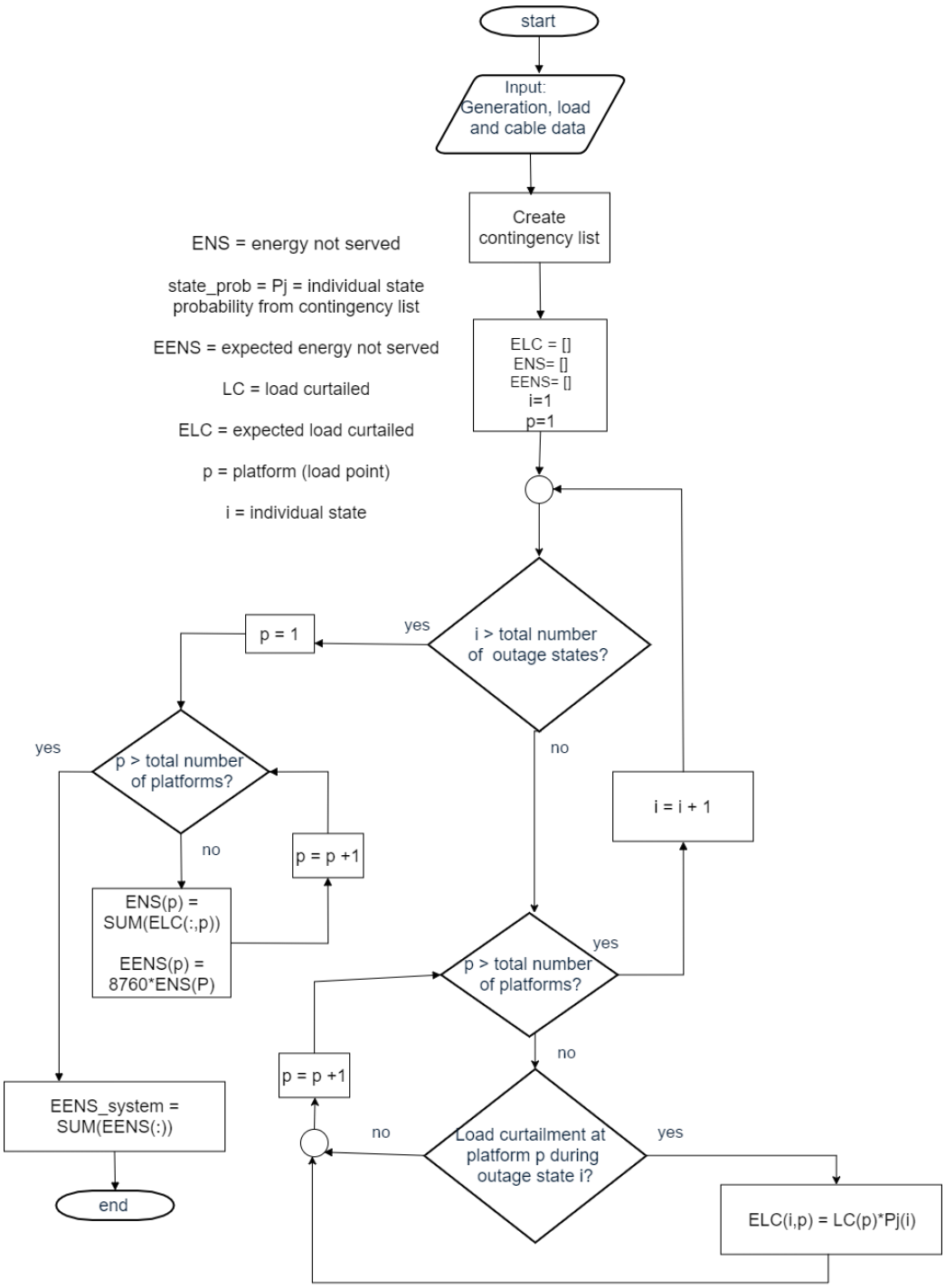

Appendix G: ELCC Flowchart

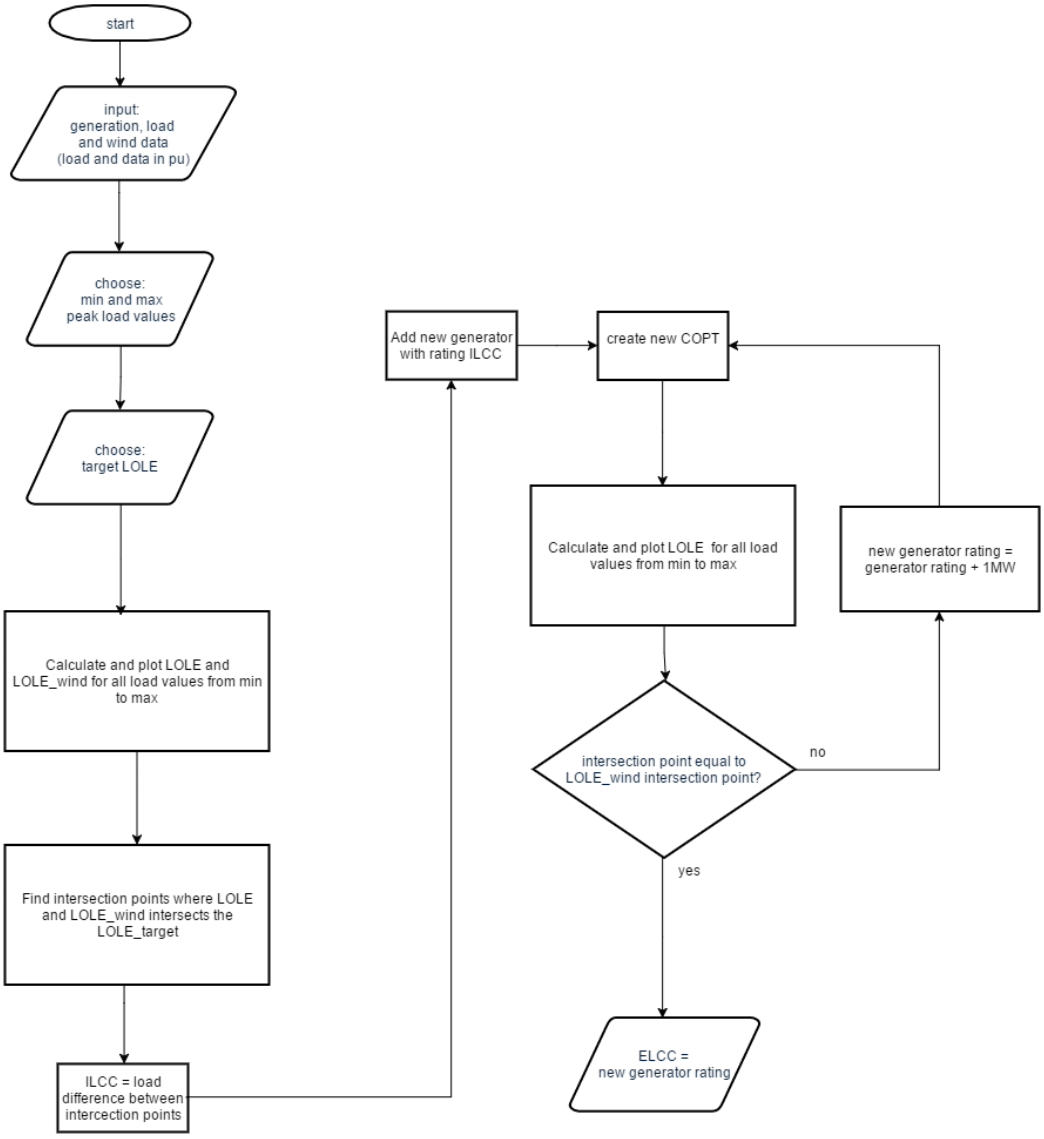

Appendix H: Cable Data ABB

Table I: Cable cross section based on current carrying capability, ABB [33]

100-300 kV XLPE 3-core cables		
Cross section mm²	Copper conductor	Aluminium conductor
	A	A
300	530	430
400	590	485
500	655	540
630	715	600
800	775	660
1000	825	720

Table II: Cable cross section based on current carrying capability, single core ABB [33]

Cross section Cu conductor	Rated voltage 100 - 420 kV	
	Wide spacing	Close spacing
mm²	A	A
185	580	445
240	670	505
300	750	560
400	845	620
500	950	690
630	1065	760
800	1180	830
1000	1290	895

Table III: Cable data based on voltage level and cross section, ABB [33]

Cross-section of con-ductor	Diameter of con-ductor	Insulation thickness	Diameter over insulation	Lead sheath thickness	Outer diameter of cable	Cable weight (Aluminium)	Cable weight (Copper)	Capaci-tance	Charging current per phase at 50 Hz	Inductance
mm²	mm	mm	mm	mm	mm	kg/m	kg/m	µF/km	A/km	mH/km
Three-core cables, nominal voltage 110 kV (Um = 123 kV)										
185	15.8	16.0	50.2	2.0	156.0	37.4	40.9	0.14	2.8	0.46
240	18.1	15.0	50.5	2.0	157.0	38.0	42.5	0.15	3.0	0.43
300	20.4	14.0	50.8	2.0	157.0	38.5	44.1	0.17	3.5	0.41
400	23.2	13.0	51.6	2.0	159.0	39.7	47.2	0.20	3.9	0.38
500	26.2	13.0	55.0	2.1	167.0	43.6	53.0	0.22	4.3	0.37
630	29.8	13.0	58.6	2.3	176.0	48.8	60.7	0.24	4.7	0.36
800	33.7	13.0	62.5	2.4	185.0	54.4	69.5	0.26	5.2	0.34
1000	37.9	13.0	67.3	2.6	197.0	61.6	80.5	0.28	5.6	0.33